UNIVERSITY OF ILLINOIS
URBANA

AERONOMY REPORT NO. 116

ROCKET MEASUREMENTS OF MESOSPHERIC IONIZATION IRREGULARITIES

by
R. B. Stoltzfus
S. A. Bowhill

June 1, 1985

Library of Congress ISSN 0568-0581

...oratory
Department of Electrical and Computer Engineering
University of Illinois
Urbana, Illinois

Supported by
National Aeronautics and Space Administration

UILU-ENG-85-2502

A E R O N O M Y R E P O R T

N O. 116

ROCKET MEASURMENTS OF MESOSPHERIC IONIZATION IRREGULARITIES

by

R. B. Stoltzfus
S. A. Bowhill

June 1, 1985

Supported by
National Aeronautics
and Space Administration
Grant NGR 14-005-181

Department of Electrical and
Computer Engineering
University of Illinois
Urbana, Illinois

ABSTRACT

The Langmuir probe technique for measurement of electron concentration in the mesosphere is capable of excellent altitude resolution, of order 1 m. Measurements from nine daytime rocket flights carrying an electron density fine structure experiment frequently show small-scale ionization structures in the altitude region 70 to 90 km. The irregularities are believed to be the result of turbulent advection of ions and electrons. This work describes the fine structure experiment flown by the University of Illinois and presents methods of analyzing the collected data. Theories of homogeneous, isotropic turbulence are reviewed. Power spectra of the measured irregularities are calculated and compared to spectra predicted by turbulence theories.

TABLE OF CONTENTS

LIST OF TABLES

LIST OF FIGURES

Page

1. INTRODUCTION

1.1 Statement of the Problem

Electron density irregularities in the mesosphere are often observed by both radar and rocket techniques. The advection of electrons and ions by atmospheric turbulence is one possible cause of the irregularities. Turbulence in the field of a scalar such as electron density may be analyzed by decomposing the spatial fluctuations into sinusoidal components. The strength of the components as a function of spatial frequency, or wave number, is called the scalar spectrum. In coherent-scatter radar studies, scattered power is measured as a function of altitude. Irregularities show up as isolated regions of high scattered power. Analysis of coherent-scatter data gives the value of the scalar spectrum at a particular wave number. In rocket studies measuring electron density the irregularities show up as small-scale fluctuations on an otherwise smooth electron density profile. Analysis of the rocket data can ideally give the scalar spectrum at all wave numbers. The measurable wave number range is limited by system noise and performance of the equipment used in the experiment.

The present study has three main objectives: (1) to review theories of isotropic, homogeneous turbulence predicting three-dimensional and one-dimensional spectra of turbulence, (2) to describe the analysis of data from the electron density fine structure experiment flown by the University of Illinois rocket program, and (3) to compare power spectra of irregularities measured by nine rocket flights with theoretical turbulence spectra.

1.2 Previous Work

Rocket studies of mesospheric electron density irregularities have been conducted by a number of groups using similar experiments. A rocket

equipped with a Langmuir probe passes through an electron density irregularity and observes temporal current fluctuations superposed on a background current. The temporal fluctuations are attributed to spatial fluctuations in electron density. If the spatial fluctuations are assumed to be isotropic, then the temporal and spatial fluctuations are related simply by the velocity of the rocket.

Prakash et al. (1969) describe the results from a number of flights at Thumba, India. Their experiment essentially measures the amplitude of the probe current in a frequency range of 70 to 1000 Hz. They observe a number of irregularities between 85 and 92 km. The irregularities occur in bands with altitude extents of the order of 100 m. Prakash et al. (1969) attribute these irregularities to atmospheric turbulence. Power spectra of the observed irregularities are not calculated.

Thrane and Grandal (1981) present fine structure measurements from two nighttime launches at the Andoya Rocket Range in Norway. One of the launch conditions was the presence of D region irregularities measured with a partial reflection radar operated at Tromso, 120 km away from the rocket range. The rocket data show ionization fine structure throughout the flight. Spectral analysis of the mesospheric irregularities show a power spectral index close to -5/3, consistent with the presence of isotropic, homogeneous turbulence.

Royrvik and Smith (1984) compare rocket and radar measurements of a single irregularity at 85 km altitude. The rocket launch took place at Chilca, Peru. Coincident coherent-scatter radar measurements were made at the Jicamarca radio observatory. Spectral analysis of the rocket data shows a power spectral index close to -5/3. The spectrum is extrapolated to the wave number measured by the Jicamarca radar, and agreement is found between

the rocket and radar results.

1.3 University of Illinois Rocket Program

The rocket program in the Aeronomy Laboratory at the University of Illinois conducts three separate experiments based on the Langmuir probe. First, the probe current is used to measure the ambient electron density as a function of altitude. Calibration between probe current and electron density is provided by a radio propagation experiment (Mechtly et al., 1967). Second, electron temperature is measured in the E region by sweeping the probe potential and analyzing the I-V characteristic of the probe (Zimmerman and Smith, 1980). Third, the ac component of the probe current is used to study electron density fine structure.

The University of Illinois has launched nine daytime flights carrying a fine structure experiment described by Klaus and Smith (1978). The experiment apparatus consists of a Langmuir probe extended from the rocket into the ionosphere. As the rocket passes through electron density irregularities, temporal fluctuations in the probe current are observed. The ac component of the probe current is amplified and telemetered to the ground. Digital analysis of the data estimates the power spectra of the irregularities.

1.4 Outline of the Investigation

Chapter 2 reviews the theory of the Langmuir probe in the D region. Debye length and various plasma parameters in the D region are discussed. The values of the parameters in the D region present certain difficulties in interpreting the probe current. Some of these problems are overcome by use of a dc mode of operation developed by Smith (1969).

Chapter 3 reviews various theories of isotropic, homogeneous turbulence. The basic parameters of fluids and fluid flows are given. The

spectral approach to describing turbulence and the relationship of three-dimensional to one-dimensional spectra are discussed. Application of dimensional and physical arguments leads to a number of important theories predicting turbulence spectra, which are presented. In particular, a scalar spectrum model by Hill and Bowhill (1976) suitable for describing atmospheric turbulence is discussed.

Chapter 4 describes the University of Illinois fine structure experiment and methods of data analysis. Using analog preprocessing, irregularities may be quickly identified and distinguished from interference. The appropriate data segments are digitized using a microcomputer based digitizer. The development and operation of the digitizer are discussed in detail. Following transfer of the data to a CDC Cyber mainframe computer, the data are Fourier analyzed to calculate power spectra of the irregularities. Software needed for the transfer and analysis is described.

Results of the data analysis are given in Chapter 5. Five of the nine flights examined reveal ionospheric irregularities. The power spectra of the irregularities are examined and various parameters of the irregularities and spectra are tabulated. Comparisons are made to the Hill and Bowhill (1976) scalar spectral model and to some spectral predictions by Rastogi and Bowhill (1976).

2. LANGMUIR PROBE THEORY

2.1 Introduction

Rockets using Langmuir probes are capable of measuring electron density and other plasma parameters in the ionosphere. In a simple Langmuir probe experiment an electrode at a known potential is inserted into a plasma. As the potential of the probe is varied the current drawn by the probe is monitored. Analysis of this I-V characteristic gives information about various properties of the plasma. Due to collisions of particles within a few Debye lengths of the probe, exact relations of the plasma parameters to probe current do not exist in the D region. Assuming a direct proportion between the current and the electron density, a calibration constant between the two may be obtained with a radio propagation experiment. When the probe is operated in a dc mode high spatial resolution is attainable, allowing detailed examination of small-scale ionization structures. Detailed discussions of Langmuir probes in the ionosphere are available in Smith (1965, 1969) and Cicerone and Bowhill (1967).

Section 2.2 discusses the D region environment and its relevant parameters. Section 2.3 presents the collisionless regime theory and the problems it faces in the D region. Section 2.4 describes the dc method of operation of the Langmuir probe in the D region. This method gives measurements of electron density and fine structure thereof.

2.2 The D Region Plasma Environment

The D region of the ionosphere may be described as a weakly ionized plasma consisting of electrons, negative ions, and positive ions. Solar radiation is believed to be the chief source of this ionization. Daytime electron concentrations typically run from 10^2 cm^{-3} at 70 km to 10^4

cm^{-3} at 90 km; the neutral concentration varies from 10^{15} to 10^{14} cm^{-3} over the same range. At these densities it is assumed that the plasma does not affect the macroscopic dynamics of the neutral atmosphere. The free electrons may thus be used as a tracer in detecting macroscopic motions of the neutral atmosphere (Thrane and Grandal, 1981). In turn, the motion of the neutral atmosphere is assumed not to alter the reaction rates of the production and recombination of ions and electrons.

An ideal plasma consists of a charge-neutral collection of positively and negatively charged particles. If the particles have different masses, then a gravitational field induces a charge separation, resulting in an electric field. Such a separation is present in the earth's ionosphere. Lemaire and Scherer (1970) show that in an isothermal ionized atmosphere in hydrostatic and diffusive equilibrium the vertical induced field is

$$E = \frac{\mu(z)}{e} g$$

where g is the acceleration due to gravity, z is the altitude, and e is the electronic charge. $\mu(z)$ is an effective particle mass:

$$\mu(z) = \frac{\sum_i Z_i m_i n_i / k_b T_i}{\sum_i Z_i^2 n_i / k_b T_i}$$

where the sums are over all i species of particles, Z_i is the degree of ionization (-1 for electrons), m_i is the mass of the i'th species, n_i is the concentration of the i'th species at altitude z, T_i is the temperature of the i'th species, and k_b is Boltzmann's constant. Since the effective mass is of the order of the ion mass, the field as given above is quite small and has little effect on the probe operation as described in this chapter.

The Debye length is a characteristic length parameterizing the response of a plasma to an imposed potential. If a potential is imposed at a point

in the plasma the particles rearrange themselves to cancel the resulting field. When equilibrium is reached the plasma exhibits a local field in the neighborhood of the imposed potential. This field decreases exponentially with distance from the imposed potential, in contrast to the inverse square decrease of a point charge's field in free space. In the absence of negative ions, Poisson's equation in one dimension gives:

$$\frac{d^2V}{dx^2} = -(1/\epsilon_0)e(N_+ - N_e)$$

where e is the electron charge, V is the potential, ϵ_0 is the permittivity of free space, N_+ is the positive ion density, and N_e is the electron density. The presence of negative ions would replace N_e by $N_e + N_-$ where N_- is the negative ion density. Chen (1965) shows that if the positively charged particles are much heavier than the negatively charged particles, then

$$V = V_o e^{-x/h}$$

where V_o is the imposed potential with respect to the plasma, and h is the Debye length defined, in rationalized units, as

$$h = (\epsilon_0 k_b T_e / N_e e^2)^{1/2} \qquad (2.1)$$

where T_e is the electron temperature, and N_e is the ambient electron concentration. At points located a few Debye lengths from the perturbing potential the field is small. It is important to note that charge neutrality does not hold within a few Debye lengths of the imposed potential. It is this net charge which shields the rest of the plasma from the imposed potential. The charged region is often referred to as the plasma sheath. Care must be taken not to visualize the sheath as a sharply bounded layer outside of which the field does not exist. The Debye length only characterizes the exponential decrease in the field.

To calculate the Debye length it is necessary to find the electron temperature and the electron density. A number of techniques are available for measuring electron density, which may be considered a well-known parameter. Given a distribution of velocities for electrons or ions it may be possible to apply a Maxwellian distribution, defining an electron or ion temperature. For low collision rates these two temperatures could be quite different from each other and that of the neutral atmosphere. Unfortunately, direct measurements of electron temperature using Langmuir probes (Banks and Kockarts, 1973; Zimmerman and Smith, 1980) are obtainable only above 100 km. Below this height, conventional Langmuir probe theory fails and electron temperature measurements must be obtained in other manners. Due to the high neutral concentration and high collision rates in the D region it is assumed that the ion and electrons are in thermal equilibrium with the neutral atmosphere (Hill and Bowhill, 1976). Neutral temperatures in the D region range from approximately 180 to 220 ^{o}K (U.S. Standard Atmosphere, 1976). Thus Debye lengths ranging from 1 to 10 cm may be expected in the D region.

2.3 Langmuir Probes in the D Region

Langmuir probes provide a simple method of measuring charged particle densities in the D region. This simplicity, unfortunately, is counterbalanced by a rather complex theory. A general probe theory does not exist for all atmospheric regions, and useful results may be obtained only under certain restrictive assumptions. This section describes the basic theory of probes in a plasma and the applicability of the theory to the D region. A more complete description of Langmuir probes is available in Chen (1965).

In the basic operation of a Langmuir probe an electrode is inserted

into the plasma and a potential imposed. The potential is swept repeatedly over a wide range, and the induced current is measured as a function of potential, the rocket body acting as an electrode for the return current. Such an arrangement is termed a bipolar probe. Figure 2.1 shows a typical I-V characteristic for a probe. At V_s, the plasma or space potential, the probe potential equals that of the plasma. No sheath forms about the probe and the plasma is undisturbed. The observed current is entirely due to the thermal migration of charges in the plasma. Since an electron mass is many orders of magnitude less than an ion's, the electron thermal velocity is much greater than the ion's (for equal ion and electron temperatures). This results in a net electron current into the probe. To induce zero current the probe potential must be lowered, accelerating positive ions and retarding electrons. At V_f, the floating potential, the sum of the electron and ion currents adds to zero. Alternatively, if the potential is raised above V_s the positive ions are retarded and the electrons are accelerated. For potentials much greater than the plasma potential the current is due totally to the thermal electrons (region A in Figure 2.1). For potentials below V_s the current is totally due to positive ions (region C in Figure 2.1). The slope of the curve in region B gives information about the electron and ion temperatures. It is important to note that an isolated conductor in a plasma assumes the floating potential (Chen, 1965). A satellite or rocket in a plasma assumes this potential. All measurements of probe potential are thus made with respect to V_f. Moreover, these measurements must account for the plasma sheath which naturally accompanies a conductor not at the plasma potential.

Quantitative predictions of the I-V behavior of a spherical probe may be made for an ideal plasma of electrons and positive ions with Maxwellian

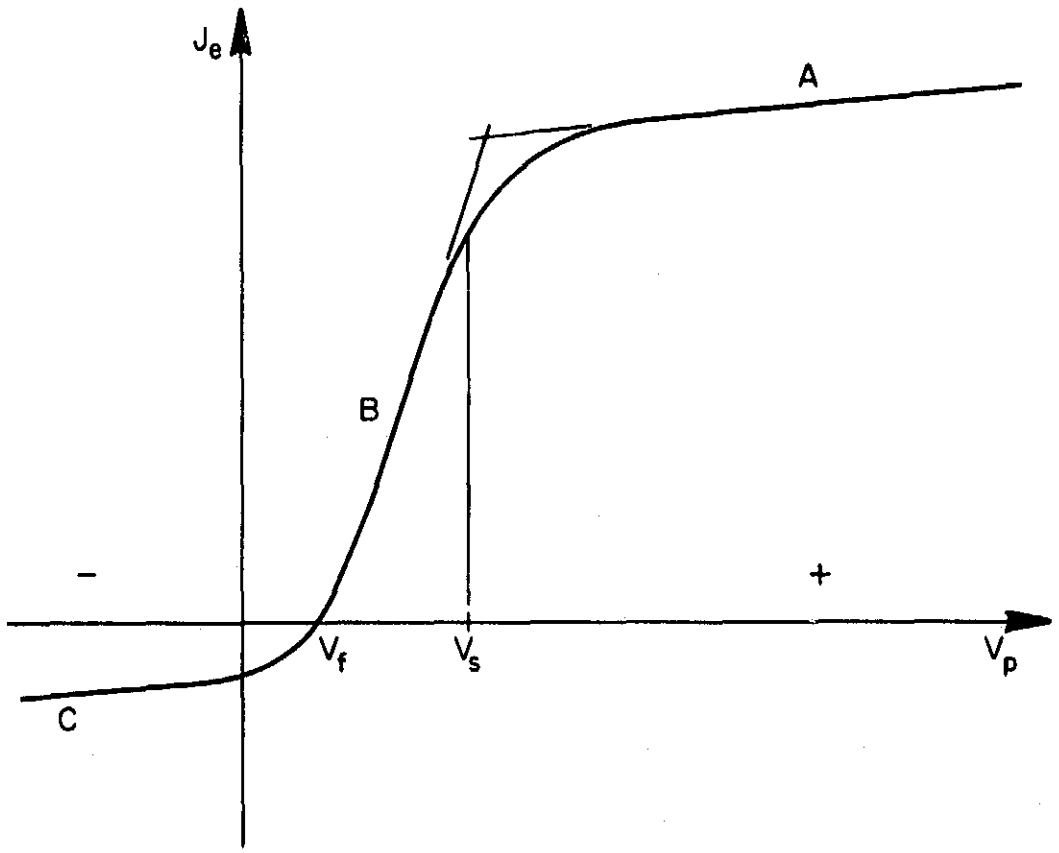

Figure 2.1 I-V characteristic for a Langmuir probe.

distributions. From Smith (1965) the number of electrons collected per unit area by a probe at the plasma potential is

$$j_e = N_e e \bar{v}_e / 4 \qquad (2.2)$$

where N_e is the electron concentration, $\bar{v}_e$ is the electron mean velocity, and j_e is the average electron current density. For a Maxwellian electron velocity distribution

$$\bar{v}_e = (8k_b T_e / \pi m_e)^{1/2} \qquad (2.3)$$

where T_e is the electron temperature, k_b is the Boltzman constant, and m_e is the mass of an electron. A similar analysis applies to positive ions. A comparison of the two current densities for equal temperatures gives

$$j_e / j_i = (m_i / m_e)^{1/2} \qquad (2.4)$$

where j_i is the ion current and m_i is the ion mass. For NO^+, a common ion in the D region, this ratio is 235. It is then quite justifiable to approximate the measured current as due to electrons only. This approximation becomes even better when the probe is above V_s and positive ions are repelled from the probe. If the electron mean free path, L_e, is much greater than both h and a_p, the probe radius, then Smith (1965) shows that for electron retarding potentials ($V < V_s$) the electron current is

$$j = j_e \exp[e(V-V_s)/k_b T_e] \qquad (2.5)$$

independent of probe shape. A probe operating under these conditions is said to be operating in the collisionless regime. For electron accelerating potentials on a small spherical probe ($h \gg a_p$)

$$j = j_e[1 + e(V-V_s)/k_b T_e] \; . \qquad (2.6)$$

Both relations give j proportional to N_e for constant T_e. This property is essential in justifying the fine structure experiment to be described in Section 2.4. From these relations it is theoretically possible to derive

electron density, electron temperature, and average ion composition.

There are a number of restrictions on the use of the above relations. Many of these restrictions are met in the D region, given due attention to the experimental apparatus. First, it must be assumed that the current drawn by the probe does not affect the plasma. Given the high electron velocities in the D region, any dearth of electrons created locally by the probe current is quickly replenished by diffusing electrons. Equation (2.3) numerically gives

$$\bar{v}_e = 6.21 \times 10^3 \, T_e^{1/2} \quad \text{m/sec}$$

or approximately 10^5 m/sec in the D region. Second, photoemission of electrons at the probe surface can interfere with current measurements. Smith (1965) finds that photoelectrons in the F region limit electron density measurements to altitudes less than 1000 km. It is assumed that this effect is absent in the D region since much of the hard solar radiation is attenuated by the atmosphere above. Third, it must be assumed that the contact potential (the bias appearing between the probe and rocket body when the internal circuitry shows no potential) remains constant over the altitude range under study. Such a bias might be caused by the dissimilar metals in the probe and rocket body (Smith, 1965). Fourth, the telemetry system and any radio propagation experiments must be designed such that they do not excite any plasma resonances near the probes.

Two important conditions do not hold in the D region. First, the above relations, equations (2.2) through (2.6), assume that the negative current is totally due to electrons. However, below 90 km negative ions are present in sufficient numbers to disqualify this assumption. Second, the above analysis has not taken collisions into account. If the Debye length is larger than or of the order of the electron mean free path ($h \geq L_e$),

then collisions can occur in the sheath, disrupting the free movement of electrons traversing the sheath to the probe. Such a free-fall condition is necessary to derive equation (2.6) (Chen, 1965). If the condition $L_e >> a_p$ is violated then collisions can occur in the region close to the probe. This region can only receive electrons from that portion of all 4π steradians not subtended by the nearby probe. The anisotropy prevents the formation of the Maxwellian velocity distribution necessary to derive equation (2.6). Due to the large variation of L_e, h, and other parameters in the D region, it is not possible to derive general relations between measured current and electron density. However, Smith (1969) suggests that the relationship is a simple proportionality, allowing the current to be calibrated by other experiments, thus extending the useful range of the Langmuir probe into the D region.

The measured current is also affected by the rocket's high speed, typically on the order of 1 km/sec. This is comparable to the mean positive ion velocity (from equation 2.3 NO^+ at 200° has $\bar{v}_+ = 664$ m/sec) in the D region but is far less than the mean electron velocity. The effect on positive ion current is discussed by Smith (1965) who gives the increase expected in ion current as a function of rocket speed divided by $\bar{v}_+$. For example, at $\bar{v}_+ = 664$ m/sec and rocket velocity of 1 km/sec the NO^+ ion current is 1.6 times the value expected for a stationary rocket. The measured electron current is largely unaffected due to the great difference between $\bar{v}_e$ and the rocket's velocity. Since the measured ion current increases, the total measured current density decreases. However, the ion current at zero rocket speed is so small compared to the electron current that the effect is negligible. The rocket's motion may also distort the current if the probe passes through the rocket's wake. Although the

electrons have sufficient velocity to quickly refill the rarefied wake region, preservation of the plasma charge neutrality demands that the plasma respond to the rarefaction at the slower ion velocity. As the rocket spins and precesses, an extended probe may sweep through the trailing rarefied wake, modulating the measured current at the spin frequency. Finally, it is important to discuss the effect of the supersonic nature of the rocket's velocity. Such high velocities are necessary in assuming a frozen atmosphere during measurements. At these velocities, however, a shock front develops ahead of the probe. This region exhibits temperatures and densities above those of the ambient atmosphere. It is found, however, that the ratio of the neutral densities $n_{shock}/n_{ambient}$ depends only on the Mach number (Thrane and Grandal, 1981) where n_{shock} is the neutral density in the shock front and $n_{ambient}$ is the neutral density in the ambient atmosphere.

2.4 DC Operation of a Rocket-Borne Langmuir Probe

In the previous section it was found that exact formulae for electron density versus current do not exist for D region measurements. Mechtly et al. (1967) describe an experiment to calibrate the current. Since collisionless regime theory does not hold in the D region, a potential sweep of the probe gives questionable results for temperature and other quantities. The probe is therefore operated at a fixed potential, sacrificing temperature data but gaining altitude resolution. This dc mode is particularly useful in discerning any fine structure in electron density. These irregularities may be related to irregularities in the neutral atmosphere. Such a relationship found by Thrane and Grandal (1981) is given here.

In the dc mode of operation the probe is set at a particular voltage,

and the electron current versus time is measured. The main assumption is that the current is proportional to the electron density over ranges in which the electron temperature is constant (Smith, 1969). The probe potential is set high enough above the floating potential that the I-V charcteristic is well into the linear part of the curve (Figure 2.1), above the plasma potential. The relation of current to electron concentration is found by means of a propagation experiment (Mechtly et al., 1967). In this experiment a circularly polarized wave at a few megahertz is launched from the ground and received at the rocket. The differential absorption and Faraday rotation of the wave are monitored as a function of height. These quantities can be used to find the electron concentration as a function of altitude. The two experiments work in tandem, the uncalibrated probe having high spatial resolution and the propagation experiment giving a coarse proportionality between concentration and current.

Amplification of the ac component of the probe current can reveal details of the fine structure in electron concentration. Such experiments have been carried out by Prakash et al. (1980), Smith and Klaus (1978), and Thrane and Grandal (1981). These irregularities can occur over ranges of tens of meters to kilometers. To measure them one asumes that the fluctuations are statistically stationary, that is,

$$N_e = \langle N_e \rangle + \Delta N_e$$

where N_e is the electron concentration and ΔN_e is the fluctuation about the mean. If in addition the proportionality between probe current and electron density is steady over a particular altitude range, then appropriate signal analysis of the current alone yields $\Delta N_e/\langle N_e \rangle$ ($= \Delta I/\langle I \rangle$) (Smith and Klaus, 1978) the percentage fluctuation. Due to the proportionality of N_e to I calibration of the current is unnecessary. Thrane and Grandal

(1981) extend the proportionality of n_{shock} to $n_{ambient}$ and show that percentage fluctuations in N_e are independent of velocity.

Further analysis is necessary to relate $\Delta N_e/\langle N_e\rangle$ to $\Delta n/\langle n\rangle$ where n is the neutral atmosphere concentration and Δn is the fluctuation about the mean, $\langle n\rangle$. The thermodynamic state equation

$$p = nkT$$

may be differentiated with respect to height in an ideal exponential atmosphere, yielding

$$-\frac{1}{H_p} = -\frac{1}{H_n} + \frac{1}{T}\frac{dT}{dz} \qquad (2.7)$$

where H_p is the pressure scale height and H_n is the neutral density scale height in the unperturbed atmosphere. The fluctuations are assumed to occur over altitude ranges small compared to the scale height. Thrane and Grandal (1981) show that for adiabatic displacements of air parcels

$$\frac{\Delta n}{\langle n\rangle} \simeq \left(\frac{1}{H_n} - \frac{1}{\gamma H_p}\right)\Delta z \qquad (2.8)$$

where Δz is the vertical displacement off equilibrium, and γ is the ratio of the specific heat of air at constant pressure to that at constant volume. Letting H_e be the scale height of the electron concentration, Thrane and Grandal (1981) find a relation similar to equation (2.8):

$$\frac{\Delta N_e}{\langle N_e\rangle} \simeq \left(\frac{1}{H_e} - \frac{1}{\gamma H_p}\right)\Delta z$$

Thus

$$\frac{\Delta n}{\langle n\rangle} = \frac{(\gamma H_p)/H_n - 1}{(\gamma H_p)/H_e - 1}\frac{\Delta N_e}{\langle N_e\rangle}$$

giving a relationship between electron density and neutral density fluctuations. This analysis assumes that fluctuations are caused only by

vertical displacements of air parcels in which the adiabatically shifted parcels' densities differ from those of the ambient atmosphere. Ambient properties in the horizontal direction are assumed to change slowly with respect to the vertical changes.

2.5 Summary

Rocket-borne Langmuir probes are capable of measuring a variety of plasma properties: electron and ion temperature and electron and ion concentrations. Collisionless regime Langmuir probe theory applies above 90 km. Below 90 km, in the D region, the Langmuir probe may be used only to measure electron density (when calibrated with an independent radio propagation experiment) and fluctuations in electron density. These fluctuations in electron concentration may then be related to fluctuations in the neutral atmosphere. Homogeneous turbulence is believed to be responsible for creating the irregularities. Mechanisms for production and a theoretical description of homogeneous turbulence are discussed in the next chapter.

3. THEORIES OF HOMOGENEOUS TURBULENCE

3.1 Introduction

Electron density fluctuations as a function of altitude in the mesosphere are often observed by both radar and rocket techniques. These fluctuations have been observed to occur in layers with a wide range of thicknesses ranging from the order of tens of meters (Rastogi and Bowhill, 1976) to the order of kilometers (Royrvik and Smith, 1984; Rottger et al., 1979). Isotropic turbulence is generally believed to cause these layers (Hocking and Vincent, 1982; Thrane and Grandal, 1981; Royrvik and Smith, 1984). Some radar investigations have indicated very narrow angular spectra for layers below 75 km (Fukao et al., 1980), suggesting very flat structures with horizontal scales greater than one Fresnel zone (Hocking and Vincent, 1982), making turbulence an unlikely mechanism for generating such layers. In the absence of coincident rocket and radar observations and under the limitations of the one-dimensional nature of rocket measurements, rocket data cannot discern the exact three-dimensional nature of the layers. One can only determine the consistency of rocket data with theoretical predictions. This chapter discusses theories of homogeneous, isotropic turbulence, providing a base for comparison with experimental results to be presented in Chapter 5. A complete development of turbulence is not intended in this chapter. More extensive presentations are available by Tennekes and Lumley (1972) and Lumley and Panofsky (1964).

Section 3.2 gives a qualitative description of turbulence and its associated parameters and measurable features. Section 3.3 reviews various sources of atmospheric turbulence. Section 3.4 discusses the Navier-Stokes equations, the problem of their closure, and their spectral interpretation.

Dimensional and similarity arguments are presented in Section 3.5, leading to a power law spectrum for certain length scales. Various theories for the spectrum at high wave numbers are examined in Section 3.6. Also, a scalar spectral model by Hill and Bowhill (1976) is applied to predict the type of spectra expected from the rocket data in this thesis.

3.2 Qualitative Description of Turbulence

Turbulence is often described as a cascade of energy from larger scales to smaller scales. A turbulent flow may be visualized as consisting of eddies of different sizes. The various scales of whirlpools and eddies seen in a river downstream from a bridge pier provide a graphic example of turbulence. These scales may be divided into three regimes with respect to their mechanisms of energy transfer. The first regime contains the largest scales (e.g., size of the bridge pier) in the flow. They draw their energy from instabilities in the mean flow. All smaller eddies find themselves in the rate of strain field of these large eddies, and energy is transferred to the smaller scales through vortex stretching (Tennekes and Lumley, 1972). Tennekes and Lumley also show that most of the energy transferred to an eddy comes from eddies with only slightly larger scales. Thus an energy cascade develops, energy being continuously transferred to decreasing scale sizes. In the second regime the mean flow no longer contributes energy to the turbulent flow. Energy is transferred to the second regime only through cascading from the larger eddies in the first regime. The cascading process continues, with little energy lost through other processes. This regime is often called the inertial regime. The cascading energy eventually is transferred to the eddies of the third regime, containing the smallest scales in the turbulent flow. At these small scales viscosity removes significant amounts of energy from the cascade. Decreasingly smaller scales

receive less and less energy as it is removed by viscous dissipation. This regime is often called the viscous range.

Fluids and fluid flows may be described by a variety of parameters. Dynamic viscosity μ, a constant for a fluid at a given temperature and independent of pressure, gives the proportionality between a fluid flow's shear stress and rate of shear strain. Kinematic viscosity, ν, a more common term in describing fluids, is the dynamic viscosity divided by the density of the fluid. Due to this dependence on density, the kinematic viscosity is a strong function of pressure, in contrast to the dynamic viscosity. Viscosity damps velocity shears, dissipating kinetic energy as heat. D, the molecular diffusivity, describes the rate of diffusion of a scalar contaminant in the fluid.

$$\frac{\partial N}{\partial t} + \underset{\sim}{V}\cdot\nabla N = D\nabla^2 N \qquad (3.1)$$

where N is the scalar concentration and $\underset{\sim}{V}$ is the velocity field. In analogy to ν, a fluid with a high D rapidly dissipates any large gradient in the scalar concentration. Another useful parameter, the Schmidt number, may be defined from ν and D:

$$Sc = \frac{\nu}{D}$$

Substitution of the thermal diffusivity, κ, for D gives the Prandtl number.

A fluid flow, described by a velocity field, may be characterized by another set of parameters. The Reynolds number is given by

$$Re = \frac{VL}{\nu} \qquad (3.2)$$

where V is a characteristic velocity of the flow, L is a characteristic length, and ν is the kinematic viscosity of the fluid. For flows with Reynolds numbers higher than some critical value, the flow becomes unstable. This number must be found experimentally and depends on the boundaries of

the flow. For stratified flows, the Richardson number, Ri, provides another criterion for the creation of turbulence:

$$Ri = \frac{\omega_B^2}{(\partial V_o/\partial z)^2} \tag{3.3a}$$

where

$$\omega_B^2 = \frac{(\gamma-1)g^2}{c^2} + \frac{g}{T}\frac{\partial T}{\partial z} \tag{3.3b}$$

ω_B is the Brunt-Vaisala frequency, V_o is the horizontal flow's mean velocity, z is perpendicular to the planes of stratified flow, λ is the ratio of the specific heats, g is the acceleration due to gravity, c is the speed of sound, and T is the temperature. The negative of the temperature gradient, $-\frac{\partial T}{\partial z}$, is known as the lapse rate. Note that for sufficiently high lapse rates the Brunt-Vaisala frequency becomes imaginary. The lapse rate at which $\omega_B = 0$ is known as the adiabatic lapse rate. An atmosphere in adiabatic equilibrium assumes this lapse rate. A lapse rate greater than the adiabatic lapse rate is termed a superadiabatic lapse rate. If Ri is less than unity the decay rate of turbulence is smaller than the generation rate. Under such conditions a turbulent flow is sustained (Hodges, 1967). However, Ri less than unity is not a sufficient condition for the creation of turbulence in a laminar flow. For this to occur Ri must fall below some critical value Ri_{cr}. Using theoretical arguments Miles (1961) and Howard (1961) propose a value of 1/4.

3.3 Sources of Turbulence in the Atmosphere

A number of mechanisms are believed responsible for the creation of atmospheric instabilities necessary for the generation of turbulence. Two important instabilities discussed here are the convective instability and the Kelvin-Helmholtz instability (KHI). Convective instability is produced by lapse rates greater than the adiabatic lapse rate. Such an inversion can

be produced by large amplitude gravity waves altering the background atmosphere. The KHI is produced in unstable wind sheers characterized by a Richardson number less than Ri_{cr}. This instability may also be induced in a stable wind shear by interaction of a gravity wave and a critical layer within the shear. A detailed theoretical treatment of the two instabilities is available in Chandrasekhar (1961). Measurements of the instabilities in the atmosphere are reviewed by Gossard and Yeh (1980).

Convective, or Rayleigh-Taylor, instabilities are the result of a vertical temperature gradient smaller than that of an adiabatic atmosphere. If a parcel of air at position z and temperature T(z) is displaced adiabatically and vertically by Δz it expands, acquiring a temperature $T(z) + \Gamma_a \Delta z$ where $\Gamma_a = -g/c_p$, g is the acceleration due to gravity at height z, and c_p is the specific heat of air at constant pressure. However, the ambient temperature at $z + \Delta z$ is $T(z + \Delta z)$. If this temperature is greater than $T(z) + \Gamma_a \Delta z$, then the parcel is cooler and hence heavier than the ambient air. The parcel tends to return to its initial position. Overshoot and subsequent oscillation of the parcel may lead to the excitation of a gravity wave. Conversely, if the ambient temperature is less than $T(z) + \Gamma_a \Delta z$, the parcel continues to rise. The convection of these parcels creates turbulent eddies as the parcels move through the ambient atmosphere.

Convective instability is more generally described as the result of an atmosphere in which ω_B^2 is negative. In such a situation ω_B is imaginary, and a displaced air parcel does not oscillate but continues to accelerate away from its initial position. A negative ω_B^2 also forces the Richardson number below zero. A negative Richardson number thus indicates convective instability. The Brunt-Vaisala frequency may be more conveniently defined in terms of potential temperature. The potential

temperature, θ, of an air parcel is that temperature the parcel would assume if adiabatically compressed or expanded to a pressure of 1000 mb.

$$\theta = T\left(\frac{1000}{P}\right)^{\frac{\gamma-1}{\gamma}}$$

where P, the pressure, is given in millibars. The Brunt-Vaisala frequency, in terms of potential temperature, is

$$\omega_B^2 = \frac{g}{\theta}\frac{\partial\theta}{\partial z}$$

The lapse rate at which $-\frac{\partial\theta}{\partial z} = 0$ is the adiabatic lapse rate. An atmosphere in adiabatic equilibrium has $\frac{\partial\theta}{\partial z} = 0$ for all z. Under such a condition a displaced air parcel neither oscillates nor accelerates. If $-\frac{\partial\theta}{\partial z}$ is greater than zero, a superadiabatic lapse, then ω_B^2 is negative. Thus the sign of the potential temperature gradient determines stability.

Such convective instabilities can result from gravity wave growth. As a gravity wave propagates upward its amplitude increases with decreasing density to preserve energy flux. The wave eventually reaches an altitude where the increased amplitude significantly modifies the background atmospheric parameters, producing regions of superadiabatic lapse rate. Hodges (1967) calculates the Richardson number as modified by a monochromatic gravity wave and finds negative values at periodic intervals for sufficiently large wave amplitudes. These planar regions of convective instability propagate with the wave, are normal to the direction of wave propagation, and occur at the minima of the wave's wind shear.

The KHI is produced in regions of high vertical shear in a horizontally stratified flow. If Ri falls below the critical value, it is energetically feasible for vertical perturbations to overcome the stabilizing effect of decreasing density with altitude. The perturbations grow and the vorticity

accumulates in billows forming a wave pattern. The billows continue to draw vorticity from the mean flow, eventually forming what are often referred to as cat's eyes. The growth of the cat's eyes from the billows is numerically simulated by Patniak et al. (1976). The eventual breakdown of the cat's eyes produces turbulence. Gossard et al. (1970), using a high resolution radar, show the development of KHI in the lower atmosphere and the resulting turbulence.

An initially stable flow can develop KHI through interaction of a gravity wave and a critical layer in the flow. A critical layer exists in a shear at that level where the flow's velocity equals the horizontal component of the incident gravity wave's phase velocity (Booker and Bretherton, 1967). The analysis of Booker and Bretherton (1967) models the interaction using a monochromatic wave incident upon an inviscid, adiabatic, Boussinesq fluid. The flow has an initial Richardson number everywhere greater than 1/4. Booker and Bretherton (1967) find that the gravity wave is strongly attenuated upon passing through a critical layer and that the wave's energy is deposited into the flow without loss through the generation of turbulence or other dissipative processes. Geller et al. (1975), using a similar model, show that the deposited energy modifies the flow such that regions of dynamic instability are produced. However, the model is incapable of showing the detailed initial development of the instability. Such a detailed simulation is described by Fritts (1978). Neither simulation can demonstrate the final turbulent breakdown of the Kelvin-Helmholtz instabilities.

3.4 Statistical and Spectral Approach

So far only a qualitative description of turbulence has been given. Due to the chaotic and three-dimensional nature of turbulence, a mathematical

treatment requires the use of random variables and statistical methods. Despite this statistical treatment the Navier-Stokes equations for fluids have no closed form solution, requiring the addition of observational and physical arguments. Such arguments are most easily applied to the power spectra of the velocity and advected scalars. Simpler spectra may be derived with various statistical assumptions. This section shows the development of these spectra and the restrictions on their use.

As with the kinetic theory of gases, turbulence requires a statistical approach. Although the motion of a fluid in a turbulent velocity field is in theory a classically deterministic process, the amount of information required to treat it as such makes a deterministic approach wholly impractical. The statistical treatment essentially examines a quantity's fluctuation about a mean and the spatial dependence of averages of those fluctuations. The quantity might be a velocity component, a temperature, or the density of an advected scalar in a velocity field. For example, the i'th velocity component $V_i(\underset{\sim}{x},t)$ and a scalar's density $N(\underset{\sim}{x},t)$ can be decomposed into a mean and a fluctuation:

$$V_i(\underset{\sim}{x},t) = U_i(\underset{\sim}{x},t) + u_i(\underset{\sim}{x},t) \qquad (3.4a)$$

$$N(\underset{\sim}{x},t) = \overline{N}(\underset{\sim}{x},t) + n(\underset{\sim}{x},t) \qquad (3.4b)$$

where

$$U_i(\underset{\sim}{x},t) = \langle V_i(\underset{\sim}{x},t)\rangle$$

$$\overline{N}(\underset{\sim}{x},t) = \langle N(\underset{\sim}{x},t)\rangle$$

and $\langle\ \rangle$ denotes an ensemble average. The calculated averages of most interest are the covariances of the fluctuations. These may be written as

$$\langle u_i(\underset{\sim}{x},t)u_j(\underset{\sim}{x}',t)\rangle \qquad (3.5a)$$

$$\langle n(\underset{\sim}{x},t)n(\underset{\sim}{x}',t)\rangle \qquad (3.5b)$$

To make practical measurements of the covariances some assumptions must be made. First, a moving probe (e.g., rocket borne Langmuir probe) is often used to measure scalar density along a path. Due to the finite velocity of the probe the turbulent field evolves during the time of the measurement. To make meaningful spatial covariances the turbulence must be assumed to be "frozen" during this time. For example, a rocket travelling at 1 km/sec traverses a turbulent layer 1 km thick in 1 second. Radar measurements (Rottger et al., 1979) indicate that turbulent layers have lifetimes on the order of minutes. The frozen-in assumption is hence quite applicable to rocket measurements of such layers. A second assumption, ergodicity, must be made from a practical point of view. This allows for replacement of the ensemble averages by spatial or time averages. In the rocket experiment described above, spatial averages are used. As a different example, measurements of wind turbulence using a fixed, ground based hot wire anemometer would replace the ensemble average by a time average.

Under the conditions of statistical homogeneity and statistical isotropy the covariances may be simplified. Statistical homogeneity, hereafter referred to as just homogeneity, implies that the probability density of the fluctuations is not a function of position. In addition, the averages $\langle V_i \rangle$ and $\langle N \rangle$ do not depend on position. Under this condition $\langle u_i(\underset{\sim}{x},t)u_j(\underset{\sim}{x}'t) \rangle$ can only be a function of $\underset{\sim}{r} = \underset{\sim}{x}' - \underset{\sim}{x}$. Due to the inherent inhomogeneity of the large energy producing scales, such an assumption can only approximate an actual flow (Batchelor, 1953), and the less restrictive, more realistic, assumption of local homogeneity is necessary. Under this condition homogeneity is restricted to small-scale variations. The covariance $\langle u_i(\underset{\sim}{x},t)u_j(\underset{\sim}{x}',t) \rangle$ is then independent of position only for small $\underset{\sim}{r}$. Statistical isotropy, a refinement of

statistical homogeneity (Kolmogorov, 1941), implies that there is no preferred direction in the velocity or scalar field. As with homogeneity, the qualifier "statistical" is implied. It is quite conceivable that a field be homogeneous yet anisotropic. For example, a field may have a homogeneous preference for u_i components over u_j components, thus representing a homogeneous anisotropic field. Isotropy, like homogeneity, is most realistically applied at small scales. This condition is called local isotropy. When both isotropy and homogeneity hold, the covariances of u_i and n depend only on $|\underset{\sim}{x} - \underset{\sim}{x}'|$. Kolmogorov (1941) claims that for flows with high Reynolds number a wide gap in k-space exists between the large and small eddies. Under such conditions Kolmogorov hypothesizes local isotropy for the smaller scales. Tennekes and Lumley (1972) make a similar claim by examining the interdependence of different sized eddies. They find that although the strain rate field of a large eddy induces anisotropy in passing energy to a small eddy, at sufficiently small scales the anisotropy is temporary, and the small eddy's mean state is isotropic.

Fluid flows may be described by the Navier-Stokes equations:

$$\frac{\partial \underset{\sim}{V}}{\partial t} + (\underset{\sim}{V}\cdot\nabla)\underset{\sim}{V} = -\frac{1}{\rho}\nabla P + \nu\nabla^2\underset{\sim}{V} \qquad (3.6a)$$

$$\nabla\cdot\underset{\sim}{V} = 0 \qquad (3.6b)$$

where V is the velocity field, P is the pressure, and ρ is the fluid density. Equation (3.6b) states that the fluid is incompressible. As mentioned earlier, turbulent flows must be described statistically. Decomposing V_i and P into $U_i + u_i$ and $\overline{P} + p$ evaluated at $\underset{\sim}{x}$ and t, assuming the tensor summation notation, and applying the incompressibility condition gives

$$\frac{\partial (U_i+u_i)}{\partial t} + \frac{\partial (U_i+u_i)(U_j+u_j)}{\partial x_j} = -\frac{1}{\rho}\frac{\partial (\overline{P}+p)}{\partial x_i} + \nu\frac{\partial^2 (U_i+u_i)}{\partial x_j \partial x_j}$$

Multiplying by $u_q(\underset{\sim}{x}',t)$ and averaging gives an equation in terms of $\langle u_q(\underset{\sim}{x}',t)u_i(\underset{\sim}{x},t)\rangle$, $\langle u_q(\underset{\sim}{x}'t)u_i(\underset{\sim}{x},t)u_j(\underset{\sim}{x},t)\rangle$, and other terms. Attempting to solve for the triple correlation using the Navier-Stokes equations leads to an equation involving a fourfold correlation. This continued predicament is referred to as the closure problem. Various statistical assumptions may be made to allow for an approximate numerical solution. Some of these methods are reviewed by Tatsumi et al. (1978). Hill and Bowhill (1976) point out that even under isotropy and homogeneity the equations only reduce to a single equation involving two unknowns: the double and triple correlations. It should also be noted that the diffusion equation

$$\frac{\partial N}{\partial t} + \underset{\sim}{V}\cdot\underset{\sim}{\nabla}N = D\underset{\sim}{\nabla}^2 N$$

is coupled to the Navier-Stokes equations, resulting in a closure problem for scalar turbulence also.

It is often physically enlightening to take the spatial Fourier transform of the covariances. The resulting spectrum facilitates comparison of the energy at various scales. The following spectral formulae are taken from Hill and Bowhill (1976). The three-dimensional velocity fluctuation power spectrum, assuming homogeneity, is given by the Fourier transform of the covariance:

$$\frac{1}{(2\pi)^3}\iiint \langle u(\underset{\sim}{x},t)\cdot u(\underset{\sim}{x}+\underset{\sim}{r},t)\rangle \exp(-i\underset{\sim}{k}\cdot\underset{\sim}{r})\, d\underset{\sim}{r}$$

Physically, this gives the strength of a velocity fluctuation at the wave vector k. Since $|\underset{\sim}{k}| = 2\pi/\lambda$ the spectrum also is a measure of fluctuations with scale size λ. This spectrum can be averaged over all directions to give the three-dimensional energy spectrum, commonly referred to as just the energy spectrum:

$$E(k,t) = \frac{1}{2}\iint k^2\, d\Omega_k \iiint \frac{1}{(2\pi)^3} \langle u(\underset{\sim}{x},t)\cdot u(\underset{\sim}{x}+\underset{\sim}{r},t)\rangle \exp(-i\underset{\sim}{k}\cdot\underset{\sim}{r})\, d\underset{\sim}{r} \tag{3.7}$$

where $d\Omega_k$ is the solid angle in k space and $k = |\underset{\sim}{k}|$. The factor of 1/2 normalizes the spectrum such that E(k,t) integrated over all k gives (1/2) $\langle \underset{\sim}{u}\cdot\underset{\sim}{u}\rangle$, called the turbulent kinetic energy. For a given magnitude k, E(k,t) gives the average energy per unit mass per unit wave number. An analogous three-dimensional spectrum also may be constructed for scalar quantities. Assuming homogeneity, the three-dimensional scalar power spectrum and its spatial average, the scalar spectrum, can be written as

$$S(\underset{\sim}{k},t) = \iiint \frac{d\underset{\sim}{r}}{(2\pi)^3} \langle n(\underset{\sim}{x},t)n(\underset{\sim}{x}+\underset{\sim}{r},t)\rangle \exp(-i\underset{\sim}{k}\cdot\underset{\sim}{r}) \tag{3.8a}$$

$$\Gamma(k,t) = \iint k^2\, d\Omega_k \iiint \frac{1}{(2\pi)^3} \langle n(\underset{\sim}{x},t)n(\underset{\sim}{x}+\underset{\sim}{r},t)\rangle \exp(-i\underset{\sim}{k}\cdot\underset{\sim}{r})\, d\underset{\sim}{r} \tag{3.8b}$$

Like the velocity energy spectrum, $\Gamma(k,t)$ is an average over all directions of k. $\Gamma(k,t)$ is normalized so that

$$\langle n^2\rangle = \int_0^\infty \Gamma(k,t)\, dk$$

Physically, $\Gamma(k,t)$ gives the strength of the scalar magnitude's fluctuation at a given wave number, whereas S(k,t) gives the same for a particular wave vector. The units of $\Gamma(k,t)$ are mean squared density per unit wave number. The two types of spectra, three-dimensional scalar power spectrum and its spatial average, the scalar spectrum, serve different functions in studying turbulence. The three-dimensional scalar power spectrum plays a major role in the theory of coherent scatter of radiation from atmospheric turbulence. The scalar spectrum is for the most part a theoretical tool for describing spectral energy in a field. Yet a third spectrum is needed to interpret in situ experimental data.

Many in situ measurements of turbulence are made in only one dimension with a rapidly moving probe. The turbulent field's spatial variation may be derived from the probe's temporal signal and speed relative to the field. However, for a measured variation of k_1, wave vectors $\underset{\sim}{k}$ with $|\underset{\sim}{k}| > k_1$ and $\underset{\sim}{k}$ not parallel to the probe's path alias as k_1 variations. One-dimensional spectra are defined as follows:

$$\Phi(k_1,t) = \frac{1}{\pi}\int_{-\infty}^{\infty} dx_1 \langle u_x(x,y,z,t)u_x(x+x_1,y,z,t)\rangle \exp(-ik_1x_1)$$

or

$$\Phi(k_1,t) = \left| \frac{1}{\pi}\int_{-\infty}^{\infty} dx_1\ u_x(x+x_1,y,z,t)\ \exp(-ik_1x_1) \right|^2 \tag{3.9a}$$

for the x velocity component and

$$\Psi(k_1,t) = \frac{1}{\pi}\int_{-\infty}^{\infty} dx_1 \langle n(x,y,z,t)n(x+x_1,y,z,t)\rangle \exp(-ik_1x_1)$$

or

$$\Psi(k_1,t) = \left| \frac{1}{\pi}\int_{-\infty}^{\infty} dx_1\ n(x+x_1,y,z,t)\ \exp(-ik_1x_1) \right|^2 \tag{3.9b}$$

for the scalar spectrum. The second forms of equations (3.9a) and (3.9b) are usually chosen for computational ease. In the isotropic case these are related to the energy spectra by

$$\Phi(k_1,t) = \int_{k_1}^{\infty} \frac{E(k,t)}{k}\ (1 - k_1^2/k^2)\ dk \tag{3.10a}$$

$$\Psi(k_1,t) = \int_{k_1}^{\infty} \frac{\Gamma(k,t)}{k}\ dk \tag{3.10b}$$

Ψ is the k space sum of $\Gamma(k,t)$ over all $k > k_1$. To obtain $\Psi(k_1,t)$ each $\Gamma(k,t)$ value is weighted by the ratio of the wave vectors from k to k + dk contributing to the aliasing and the total number of wave vectors ending on a sphere of radius k. The energy relationship, equation (3.10a), is given

by Hill and Bowhill (1976). The above equations are valid only under isotropy. Consequently if the turbulent field is locally isotropic only for $k_1 > k_1'$, then the equations apply only to that range. It should be noted that for $\Gamma(k,t)$ or $E(k,t)$ proportional to a power of k, the related one-dimensional spectrum has the same charateristic power law. If such a power law is limited to a particular range of k, then the observed break points in the one-dimensional spectrum differ from those in the energy spectrum. Figure 3.1 compares a scalar spectrum and its corresponding one-dimensional spectrum calculated from equation (3.10b).

Under the restrictions of homogeneity and isotropy, the Navier-Stokes equations yield the following for $E(k,t)$ and $\Gamma(k,t)$ (Hinze 1975):

$$\frac{\partial E(k,t)}{\partial t} = T_u(k,t) = -2\nu k^2 E(k,t) \qquad (3.11)$$

$$\frac{\partial \Gamma(k,t)}{\partial t} - T(k,t) = -2Dk^2 \Gamma(k,t) \qquad (3.12)$$

where $T_u(k)$ and $T(k)$ are called the spectral transfer functions. $T_u(k)$ has the units energy per unit mass per unit wave number per unit time and represents the loss of energy by viscous dissipation at a scale size k. Metaphorically, it is the leakage in the energy cascade described in Section 3.2. $T(k)$ has the units of mean squared scalar fluctuation per unit wave number per unit time. It too represents dissipation of spectral content at a wave number of size k. Two important parameters may be defined from the spectra $\Gamma(k,t)$ and $E(k,t)$. These are the energy dissipation rate and the mean squared scalar dissipation rate χ:

$$\chi = 2D \int_0^\infty k^2 \Gamma(k,t) dk$$

$$\varepsilon = 2\nu \int_0^\infty k^2 E(k,t) dk$$

ε measures the rate at which kinetic energy is dissipated by viscosity.

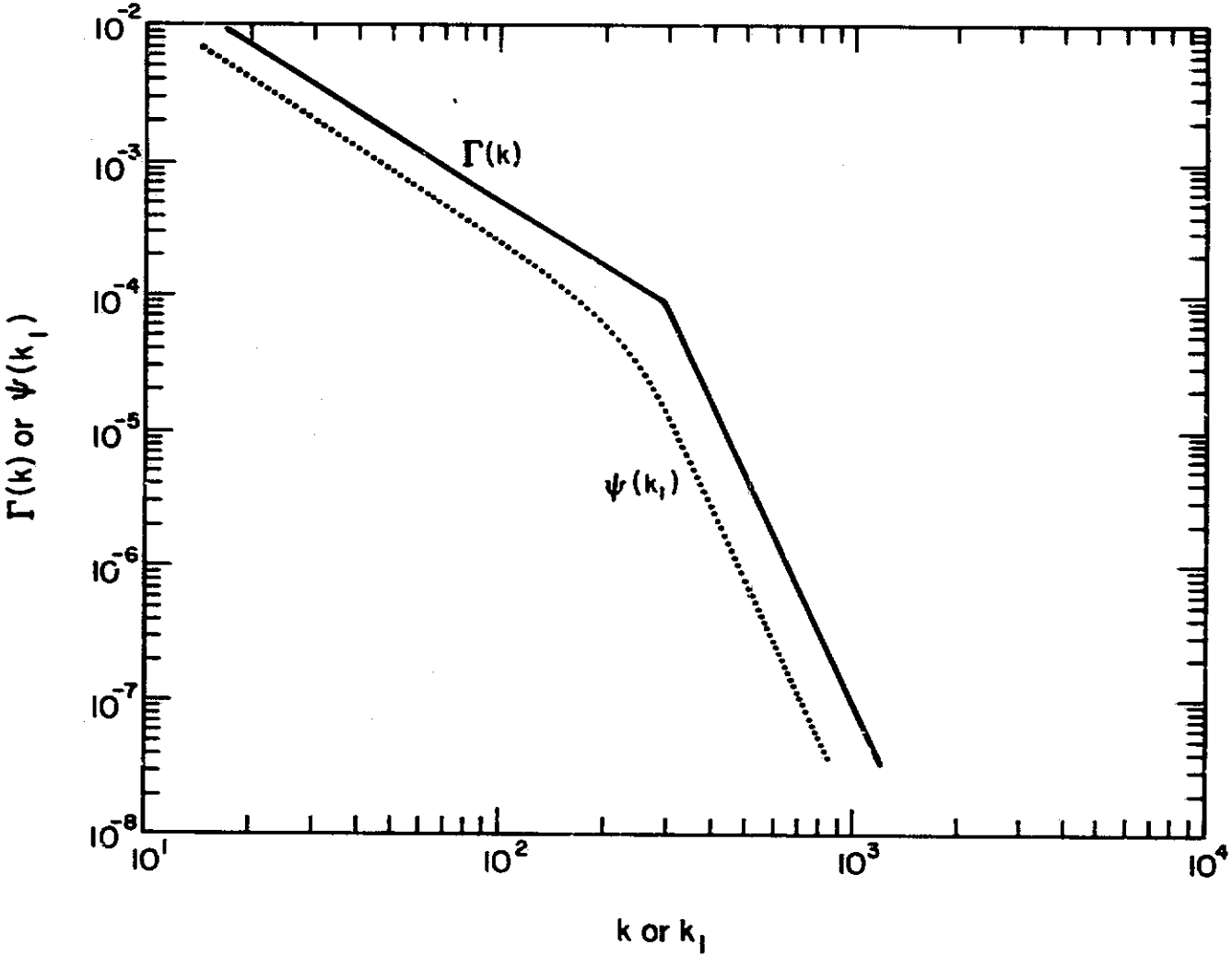

Figure 3.1 Comparison of a scalar spectrum $\Gamma(k)$ and its calculated one-dimensional spectrum $\Psi(k_1)$.

Similarly, χ measures the rate at which mean squared fluctuations are dissipated by molecular diffusion. These quantities aid in the dimensional analysis of the turbulence spectrum.

3.5 Dimensional Analysis and Turbulence Spectra

Applying local homogeneity and isotropy, dimensional and similarity arguments leads to a power law form of the energy and scalar spectra in the inertial range. The range over which this dependence applies is derived in a similar fashion. Spectra derived by Batchelor (1959) and Batchelor et al. (1959) for wave numbers above the inertial range are also presented here. Models of a scalar flux function, defined from the spectral transfer function T(k), are examined and lead to refinements of the simple power law spectra.

In addition to local isotropy and homogeneity Kolmogorov (1941) introduced a third concept: local similarity. Under local similarity, if there is a large wave number range between the scale sizes at which the turbulence is created and the scale sizes at which viscosity becomes important, then the spectrum for large k is independent of the detailed morphology of the large scales at which energy is drawn from the mean flow. Such a wide range of scales is present in flows with high Reynolds number (Kolmogorov 1941). Due to this independence turbulence produced by different sources in different media is found to be comparable at scales where local similarity holds. The comparison is subject only to certain parameters of the fluid and the flow. For example, a knowledge of these similarity parameters allows for comparison between turbulence generated in the ocean and turbulence generated in the atmosphere although the media, energy sources, and scales are quite different. Local similarity is obeyed under local statistical equilibrium (Batchelor, 1953). This requires that

the time evolution at small scales proceed much more rapidly than at large scales. Equilibrium is established at small scales with negligible influence by the large-scale evolution. Small-scale structures may then be studied in general without considering the detailed time evolution at the large scales or the particular method of the turbulence's generation.

Before deriving the various spectra, a few characteristic wave numbers need to be defined. As mentioned previously, turbulent energy cascades from larger scales to smaller scales, the scales being divisible into three regimes with respect to their methods of energy transfer. The concept of an inertial range may be extended to scalar fluctuations. The analogous regime is called the convective range: scalar fluctuations therein are not dissipated by diffusion. Similarly, the diffusive range is analogous to the viscous range. k_d, called the inner scale or Kolmogorov scale, is a measure of the wave number at which viscosity begins to significantly damp the velocity fluctuations. k_d identifies the boundary between the inertial and viscous ranges. k_b, sometimes called the Batchelor wave number, defines a scale beyond which diffusion damps out the scalar concentration fluctuations which are already subject to viscous damping. k_c, referred to as the Obukhov-Corrsin wave number, defines a scale beyond which diffusion effects are important in the absence of viscous damping.

$$k_d = (\varepsilon/\nu^3)^{1/4} \tag{3.13a}$$

$$k_b = (\varepsilon/\nu D^2)^{1/4} \tag{3.13b}$$

$$k_c = (\varepsilon/D^3)^{1/4} \tag{3.13c}$$

Batchelor (1959) shows that k_c applies only when $D \gg \nu$ and that k_b applies when $\nu \gg D$. It should be noted that scalar fluctuations may persist for wave numbers beyond k_d when $\nu \gg D$. In that case $k_b \gg k_d$.

Assuming similarity, isotropy, and homogeneity to apply locally,

Kolmogorov (1941) hypothesized that the structure of turbulence should depend only on the similarity parameters ε and ν. Using dimensional analysis Tennekes and Lumley (1972) find that

$$E(k) = \varepsilon^m \nu^n f(k/k_d)$$

where m and n are constants, $f(k/k_d)$ is a nondimensional function, and k_d depends only on ε and ν. Given the units for ν, ε, and E(k) the only possible choice for m and n is 1/4 and 5/4, respectively. This equation implies that for all flows $E(k)/(\varepsilon\nu^5)^{1/4}$ should yield the same dimensionless curve $f(k/k_d)$ at scales subject to homogeneity, isotropy, and similarity. Kolmogorov (1941) further argued that in the inertial range viscosity is unimportant. E(k) then depends only on ε. This condition requires that $f(k/k_d)$ cancel out the $\nu^{5/4}$ constant in front, leading to the energy spectrum

$$E(k) = \alpha\varepsilon^{2/3}k^{-5/3} \qquad k \ll k_d$$

where α is a nondimensional constant called the Kolmogorov constant. $k \ll k_d$ is a reminder that this spectrum applies only for k for which viscosity is unimportant. It should also be noted that the above development assumes locally a steady state turbulence field, eliminating the t dependence from E(k,t).

By similar methods Boston and Burling (1972) use the similarity parameters χ, ν, ε, and D to find the form for the scalar spectrum:

$$\Gamma(k) = \chi\varepsilon^{-3/4}\nu^{5/4}\psi(\nu/D, k/k_d)$$

where $\psi(\nu/D, k/k_d)$ is a dimensionless function. An inertial range may be found by disallowing effects of ν and D.

$$\Gamma(k) = \beta\chi\varepsilon^{-1/3}k^{-5/3} \qquad k \ll \text{smaller of } k_d \text{ and } k_c$$

where β is a dimensionless constant.

The shape of the scalar spectrum beyond the inertial range has been

studied by Batchelor (1959) and Batchelor et al. (1959). The relation between D and ν affects not only the cutoff wave numbers k_d, k_b, and k_c but also the spectral shape and slope. For $D \ll \nu$ the scalar fluctuations can occur at wave numbers beyond k_d in spite of the loss of kinetic energy through viscous damping. Batchelor (1959) shows that this leads to a scalar spectrum

$$\Gamma(k) = -\chi\sigma^{-1}k^{-1}\exp(Dk^2/\sigma) \qquad (3.14)$$

where σ is an average strain rate estimated by Batchelor (1959) to be

$$\sigma = -.5(\varepsilon/\nu)^{1/2} \qquad (3.15)$$

The argument of the exponent in equation (3.14) then becomes $-2(k/k_b)$. Thus for $k_d \ll k \ll k_b$ the scalar spectrum varies as k^{-1}. This range is termed the viscous-convective range since viscosity dominates the energy spectrum and diffusion is unimportant in the scalar spectrum. The range $k > k_b$ is called the viscous-diffusive range since both viscosity and diffusion affect the spectra. In the case $D \gg \nu$ Batchelor et al. (1959) predict

$$\Gamma(k) = (1/3)\,\alpha\,\chi\,\varepsilon^{2/3}D^{-3}k^{-17/3} \qquad k_c \ll k \ll k_d.$$

This range is called the inertial-diffusive range since the scalar fluctuations are damped but viscosity has little effect. The upper k range where both viscosity and diffusion become important is called the viscous-diffusive range just as in the $D \ll \nu$ case. These ranges are illustrated in Figure 3.2. The middle spectrum gives a hypothetical energy spectrum. The expected scalar spectra for $\nu \gg D$ and $\nu \ll D$ are shown above and below the energy spectrum. For $D \gg \nu$ the viscous-diffusive range is not shown. This range is not considered by Batchelor et al. (1959). Due to the very steep slope in the inertial-diffusive range extremely low values of $\Gamma(k)$ are expected in the viscous-diffusive range. Relevant measurements and studies are not abundant. In the case $D \approx \nu$ the viscous and diffusive

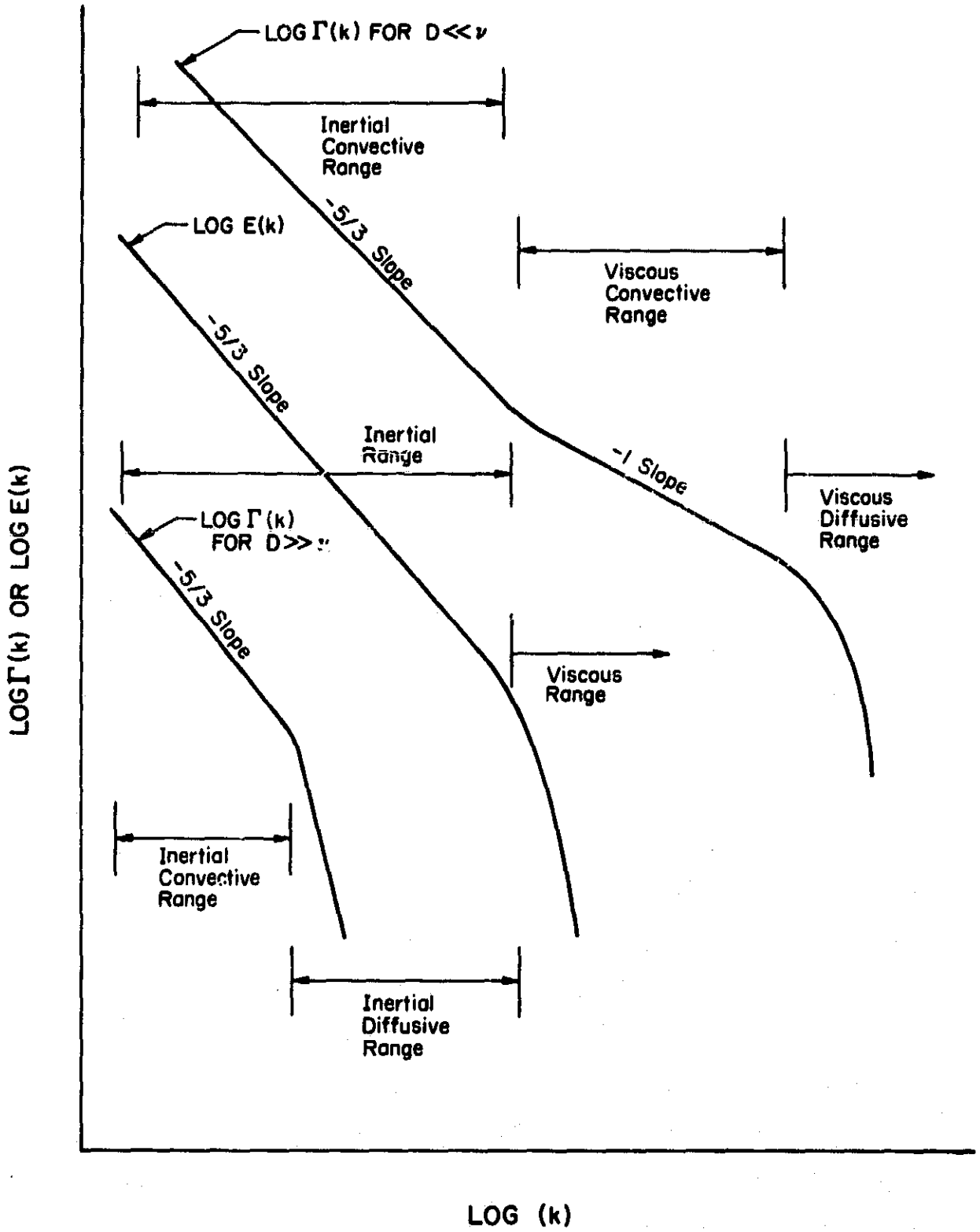

Figure 3.2 Energy and scalar spectra illustrating the various wave number ranges (Hill and Bowhill, 1976).

effects occur at approximately the same wave number. This situation is not addressed by Batchelor (1959) or Batchelor et al. (1959). Its discussion here is deferred until the presentation of the model by Hill and Bowhill (1976) in Section 3.6.

As an alternative to directly estimating $\Gamma(k)$, the spectra may be derived by modelling T(k) and working from the steady state equation (3.12). Models of T(k) leading to scalar spectra are extensively reviewed in Hill and Bowhill (1976). Three of the models are presented here. To model T(k), the spectral flux function F(k) needs to be developed.

$$-\frac{\partial F(k)}{\partial k} = T(k) \qquad (3.16)$$

Physically, F(k) describes the rate of the spectral energy cascade through a scale size with wave number k. Its units are mean squared scalar per unit time. In the inertial range the flux should be approximately constant and equal to χ. Since viscosity is unimportant, T(k) should be quite small. T(k) should increase considerably in the diffusive regime.

Using results for spectral flux from Corrsin (1964), Pao (1964) shows that

$$\Gamma(k) \propto k^{-5/3} \exp[(-3/2\ell)(k/k_c)^{4/3}] \qquad k << k_d \qquad (3.17a)$$

$$\Gamma(k) \propto k^{-1} \exp[(-D/\ell'\sigma)k^2] \qquad k >> k_d \qquad (3.17b)$$

where ℓ and ℓ' are nondimensional constants and σ is the strain rate given by equation (3.15). If $\nu >> D$ and ℓ is assumed to be of the order of unity, then $k_c >> k_d$, making the exponential term in equation (3.17a) close to unity for $k << k_d$. This results in the familiar -5/3 power law for the inertial range. For $\ell' = -1$ equation (3.17b) is of the same form as Batchelor's, equation (3.14), predicting an exponential decrease with k above k_b. If, however, $D >> \nu$ then equation (3.17a) predicts a rapid decrease in

in $\Gamma(k)$ for $k << k_c$. This decrease with k is steeper than the -17/3 power law predicted by Batchelor.

For high Pr or Sc in the viscous-convective and viscous-diffusive ranges a model by Kraichnan (1968) predicts the scalar flux function to be

$$F(k) = \frac{\Lambda}{15} k^4 \frac{\partial}{\partial k} [k^{-2} \Gamma(k)]$$

where Λ is independent of wave number but increases with Reynolds number. Assuming a steady state in equation (3.12) gives (Mjolsness, 1975)

$$\Gamma(k) = 5(\chi/\Lambda)k^{-1}(1+Z)\exp(-Z)$$

where

$$Z = (30D/\Lambda)^{1/2} k$$

Mjolsness (1975) also derives the corresponding one-dimensional spectrum

$$\Psi(k_1) = 5(\chi/\Lambda)\, k_1^{-1} \exp(-Z_1)$$

If $Z << 1$ the scalar spectrum is approximately

$$\Gamma(k) \propto k^{-1}$$

the dependence found by Batchelor (1959) in equation (3.14). For large k, Z also becomes large, causing an exponential decrease in the spectrum.

Hill and Bowhill (1976) also analyze a model by Howells (1960) which is applicable for all Pr and Sc. They find that the proportionality

$$\Gamma(k) \propto k^{-5/3} [C + C'(\frac{k}{k_c})^{-8/3}]$$

holds in the inertial-convective range with C and C′ constants. C′ is taken to be small since the spectrum should approach a -5/3 power law for $k << k_d$ as k becomes small although still in the inertial range. The viscous-convective and viscous-diffusive range spectra agree with the form of Batchelor's, equation (3.14). For $D >> \nu$ the model predicts an inertial-diffusive spectrum of the same form as equation (3.17a).

In summary, all models agree on the -5/3 power law for k well inside the inertial range. For $\nu >> D$ most models predict a scalar spectrum proportional to k^{-1} for $k_d << k << k_b$. The models differ substantially for the inertial-diffusive range ($D << \nu$), Batchelor et al. (1959) predicting a power law and other models predicting an exponential decrease above k_c. None make solid claims to the spectral behavior for $D \approx \nu$. This is unfortunate as such conditions are found in the middle atmosphere.

3.6 Estimation of Spectral Form in the Middle Atmosphere Using a Model by Hill and Bowhill (1976)

The scalar spectrum models given so far say little about the spectrum between ranges and apply only for the asymptotic cases of $\nu >> D$ and $\nu << D$. Hill and Bowhill (1976) have devised a spectral model, based on Corrsin (1964) and Pao's (1964) results for F(k) to describe the spectrum for all spectral ranges and all values of Sc and Pr. This section presents Hill and Bowhill's (1976) model with some clarifications added by Hill (1978). A spectral shape for middle atmospheric turbulence, based on estimates of Sc for those altitudes, is also predicted.

The Corrsin-Pao model determines the scalar spectrum by modelling the scalar flux as (Corrsin, 1964):

$$F(k) = s(k)\ \Gamma(k)$$

where s(k), called the flux rate, is estimated by Pao (1964) to be

$$s(k) = \ell\, \varepsilon^{1/3} k^{5/3} \qquad k << k_d \qquad (3.18a)$$

$$s(k) = \ell' \sigma k \qquad k >> k_d\ . \qquad (3.18b)$$

This applies to both the cases $D >> \nu$ and $\nu >> D$ (Pao, 1964). Pao describes s(k) physically as the rate that a spectral element is tranferred across k. Since $\Gamma(k)$ is a measure of spectral content at k the product of $\Gamma(k)$ and

$s(k)$ is dimensionally the spectral flux $F(k)$, as Corrsin's hypothesis states. Hill and Bowhill (1976) hypothesize that the flux rate dependence on k varies from 5/3 to 1 in the k range close to k_d. The scalar spectrum then also has a smooth transition. A characteristic wave number k* located between the inertial-convective and viscous-convective ranges may be defined:

$$\left.\frac{\partial\, \ln[\Gamma(k)]}{\partial\, [\ln(k)]}\right|_{k = k^*} = -\frac{4}{3} \qquad \text{for } \nu >> D$$

Although the corresponding one-dimensional scalar spectrum has a shape similar to the three-dimensional scalar spectrum, it is found that $k_1^* < k^*$ where k_1^* is the transitional wave number for the corresponding one-dimensional spectrum. To form $s(k)$, and subsequently $\Gamma(k)$, Hill and Bowhill (1976) form a nondimensional wave number expression,

$$K = \ln(k/k^*) \tag{3.19}$$

and create a parameter

$$\phi(K) = -4/3 + 1/3 \tanh(aK) \tag{3.20}$$

which varies from -5/3 to -1 over the range of all k. The value of a determines the rate at which $\phi(K)$ changes from -5/3 to -1. $s(k)$ is then proposed to be

$$s(k) = s(k_0) \exp\left[-\int_{K_o}^{K} \phi(y)dy\right]$$

where k_0 is the lowest wave number in the inertial-convective range. To find $\Gamma(k)$, $F(k)$ is formed by multiplying $s(k)$ and $\Gamma(k)$ and substituting into the steady state version of equation (3.12), giving a differential equation for $\Gamma(k)$. Taking k_0 to approach zero, Hill and Bowhill (1976) find the solution to be

$$\Gamma(k) = \chi\beta\varepsilon^{-1/3}\,(k^*)^{-5/3}\,\tilde{\Gamma}(K)$$

where $\tilde{\Gamma}(K)$ is given by

$$\ln[\tilde{\Gamma}(K)] = -\frac{4}{3}K + \frac{1}{3a}\ln[2\cosh(aK)] - \xi\int_{-\infty}^{K} e^{5y/3}[2\cosh(ay)]^{1/3a}\,dy$$

$$\xi = 2\beta(k^*/k_c)^{4/3}$$

k^*/k_d and a are assumed constant over all ν/D (Hill, 1978). The model makes no assumptions about D's relation to ν. Although k^* is defined above for $D \ll \nu$, Hill (1978) points out that for $D \gg \nu$, k^* represents the transition wave number between the inertial-diffusive and the viscous-diffusive range. Figure 3.3 shows the calculated normalized one-dimensional spectra as a function of k_1/k^* for various values of the parameter ξ where symbols with subscript 1 are associated with the corresponding one-dimensional spectrum $\tilde{\Psi}(K_1)$.

It is of interest to estimate the type of spectra the above model predicts for middle atmospheric parameters. Since only a general shape is desired, the important parameter to estimate is ξ. Many experiments have made measurements of the constant β_1. Experiments reviewed by Hill and Bowhill (1976) give a range centered about 0.6. They estimate that $\beta = 5\beta_1/3$, making β of the order of unity. Values of k_c and k_d vary with altitude. Three parameters are necessary to compute k_c and k_d: ν, ε, and D. As an example, at 80 km D is 1.0×10^4 cm^2/sec (Heicklen, 1976), and ν is 7.15×10^{-1} m^2/sec (U.S. Standard Atmosphere, 1976). Since ν is so close to D (i.e., $Sc \approx 1$), k_d and k_c are quite close together. k^*, the transition wave number between the inertial- and viscous-diffusive ranges is between these two numbers, making k^*/k_c close to unity. Thus ξ is of the order of unity, independent of ε. Referring to Figure 3.3 it is observed that Hill's model predicts neither a well-defined inertial-diffusive or

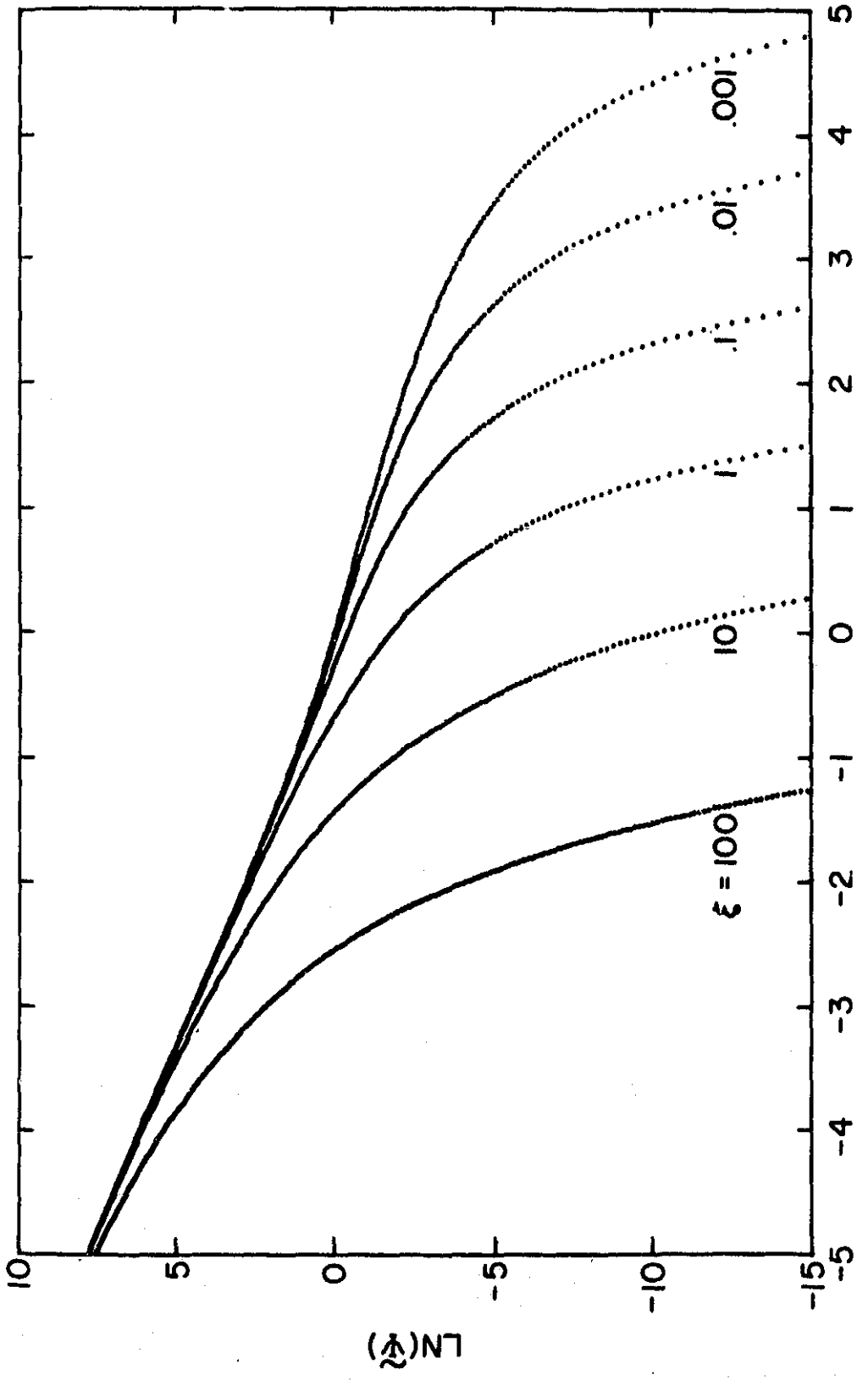

Figure 3.3 One-dimensional spectra for various values of the parameter ξ (Hill and Bowhill, 1976).

viscous-convective range. The slope of the spectrum should be -5/3 up until a rolloff at the characteristic k value of k_d or k_c, whichever is smaller. Comparisons to actual data from the University of Illinois rockets are given in Chapter 5.

4. FINE STRUCTURE EXPERIMENT AND METHODS OF DATA ANALYSIS

4.1 Introduction

To measure the spectrum of electron density irregularities in the D region a Langmuir probe is mounted on a sounding rocket and flown through the ionosphere. The fine structure experiment flown by the University of Illinois is described by Klaus and Smith (1978). All flights have carried this same configuration, with two exceptions described in Roth (1982b). In the fine structure experiment the probe current, assumed proportional to the electron density over regions of constant electron temperature, is measured as a function of time. Rapid current fluctuations superposed upon the relatively slowly varying mean current are sometimes observed. Signal processing on board the rocket converts these current fluctuations to $\Delta N_e / \langle N_e \rangle$ where ΔN_e is the fluctuation in electron density about a mean value $\langle N_e \rangle$. This signal is then telemetered to ground and recorded on an FM tape recorder. Analog preprocessing of these data helps to distinguish possible ionospheric irregularities from interference caused by other experiments on board the rocket.

Once suitable regions of interest have been established, the analog data are digitized for further processing. The digitizer consists of an 8-bit A/D peripheral card controlled by an Apple II microcomputer. The data are digitized at a 5 kHz rate and stored on floppy disk. Each data file contains 25000 bytes, or 5 seconds of data. These data are then transferred to a CDC Cyber mainframe computer. After additional formatting the data are segmented and Fourier analyzed with a FORTRAN program called SPECTRA. This program estimates the power spectrum of a data segment by calculating the square magnitude of the discrete Fourier transform (DFT) of the segment.

It should be emphasized that these spectra represent a one-dimensional spatial spectrum, where isotropy is assumed in converting the temporal variations to spatial variations. The theories of turbulence described in Chapter 3 are concerned with three-dimensional spectra, and theoretical one-dimensional spectra are derived therefrom only under the assumption of isotropy. Since no independent measure of isotropy is usually made during the rocket experiments, spectra calculated in this chapter cannot be directly compared with the theoretical one-dimensional spectra; they can at most demonstrate consistency with theory.

Section 4.2 describes the University of Illinois fine structure experiment. Section 4.3 discusses three possible sources of noise and distortion. An analog preprocessing method is presented in Section 4.4. Section 4.5 discusses the digitizing of the analog data. Section 4.6 describes postprocessing on a mainframe computer.

4.2 Fine Structure Experiment

The fine structure experiment carried out by the University of Illinois uses essentially the same instrumentation as described by Klaus and Smith (1978). A Langmuir probe is extended from the rocket body into the ionosphere and held at 4.05 V above the potential of the rocket body. The probe may be either a single electrode at the rocket nose or a pair of electrodes in parallel extended from the sides of the rocket. As the rocket passes through the ionosphere, spatial fluctuations in electron concentration are observed as current fluctuations in time. The mean current is usually in the range of 10^{-8} to 10^{-5} A in the D region. A plot of current versus height for the 28 May 1975 Peru flight is shown in Figure 4.1. The current is processed by a logarithmic electrometer and an ac amplifier to give the percentage fluctuation in electron density,

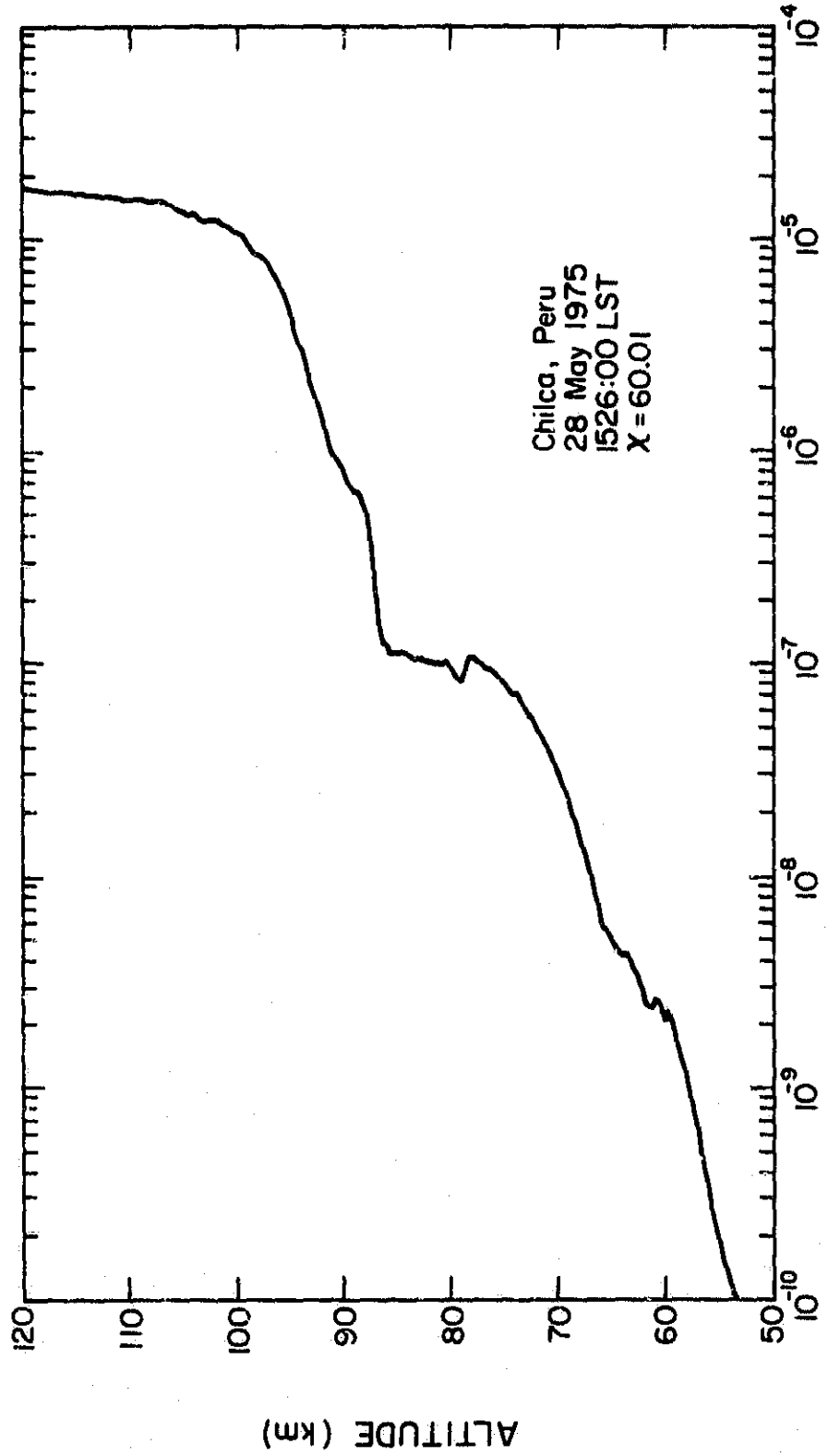

Figure 4.1 Probe current from 28 May 1975 Peru flight.

$\Delta N_e/\langle N_e \rangle$, as a function of time. This signal, along with data from other experiments on the rocket, is telemetered to the ground and stored on an FM tape recorder.

A block diagram of the system is shown in Figure 4.2. For fine structure measurements the sweep generator is held constant at 4.05 V, the sweep mode being activated to collect electron temperature data. The log electrometer produces a voltage proportional to the logarithm of the input current. Its output is 0.80 V per decade of probe current. Klaus and Smith (1978) investigate the frequency response of the logarithmic electrometer and find that it acts as a low pass filter. The upper 3 dB point is determined by measuring the rise time of the output in response to a current input consisting of a square wave superposed on a dc current. At an input dc current of 10^{-8} A and a square wave adjusted to produce a 50 mV output swing, Klaus and Smith (1978) find the upper 3 dB frequency to be 2.5 kHz. Furthermore, Zimmerman and Smith (1980) find that the 3 dB frequency increases with an increasing dc current component. Since currents greater than 10^{-8} A are expected in the D region (Figure 4.1), the frequency response of the electrometer should extend at least up to 2.5 kHz. The output of the electrometer is fed to an ac amplifier. This has a measured upper 3 dB frequency of at least 1 kHz and a gain of 100. Frequency response measurments vary between devices. Measurements of three amplifiers are presented in Appendix I. In addition, the amplifier has a single pole roll-off below 50 Hz, ensuring that the amplifier is not saturated by low frequency noise expected at the spin frequency of the rocket (4 to 8 Hz).

To predict the output of this system it is assumed that the input current, I, may be decomposed into a mean and a fluctuating component:

$$I = \langle I \rangle + \Delta I$$

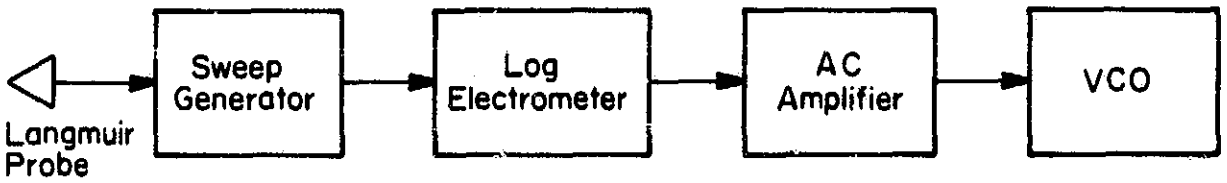

Figure 4.2 Block diagram of dc probe and fine structure experiment. Sweep generator is held at 4.05 V for electron density fine structure measurements (Klaus and Smith, 1978).

where < > represents a time average. This current is assumed proportional to the electron density as described in Chapter 2. The electrometer output, V_{LE}, is

$$V_{LE} = 0.80 \log (\langle I \rangle + \Delta I) .$$

Conversion to the natural logarithm allows expansion of V_{LE} to

$$V_{LE} = 0.80 \frac{\ln (\langle I \rangle)}{\ln 10} + 0.80 \frac{\ln (1 + \Delta I/\langle I \rangle)}{\ln 10}$$

If the fluctuations in current are small compared to the mean current, then the output may be approximated by

$$V_{LE} = 0.80 \frac{\ln (\langle I \rangle)}{\ln 10} + \frac{0.80}{\ln 10} \frac{\Delta I}{\langle I \rangle} \qquad (4.1)$$

The constant component of V_{LE} disappears due to the ac coupling of the ac amplifier following the logarithmic electrometer:

$$V_{AC} = 100 \frac{0.80}{\ln 10} \frac{\Delta I}{\langle I \rangle} \qquad (4.2)$$

where V_{AC} is the ac amplifier output. Since current and electron density are assumed to be proportional, this is equivalent to $35\ \Delta N_e/\langle N_e \rangle$, a 0.35 V deviation for a 1.0 % deviation in electron density.

The data signal on the rocket is telemetered to the ground and stored on analog tape. Following the ac amplifier the $\Delta N_e/\langle N_e \rangle$ signal is centered about zero volts. This is stepped up to 2.5 V to conform to the 0 to 5 V input swing allowed by the voltage controlled oscillator (VCO) of the telemetry system. In the IRIG FM telemetry system employed by the University of Illinois the VCO output frequency varies by $\pm$ 7.5 % for a $\pm$ 2.5 V input. The modulation index is 5. Each experiment on the rocket is assigned an IRIG channel. As an example, Table 4.1 gives the IRIG channel assignment for each experiment on the 28 May 1975 Peru flight. The

Table 4.1 IRIG telemetry channel assignments for 28 May 1975 Peru flight.

Channel Number	Center Frequency* (kHz)	Information Bandwidth** (Hz)	Signal
19	93	1395	RF probe, output
18	70	1050	Tip probe, fine structure
17	52.5	790	Receiver #1, modulation
16	40	600	Receiver #2, modulation
15	30	450	Tip probe, log output
14	22	330	Boom probe, log output
13	14.5	220	Boom probe, linear output
12	10.5	160	RF probe, monitor
11	7.35	110	Receiver #1, AGC
10	5.4	81	Receiver #2, AGC
9	3.9	59	Magnetometer

*deviation = ±7.5%
**modulation index = 5

channel assignment depends on the desired bandwidth. Channel 18 is usually selected for the fine structure experiment, giving a bandwidth of 1050 Hz. The various channels are combined and transmitted to ground on a 240.2 MHz carrier. The telemetry ground station strips off the 240.2 MHz carrier and records the raw FM signal (containing all channels) on one track of an FM tape recorder. This track is usually called the "combiner" track. In addition to this data signal the ground station simultaneously records a number of other signals on different tracks. To aid in the digitization of the data a 100 kHz reference signal is recorded on a separate track. Another track, called the "station multiplex" (labelled MUX), contains two time codes for absolute determination of elapsed time on the tape, a voice record of the flight progress, and miscellaneous data from instruments monitoring the telemetry signal.

4.3 Sources of Noise and Distortion

There are a number of noise sources which must be identified to properly analyze the data. A periodic modulation of the fine structure signal at the rocket spin frequency is often observed. Axial spin provides stability for the rocket. The spin frequency, nearly constant throughout a particular flight, is generally from 4 to 8 Hz. This is most accurately measured by an on board magnetometer measuring the component of the earth's magnetic field along the axis of the magnetometer. The strength and character of the effect on the fine structure signal varies from rocket to rocket, and even during the same flight the effect slowly changes with time. Figure 4.3 shows a segment of data exhibiting severe spin contamination. The most probable source of this noise is the passing of the Langmuir probe through the rarefied wake of the rocket. This is borne out in the observation that spin noise shows up strongly in flights using boom probes

as opposed to nose tip probes. Figure 4.3 exhibits a spin frequency of 3.984 Hz from a rocket equipped with boom probes. The existence of two oscillations every spin period is consistent with the suggestion that the booms are passing through the wake of the rocket: in one revolution each of the two booms passes through the wake once. It is assumed that this spin noise is an added component to the fine structure signal. Modelling the noise as band limited and consisting only of harmonics of the spin frequency opens the possibility of filtering out the spin noise.

A second source of noise is the distortion added by the logarithmic electrometer. In the analysis leading to equations (4.1) and (4.2) it is assumed that $\Delta N_e/\langle N_e \rangle \ll 1$. Smith and Royrvik (1985) discusses the generation of harmonics by the electrometer for a sinusoidal input. He finds that the strength of each harmonic falls off rapidly as the order of the harmonic increases. The signal expected from the probe contains a large range of frequencies. If the power spectrum obeys a power law, k^{-n}, and has a large spectral index, -n, then harmonics from the lower frequencies could be comparable to the strength of the spectrum at high frequencies. This would lead to overestimation of the spectrum at high frequencies. Smith and Royrvik (1985) concludes that for a power spectral index of -7 or greater the distortion is negligible. Spectra with smaller spectral indices are not expected from the fine structure experiment. However, spectra with exponential decreases as described in Section 3.5 could indeed be affected by this distortion. Fortunately, most of the information extracted from the spectra resides in the wave number ranges below the exponential decrease. Efforts to obtain information from the higher frequency ranges of a steeply sloping spectrum must not overlook the possibility of distortion.

A third source of noise is interference from other experiments on board

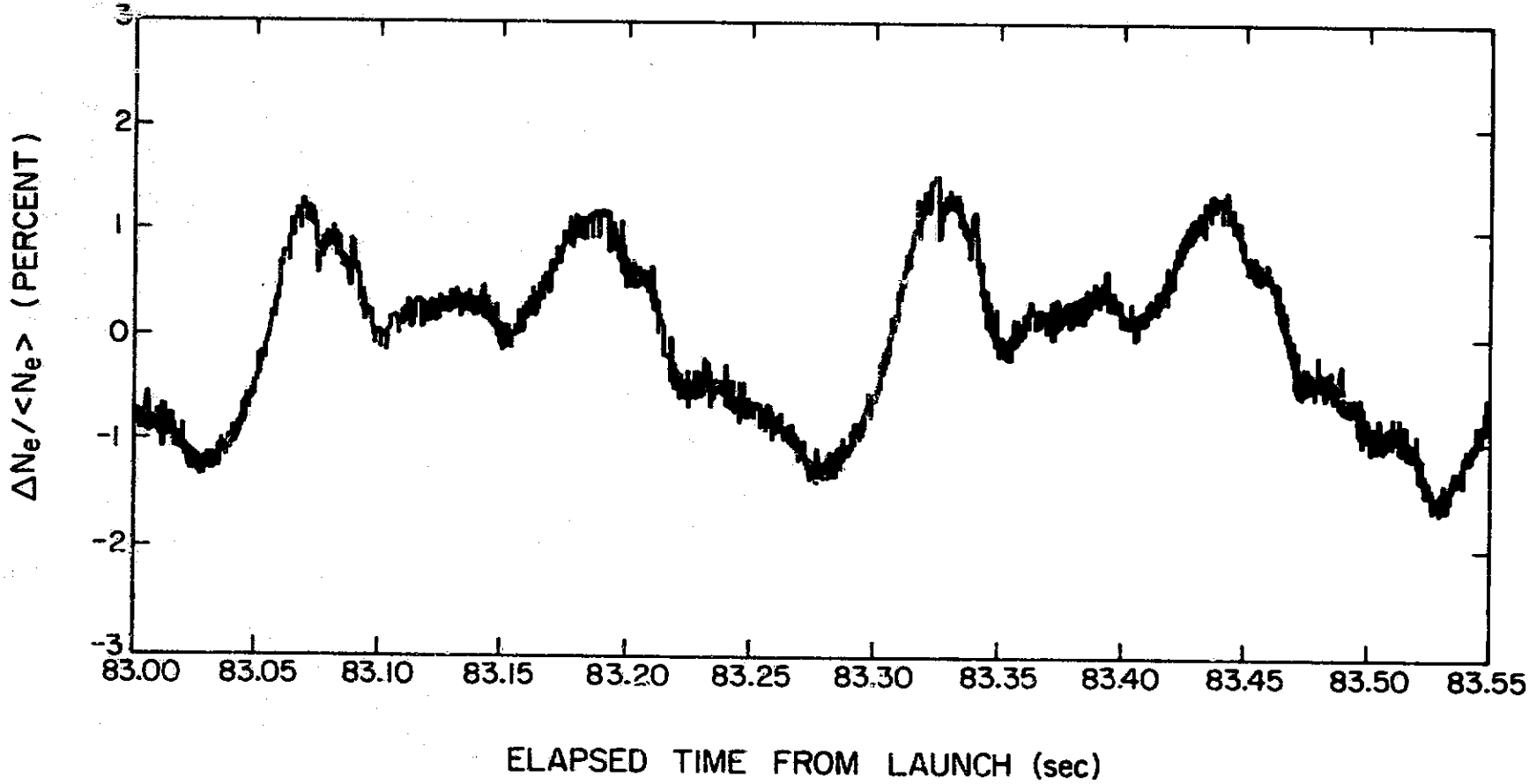

Figure 4.3 Spin contamination of fine structure signal from 18 January 1976 Wallops Island flight at 81.0 km. Launch time is 14 12 (LST).

the rocket. The fine structure experiment is especially susceptible to voltage transients that temporarily change the potential between the rocket body and probe. Other probe experiments on the rocket which use the rocket body as an electrode can generate such transients. Transients can also be generated by mechanical vibrations of the rocket. As an example, Table 4.2 gives various events during a flight that could lead to electrical noise. Door ejection and boom erection refer to the insertion of the boom-mounted Langmuir probes into the ionosphere. These events are quite violent and vibrations can persist for about a second. An aural replay of the fine structure signal exhibits surprisingly distinct metallic vibrations corresponding to these events. Fortunately, the noise from these various sources of interference is easily identified, and although it is much stronger than the first two sources of noise described, its transient nature only causes isolated data dropouts as opposed to persistent contamination of the signal.

4.4 Analog Preprocessing

An analog processing method developed by Klaus and Smith (1978) allows for easy identification of irregularities and a rough estimation of their spectra. The basic purpose of the system is to plot in various frequency bands the rms amplitude of the fine structure signal as a function of time. A block diagram is shown in Figure 4.4. The FM tape recorder plays back the combiner track, and the tunable discriminator decodes the desired channel. The 100 kHz reference signal is passed through a discriminator with a center frequency at 100 kHz. Tape speed fluctuations cause fluctuations in both the data signal and the recorded reference signal. The 100 kHz discriminator produces a voltage proportional to the tape speed fluctuation. Adding this difference signal to the discriminator output prevents

Table 4.2 Flight log from 28 May Peru flight.

Nike Apache 14.532

Site : Chilca Peru

Date : 28 May 1975 (Day 148)

Launch Time : 20 26 Universal Time (nominal)

15 26 Local Standard Time

20 25 : 59.7 (actual)

Second Stage Ignition	20 26 : 19.5 UT
40 kft Baroswitch	20 26 : 21.0 UT
70 kft Baroswitch	20 26 : 27.0 UT
Door Ejection (61 km)	20 26 : 50.6 UT
Boom Erection (62 km)	20 26 : 51.1 UT
Probe Sweep On (128 km)	20 27 : 41.1 UT
70 kft Baroswitch Off	20 32 : 50.1 UT
40 kft Baroswitch Off	20 32 : 54.5 UT
Loss of Signal (Splash)	20 33 : 07.7 UT

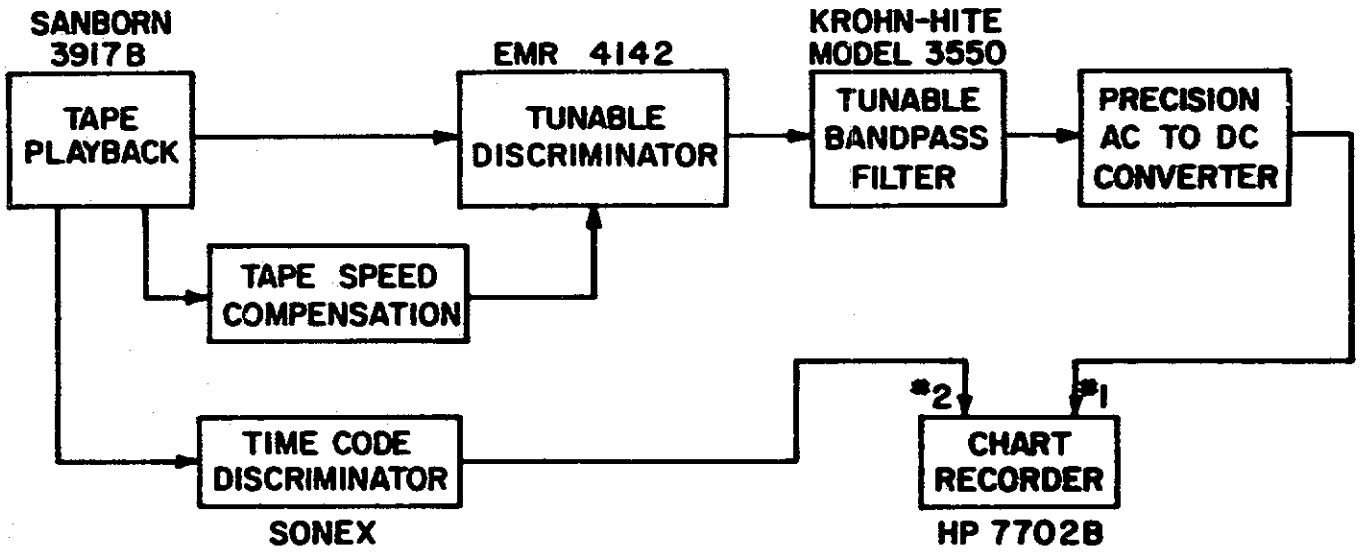

Figure 4.4 Analog data reduction system (Klaus and Smith, 1978).

fluctuations in tape speed from distorting the amplitude. The delay of the 100 kHz discriminator is matched by a 75 μsec delay added to the data line, preserving synchronicity between the tape speed compensation and data signals. Due to the FM nature of the tape, jitter in the tape speed causes jitter in both amplitude and phase of the output. The phase jitter is uncorrectable by analog means and must simply be tolerated as a source of noise. The compensated signal is then fed to a bandpass filter. The frequency bandwidths are chosen to increase geometrically (e.g., 10-20 Hz, 20-40 Hz, 40-80 Hz, etc.). This gives spectral content at evenly spaced points on a logarithmic scale. The bandpass filtered signal is fed to an ac-to-dc converter and the resulting rms voltage is recorded on a chart recorder. A time code is simultaneously plotted. The result is a plot such as that in Figure 4.5, from the 28 May 1975 Peru flight. The frequency bands are converted to wave number bands by multiplying the frequencies by $2\pi/v$ where v is the rocket speed.

This plot gives a broad view of the data, allowing for quick comparisons between structures at different altitudes. The regularly spaced spikes seen clearly in the 0.18 - 0.36 rad/m band result from another probe measuring plasma resonance. The spike at 70.3 km is attributed to interference from an unknown source. Magnification of the raw fine structure data at 70.3 km is shown in Figure 4.6. A similar extraordinarily large signal swing occurs at 84.8 km. The apparent extended bandwidth of this spike observed in Figure 4.5 arises from clipping of the signal. Since the 28 May 1975 Peru flight is an equatorial flight the beginning of the electrojet is visible at 90 km. The regions of most interest are the altitudes between 75 and 80 km and the irregularity at 87.5 km. Once the regions of interest have been identified from this broad overview, detailed

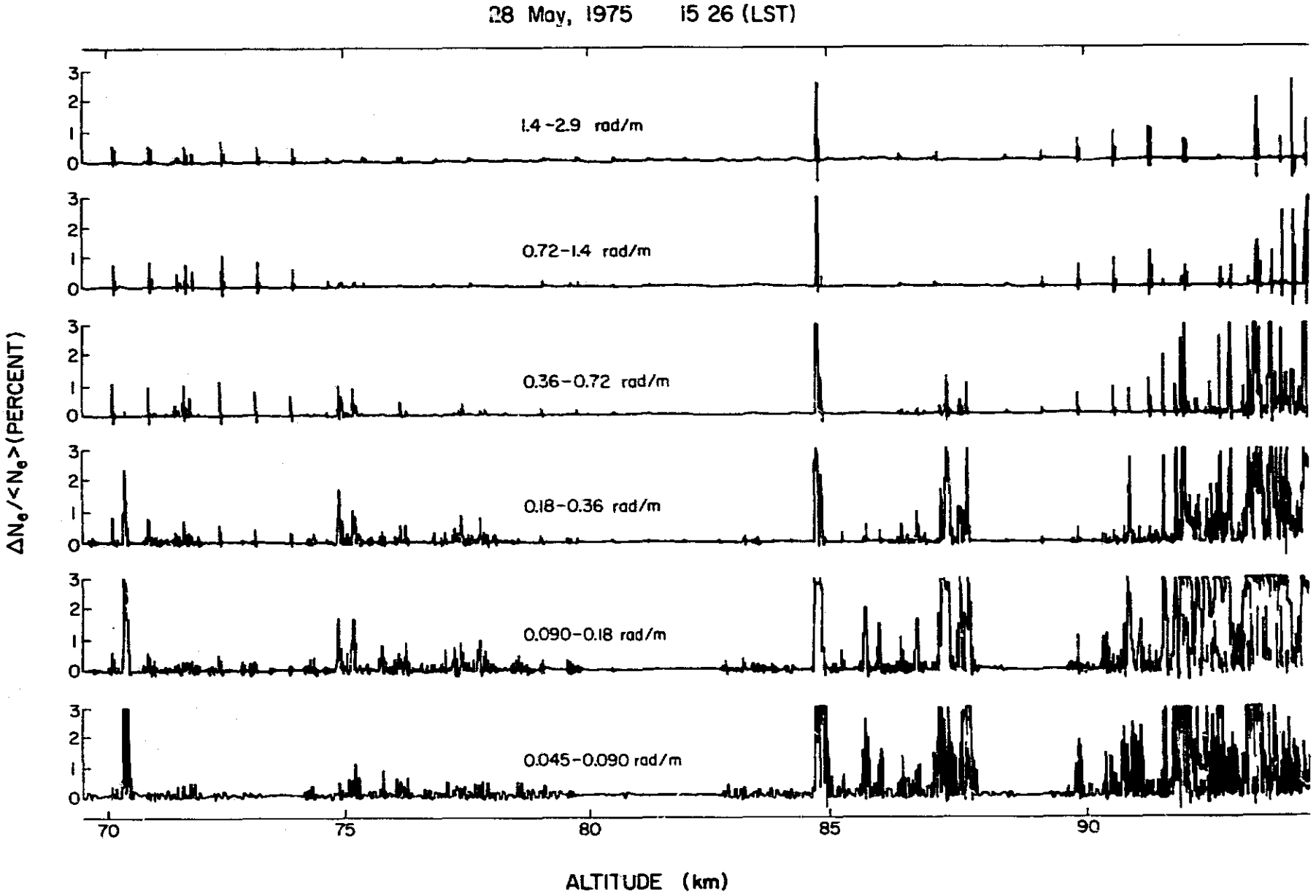

Figure 4.5 Fine structure signal filtered into wave number bands.

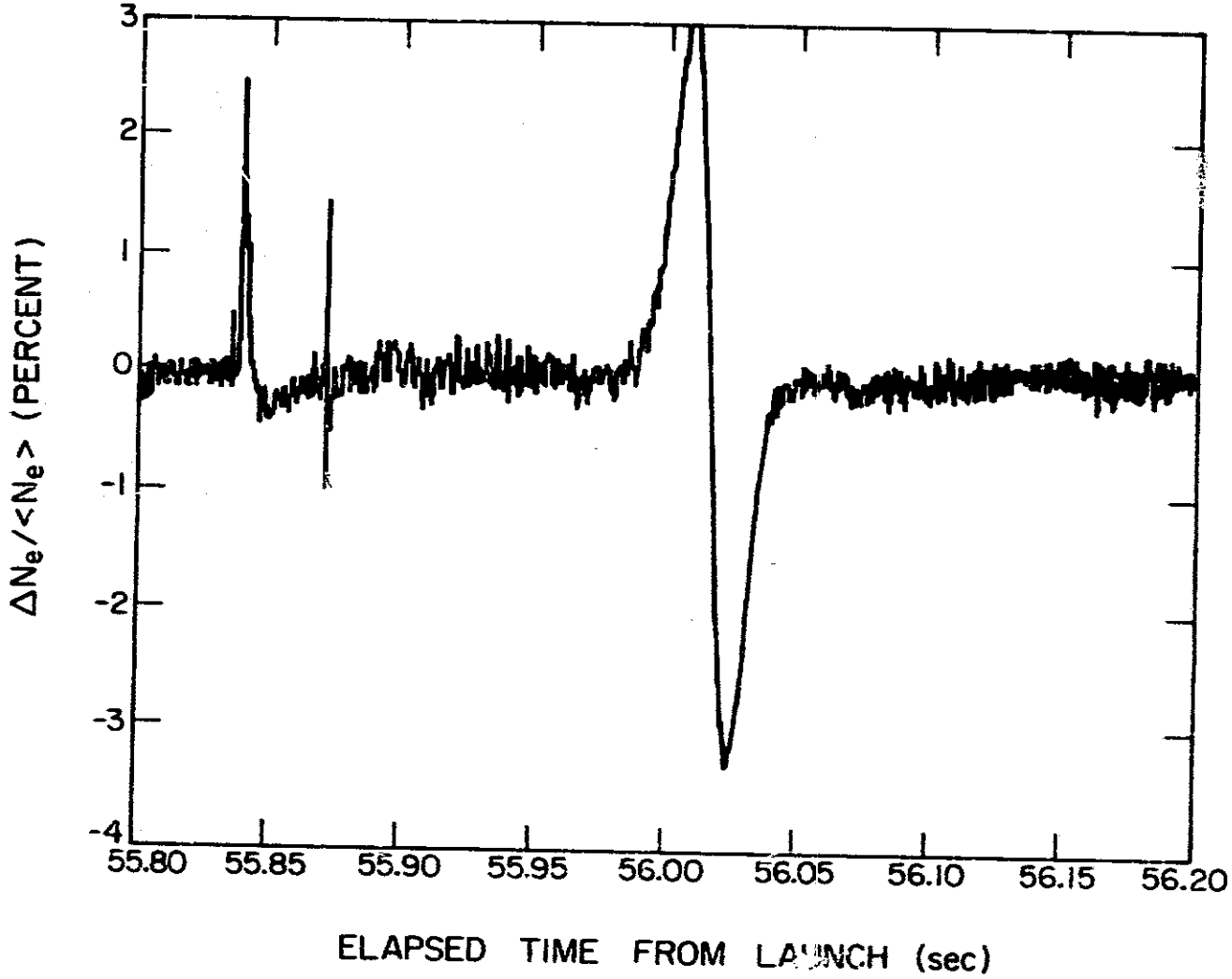

Figure 4.6 Portion of fine structure signal from 28 May 1975 Peru flight at 69.6 km. Launch time is 15 26 (LST).

inspection may begin at the proper altitudes.

4.5 Digitizer

To perform further analysis the analog data must be digitized. Prior to the development of the present digitizer system all digitization was carried out at the NASA facility at Wallops Island, Virginia. Since the turnaround time for the digitization varied from weeks to months, a digitizer system based on an Apple II microcomputer was developed at the University of Illinois capable of an 8-bit resolution, a digitizing rate of 5 kHz, and a continuous record size of 25 kilobytes. This system solves a number of problems with the old system. The Wallops Island system returns a digitial tape in a format compatible with a PDP computer. To use these data on the CDC mainframe this tape must be converted to CDC format with a conversion program (McInerney and Smith, 1984). The program is quite lengthy and complicated, requiring the user to have a fair degree of familiarity with the CDC Cyber tape system at the University of Illinois. To obtain data from the converted tapes, another Cyber program must be run to control the mounting and playback of the tapes. The data generated are in a rather bulky format, making disk storage expensive.

In the new system the turnaround time for digitization is of the order of days, and the data are stored conveniently on floppy disks rather than on tapes. The data are transferred to the Cyber via a telephone modem. Essentially, the new system shifts control of the data to the user, avoiding complications and delays. Familiarity with the analog tape system is necessary to the extent needed for the analog processing described in Section 4.3. It is not suggested that the new system is suitable for all applications; it is most efficient when handling small amounts of data. The time overhead needed for the old system can pay off in studies requiring

large quantities of continuous data. In smaller projects this overhead may dominate the expended effort, making the microcomputer system a more attractive choice.

A block diagram of the digitizer system is shown in Figure 4.7. The recorder plays back the FM combiner tr ck, the 100 kHz reference, and the two time codes. The EMR tunable discriminator selects the appropriate data channel and corrects for tape speed fluctuations as described in Section 4.4. In addition, the discriminator has a built-in low pass filter necessary for reducing the cross talk from adjacent data channels. As suggested by Table 4.1, this filter is set to 1050 Hz for IRIG channel 18. The tape speed compensated data are sent to the A/D card for processing by the Apple computer. To assist in sampling data at regular intervals with respect to the tape, the 100 kHz reference signal is converted to a logic signal by a phase locked loop circuit. The Apple repeatedly counts a fixed number of these logic pulses and takes a sample, resulting in a constant sampling rate.

Use of the Apple internal clock for timing is avoided for a number of reasons. First, fluctuations in tape speed would cause the data to be sampled at irregular intervals with respect to the tape time frame. The 100 kHz reference exhibits the same fluctuations as the tape, providing a clock synchronized to the data. Second, the Apple 1.023 MHz clock is not regular: every 65th μsec an approximately 140 nsec delay is added for videoscreen control. Continuing with Figure 4.7, to ensure that the digitization starts at a precise time, a 1 pulse per second (1 pps) clock signal is obtained from the Datum time decoder, giving a positive transition exactly on the second. This transition is used to trigger the digitization at a precise and reproducible instant.

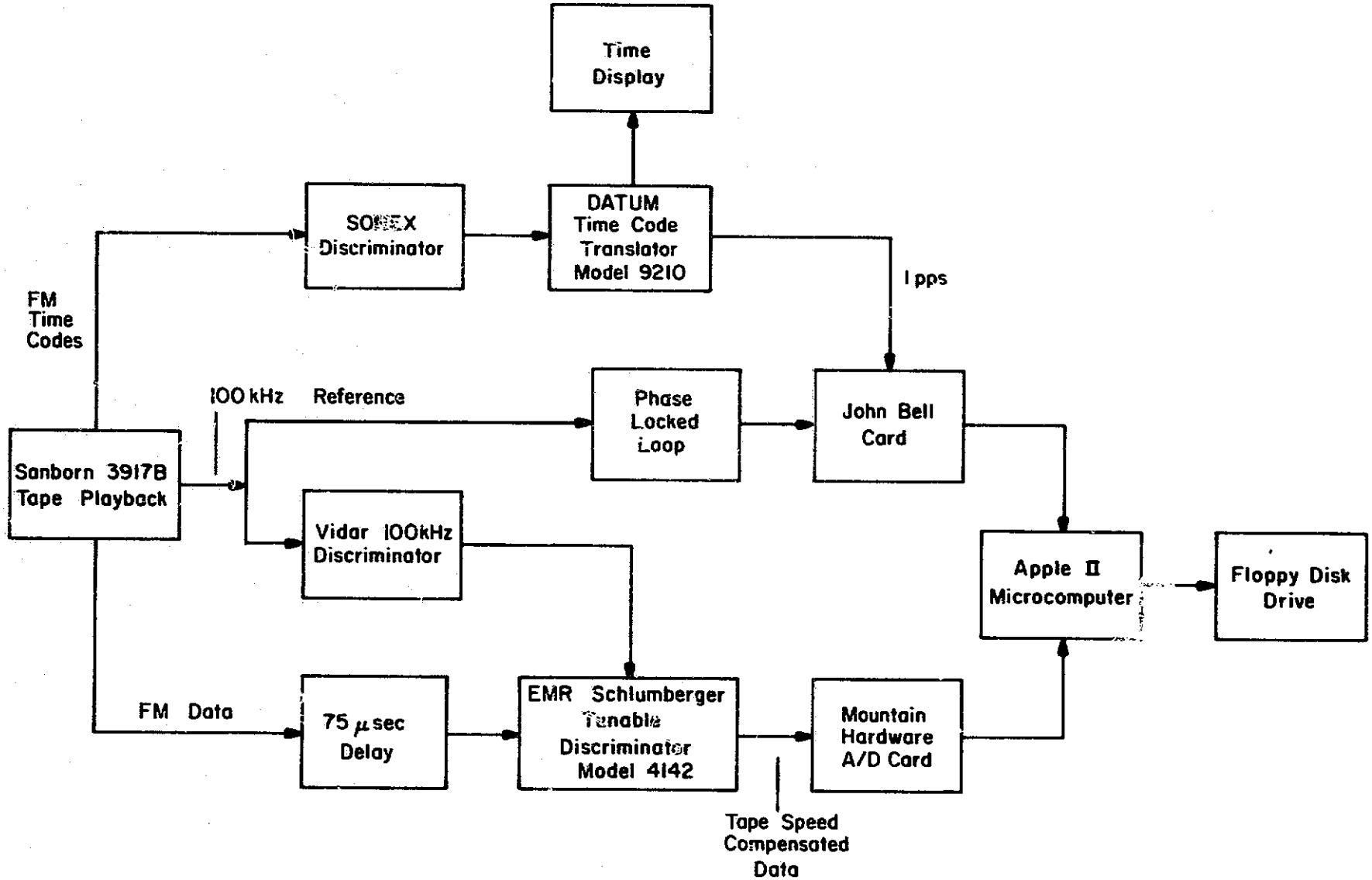

Figure 4.7 Digitizer system.

The A/D card is made by Mountain Computer and is capable of taking a sample every 9 μsec. The card can sample data on any one of 16 input channels. The input lines are bundled in a standard 26 wire ribbon cable. To minimize high frequency noise on this unshielded cable, the cable is wrapped in copper tape. The analog to digital converter on the card accepts an input in the range -5 to 5 V, converting this to a digital value in the range 0 to 255. The -5 to 5 V range is not adjustable, so any scaling of the input must take place external to the card. Software controlling the card is straightforward. Each of the 16 inputs is treated as a memory location in the Apple peripheral card I/O space (addresses $C080 - $C0FF). If the card is in slot S, channel X may be read from address $C080 + S * $10 + X. Each time the address is queried the card begins another sample. Two read commands are thus required to take a valid sample: one to start sampling and one to load the result into the Apple.

Interfacing of the timing signals to the Apple is performed by a 6522 Versatile Interface Adapter (VIA) on a peripheral card made by John Bell Engineering. A system diagram of the VIA is shown in Figure 4.8. The card occupies 16 bytes of address space in the Apple II peripheral card ROM space ($C100 - $C7FF). The various functions on the 6522 can request servicing from the Apple by setting a bit in the interrupt flag register (IFR). Each bit in the IFR has a corresponding bit in the interrupt enable register (IER). Preconfigured high, this corresponding bit enables a set bit in the IFR to pull the Apple $\overline{\text{IRQ}}$ line low, initiating an interrupt.

The first timing signal required by the digitizer is a trigger to begin taking data. This is derived from the 1 pps signal from the time decoder, attached to line CA1 of the VIA. By configuring the peripheral control register (PCR) bit 0 high any positive transition on CA1 sets IFR bit 1.

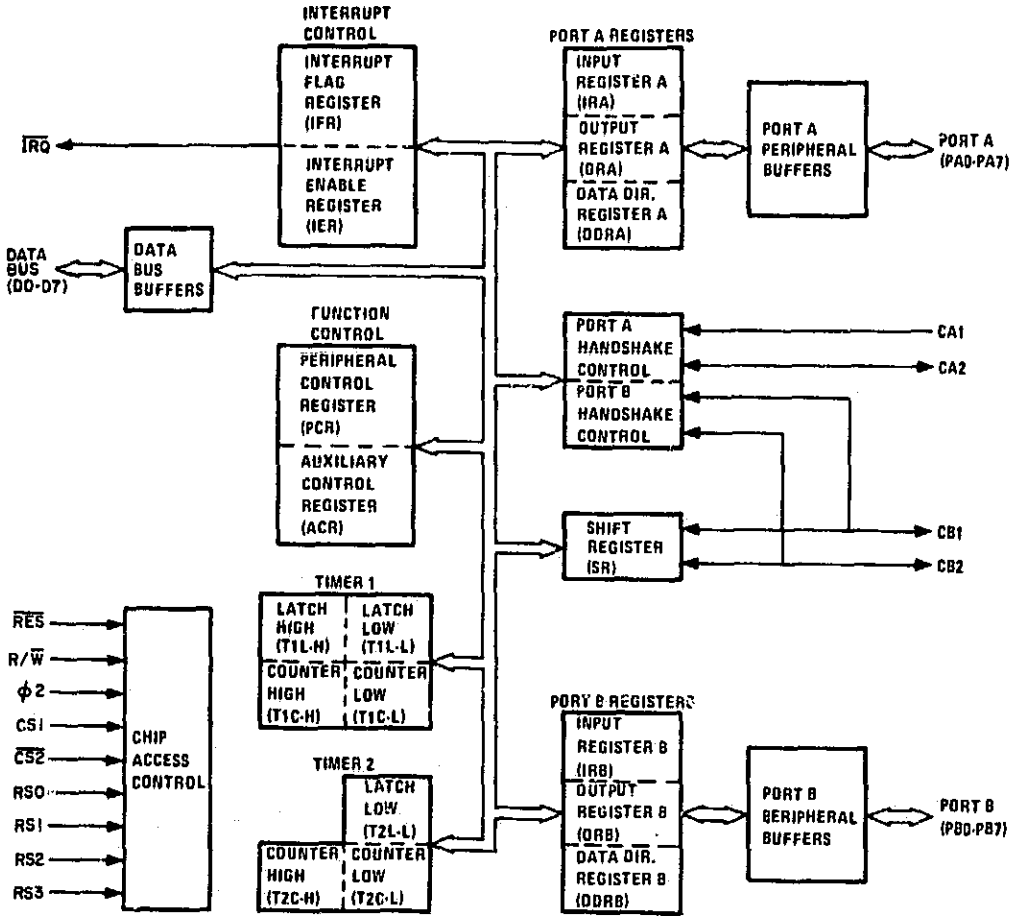

Figure 4.8 6522 system diagram.

IER bit 1 is low, disabling IFR bit 1 from pulling $\overline{IRQ}$ low. The Apple, waiting in a loop which continually examines the IFR, exits the loop when IFR bit 1 goes high, starting the sampling.

The second timing signal needed by the digitizer is an interrupt every 20 cycles of the 100 kHz reference (for a 5kHz digitizing rate). There are two timers on the VIA: TIMER1 and TIMER2. TIMER2 is used to count the 100 kHz reference pulses from the phase locked loop circuit, the output of which is attached to line PB6 of the VIA. Each negative transition causes the counter value in TIMER2 to decrement by one. When the counter value decrements from $0000 to $FFFF, TIMER2 sets IFR bit 5. Since IER bit 5 is set high, the VIA pulls $\overline{IRQ}$ low. The starting values of the counting registers are written by the interrupt service routine to the TIMER2 low latch and high counter byte. The second act, writing to the high counter byte, causes the VIA to place the low latch value into the low counter byte, to clear IFR bit 5, and to start TIMER2 counting pulses. Appropriately refilling the counter every interrupt cycle results in an interrupt request every 20 reference cycles.

A flow chart of the digitizer software is shown in Figure 4.9. The system consists of a BASIC program named DIGITIZER CONTROL and a collection of assembly language subroutines called DIGIAUTOSTART.OBJ0 (complete listing in Appendix II.1). DIGITIZER CONTROL, listed in Figure 4.10, uses POKE statements to pass various parameters to DIGIAUTOSTART.OBJ0. These include the number of samples to be taken and various addresses. DIGIAUTOSTART.OBJ0 is assumed to begin at $8000. However, a NOP instruction is placed at $7FFF, and line 470 calls this address. This odd starting point is due to an idiosyncrasy of the Apple II that prevents a BASIC program from calling address $8000. The first subroutine called by DIGITIZER CONTROL (called in

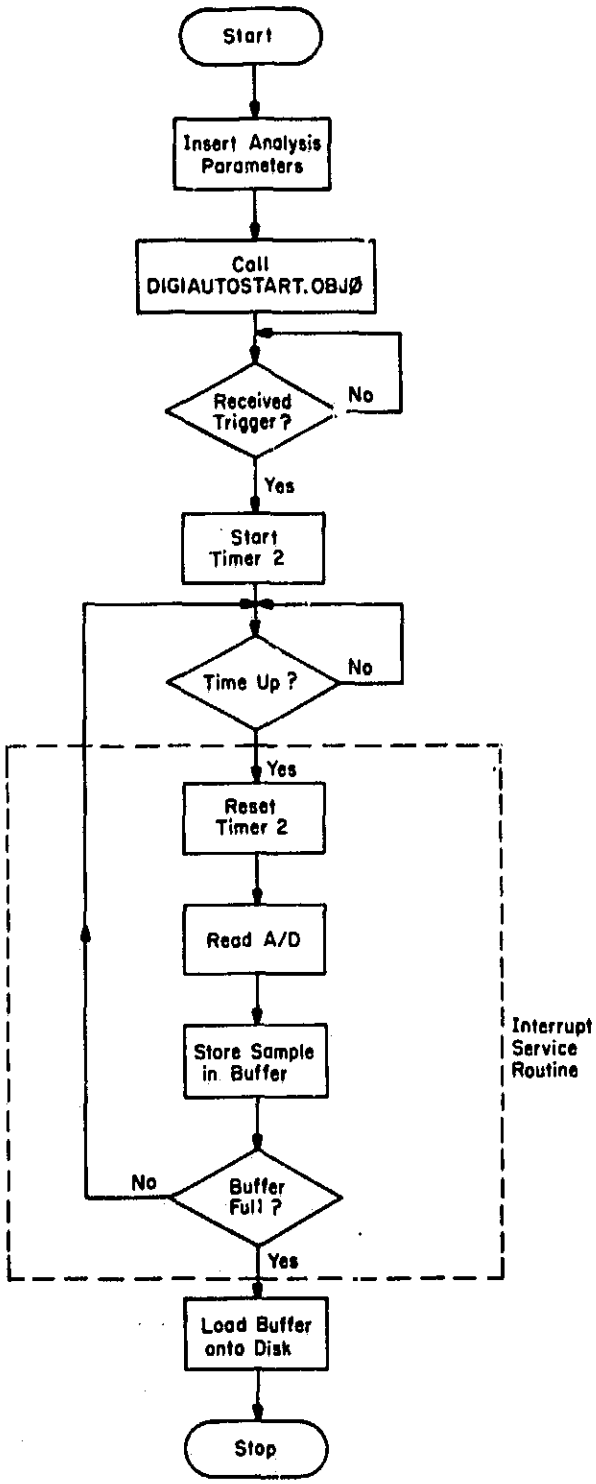

Figure 4.9 Digitizer software flow chart.

```
 50 REM  DIGITIZER CONTROL
 60 REM  THIS PROGRAM CONTROLS THE ASSEMBLER PROGRAM DIGIAUTOSTART.OBJ0.
100 REM  TO SAVE MEMORY SPACE, REMOVE ALL REMARKS BEFORE LOADING.
200 D$="": REM  D$ EQUALS CTRL D.
400 POKE -32754,47: REM    CHANNEL PARAMETER = A/D SLOT * 16 + A/D INPUT
        CHANNEL.
410 POKE -32753,16: REM  HIGH BYTE OF BUFFER ADDRESS. LOW BYTE ASSUMED ZERO.

420 POKE -32752,168: REM  LOW BYTE OF NUMBER OF SAMPLES TO BE TAKEN.
430 POKE -32751,97: REM  HIGH BYTE OF NUMBER OF SAMPLES.
460 POKE -32748,128: REM  HIGH BYTE OF INTERRUPT SERVICE ROUTINE.
465 POKE 32767,234: REM  PUTS A NOP AT $7FFF.
470 CALL 32767: REM    CALLS DIGIAUTOSTART.OBJ0 AT $7FFF.  FIRST
472 REM                ROUTINE INITIALIZES THE BUFFER AND PERIPHERAL CARDS.
480 CALL -32757: REM  CALLS THE WAIT LOOP FROM WHICH INTERRUPT OCCURS.
500 PRINT D$;"BSAVE R######TYP@XXS,A$1000,L25000"
600 END
```

Figure 4.10 Integer BASIC program DIGITIZER CONTROL.

line 470) configures the VIA and creates a buffer to hold the sampled data. Before returning to DIGITIZER CONTROL, the subroutine waits for the positive transition on line CA1. Once triggered the subroutine starts the counter on the VIA and returns to DIGITIZER CONTROL. The next subroutine called is simply a wait loop (called in line 480). When the VIA counter finishes counting down, IFR bit 5 is set, pulling $\overline{IRQ}$ low. An interrupt service routine takes a sample from the A/D card, restarts TIMER2, places the sample in the buffer, and returns to the wait loop. Since five seconds of data are needed, the buffer is 25000 ($61A8) bytes long. When the final sample is taken the interrupt service routine does not return to the wait loop but rather to DIGITIZER CONTROL. The buffer is then saved on floppy disk in binary format.

Once the external hardware of the digitizer system is set up, running the program only requires loading the appropriate files into the Apple and starting the sampling at the desired time. The two files needed are DIGITIZER CONTROL and DIGIAUTOSTART.OBJ0. Omission of address parameters in loading DIGIAUTOSTART.OBJ0 causes the file to be loaded at the default address $8000. Loading at another address necessitates changing the POKE statements of DIGITIZER CONTROL. An alternate starting address also requires the reassembly of the assembly code of DIGIAUTOSTART.OBJ0. A memory map showing the addresses used by the digitizer is given in Figure 4.11. To take a 5 second data segment at, for example, 50 seconds into a flight, the analog tape is started about 20 seconds earlier. When the time code translator displays 49 seconds DIGITIZER CONTROL is run. Digitization then starts at exactly 50 seconds, the next positive transition on CA1. After five seconds the sampling stops and the buffer is written to disk. The file name has the following format: "R" + rocket number + file type +

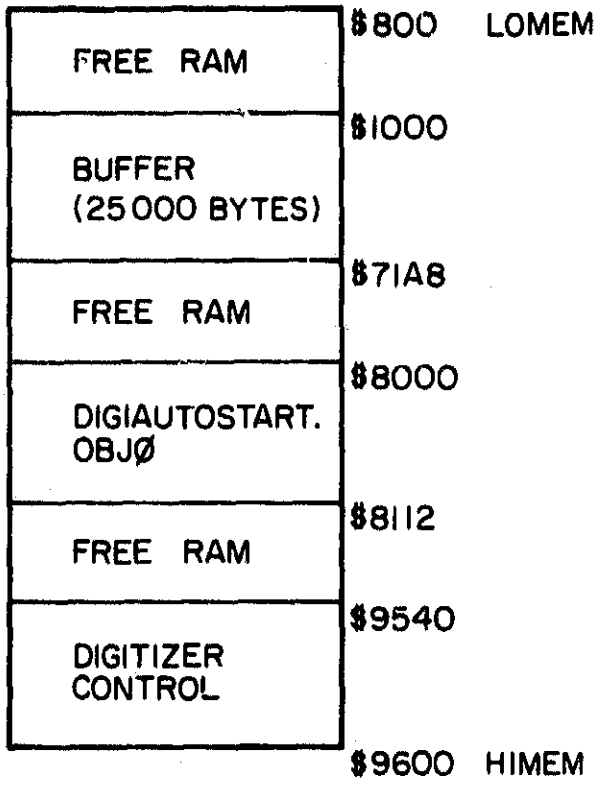

Figure 4.11 Memory map for digitizer software.

"@" + elapsed flight time from launch to first sample + "S". For example, a data file for the 28 May 1975 Peru flight (code number 14.532) at 50 seconds into the flight would be labelled R14532DAT@50S. This name must be substituted into DIGITIZER CONTROL before the program is run.

To achieve the highest resolution possible the data signal is amplified to the threshold of saturating the ±5 V input range. This amplification is provided by the EMR discriminator. To calibrate the amplified data the digitizer is run with a frequency generator substituted for the FM data from the tape recorder. A block diagram is given in Figure 4.12. Since the frequency generator does not suffer from tape speed fluctuations, the 100 kHz reference is disconnected from the EMR discriminator and the delay is omitted, eliminating tape speed compensation. The frequency generator mimicks the output of a VCO. Stepping the frequency generator from 7.5% below to 7.5% above the center frequency of the VCO simulates stepping the VCO input from 0 to 5 V. The digitized values for a number of frequencies are taken with the A/D system, treating the generator as a data signal. This provides a calibration between VCO input and digitized output. Since the frequency generator does not exhibit tape speed fluctuations the tape speed compensation is disabled.

4.6 Data Postprocessing

The final process in the data analysis is transferring the binary files from floppy disk to the Cyber mainframe computer and performing spectral analysis. Properly transferring and formatting the data is a three-step process. The binary files must first be converted to text files. Next, these files are transferred to the Cyber via a 300 baud modem. Finally, on the Cyber the data must again be reformatted to simulate files created from Wallops Island tapes. Once the files are in the proper format they may be

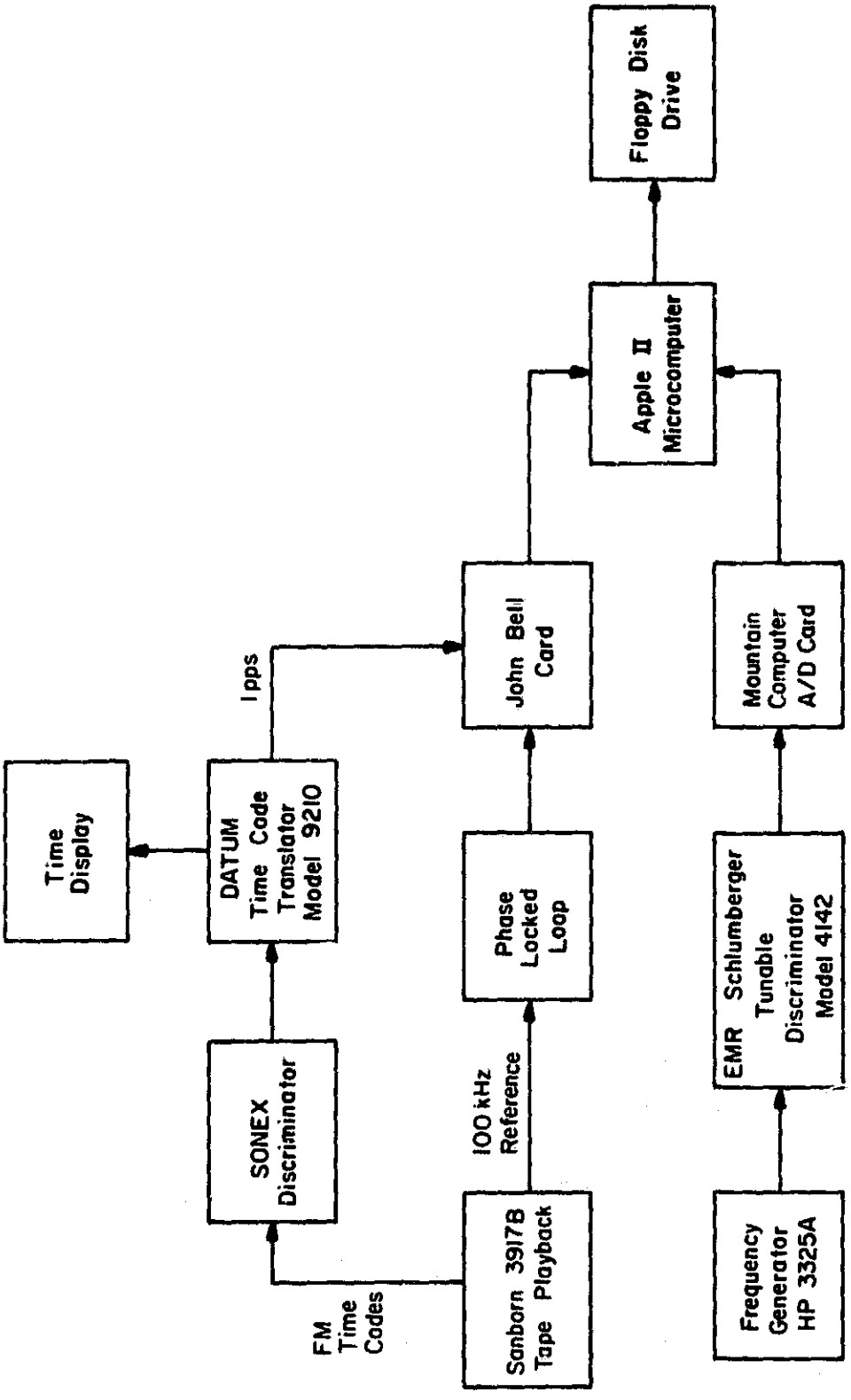

Figure 4.12 Calibration for digitizer system.

submitted to SPECTRA and other programs. SPECTRA estimates the power spectrum of an irregularity by processing the discrete Fourier transform (DFT) of a number of data segments. The estimate is then compensated for the filtering imposed by the experimental apparatus. The corrected estimate is plotted on a high resolution graphics terminal. The spectrum may be stored while others are calculated. Further processing can calculate averages, differences, and smoothing of the stored spectra. In an attempt to reduce the effects of spin noise, a simple moving average can be applied to the data before spectral analysis. In some cases this allows for a more confident estimation of the spectrum at lower wave numbers.

To transfer a binary data file to the Cyber it must first be converted to a text file. The binary file is stored in memory starting at $1000. An APPLESOFT program called TEXTIFY (listing in Appendix II.2), stored at $800, converts segments of 20 bytes into text strings 60 characters long. Single and double digit numbers are padded with zeros. These strings are collected into a text file and stored on floppy disk. Due to Apple DOS limits on file sizes, one binary file, 25000 bytes or 99 disk sectors, must be converted to two text files with a total of 302 sectors.

These text files are then transferred to the Cyber via a telephone modem. The transfer is supervised by a set of programs called APPLE TERM (Version 3.0), written by Neil Remy for the Computing Services Office at the University of Illinois. The modem used is a 300 baud Micromodem II made by D.C. Hayes and Associates, Inc. It may be inserted into any of the peripheral card slots in the Apple. Booting APPLE TERM loads various subroutines and asks the user for the telephone number of the Cyber hookup. Once connected, the Apple acts as a Cyber terminal. The user opens a destination file for the text files using the Cyber's ICE editor. A useful

file name format is "D" + the last three digits of the flight number + "A" + the elapsed seconds from launch corresponding to the first datum in the file (e.g., D532A50). After opening the file the insert mode is invoked. The Cyber displays a line number and a question mark, the insert mode prompt. To start the transfer the user types <ESC> T. APPLE TERM then takes control of the keyboard, opens the specified text file, and sends the data. Each line of the ICE file receives one record of the text file. Upon completion of the transfer the user saves the ICE file.

At this point the ICE file is still not in the format acceptable to many programs developed for rocket data analysis. These accept the Wallops Island format. In this format, diagrammed in Figure 4.13, the data are segmented into records, each with 1251 bytes. Each record consists of one real byte giving the starting time of the record, followed by 1250 integers divided into 250 frames. A frame has five channels, each of which is assigned to a different experiment. This channel arrangement facilitates synchronous comparisons between two or more experiments. Thus each record contains 250 samples from a single experiment. If data from only a single experiment are needed, this format is rather uneconomical in memory usage when compared to the ICE files.

Conversion of the ICE files to the Wallops Island format requires a simple FORTRAN program called APL2CDC (complete listing in Appendix II.3). Program APL2CDC reads in data from the ICE file, inserts the proper time bytes, packs each data point into a frame with four filler points, and writes out the constructed records to a new file. The unformatted write statement used writes out a whole 1251 point array at once. Other programs reading this file must use a corresponding unformatted read statement with an identically sized input array. Files created with unformatted write

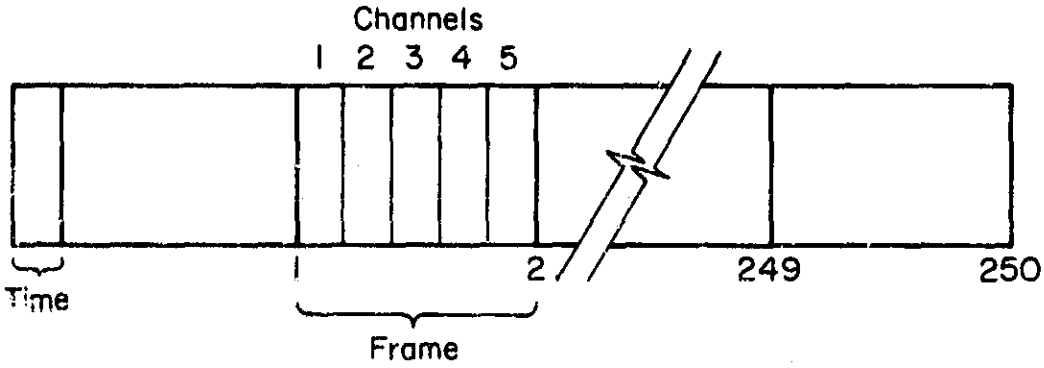

Figure 4.13 Format of a data record using the Wallops Island format.

statements cannot be edited by ICE. Due to the approximately fivefold increase in file size, limits on the Cyber system force the new file to be a direct access file, as opposed to the original indirect access file. The only major difference between the two file types lies in the way the Cyber stores them. In a FORTRAN program, both file types are read from and written to in the same manner. Since the Wallops Island format entails an appreciable increase in storage costs and required memory, long-term data storage is most efficient using the ICE files.

Once in the appropriate format the data may be Fourier analyzed and the power spectrum estimated. This is accomplished with an interactive FORTRAN program called SPECTRA (complete listing in Appendix II.4). A flow chart of SPECTRA is shown in Figures 4.14 and 4.15. SPECTRA, written by Bruce Tomei (in Roth, 1982b), employs a power spectrum estimation method developed by Welch (1967). In this method consecutive, possibly overlapping, periodograms are averaged together. An introduction to various methods of power spectrum estimation is available in Oppenheim and Schafer (1975). SPECTRA requires access to two software libraries available on the Cyber: International Math and Statistical Library (IMSL) and the Graphics Compatability System (GCS) library of plotting routines. SPECTRA first asks a number of questions allowing the user to control the analysis. These include the starting time of the data of interest, the number of data points desired, and the DFT block length. The starting time is approximately known from the analog preprocessing. A plot of the digital data allows for an even more precise determination of a starting point. Such plots are made by a FORTRAN program called DATPLOT (complete listing in Appendix II.5). The number of points to which SPECTRA is applied is also determined from a DATPLOT output. Figure 4.3 is an example of a plot by DATPLOT. The time

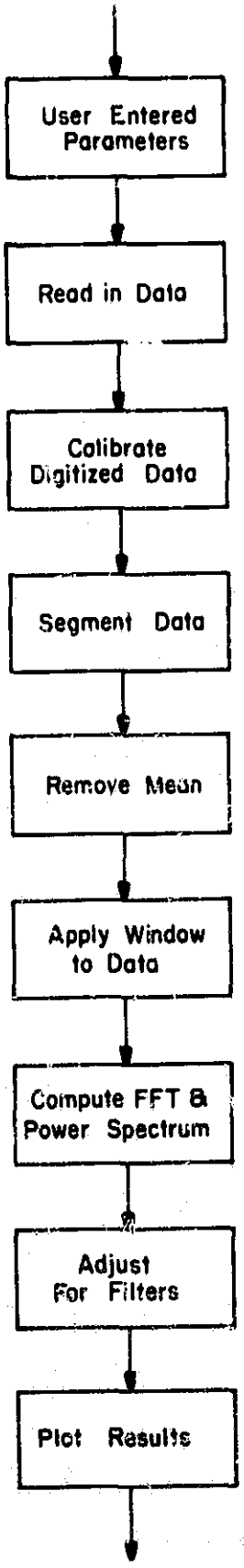

Figure 4.14 Spectra calculation from program SPECTRA.

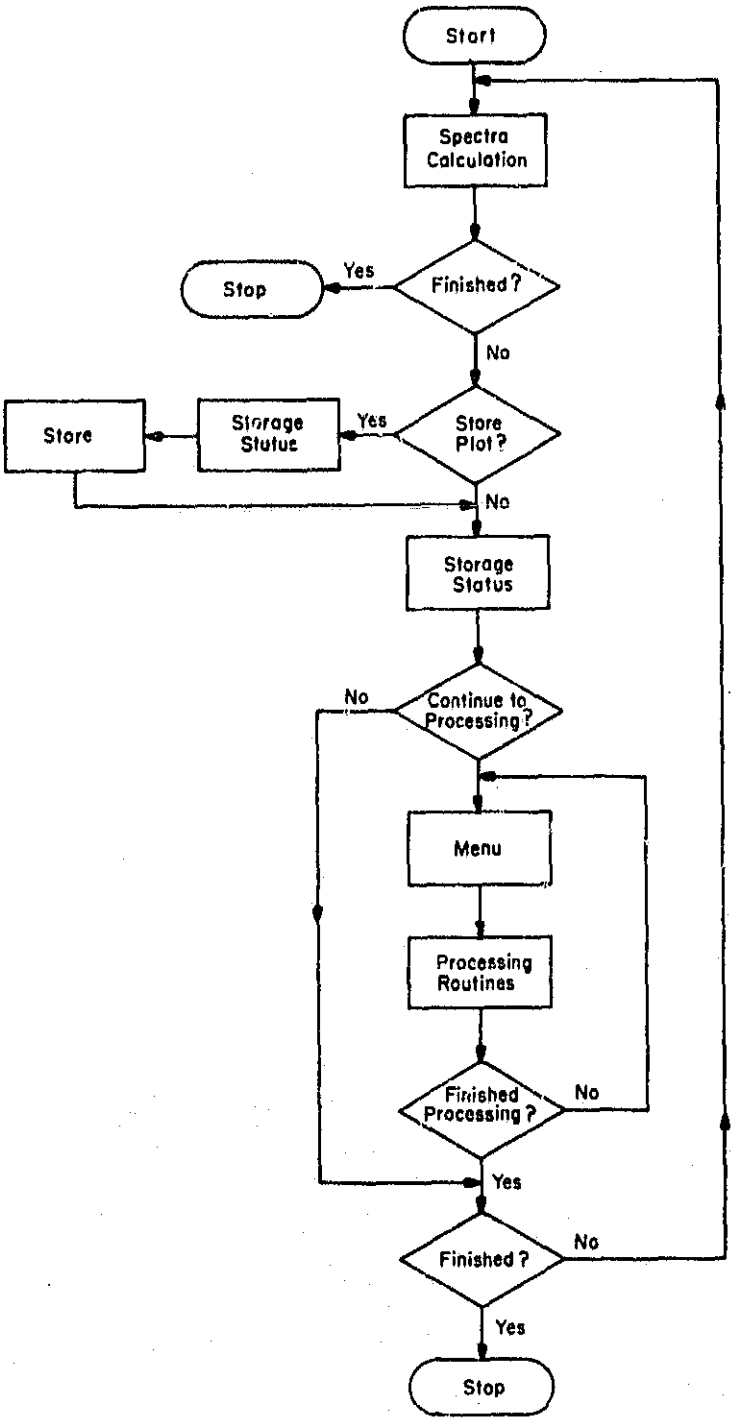

Figure 4.15 Flow chart for program SPECTRA.

span of interest is multiplied by the digitizing rate to give the number of points to be analyzed. This sequence of points may be divided into smaller, possibly overlapping segments. It is these segments to which the Fourier analysis is applied.

The chosen length of the DFT may either match or exceed an individual data segment length, an inadequately long data segment being padded with zeros. When the data are segmented, the digital values are calibrated to give values of $\Delta N_e/\langle N_e \rangle$. A Hanning window is applied to each segment to produce a better power spectrum estimate. The DFT of each windowed data segment is found with a fast Fourier transform (FFT) routine in IMSL. The squared magnitude of the DFT times some scaling constants gives the power spectrum estimate. To correct for the various filters in the rocket experiment, SPECTRA divides the spectrum by the theoretical transfer function of the filters. This corrected spectrum is plotted using GCS graphics routines. The individual spectra are then averaged together to give a best estimate of the power spectrum. The averaged spectrum may be stored while a different averaged spectrum is calculated. Two spectra may be stored at one time.

A number of modifications to SPECTRA allow for further processing of the spectra. The aim of these processes is to produce a better estimate of the spectral index. First, two stored spectra may be averaged together. This allows for the spectra of two nonconsecutive segments to be averaged. Such an average may be necessary to avoid a data segment flawed by interference. Second, the difference of two spectra may be calculated. With this function an estimate of the background noise power spectrum may be subtracted from another spectrum with both signal and noise. Third, a spectrum may be smoothed by dividing the frequencies into groups whose size

increases with frequency by a constant factor. This has the effect of dividing a logarithmic frequency axis into equal segments. The corresponding magnitudes in each frequency range are averaged and plotted.

To study the effects of spin on the power spectrum, a moving average is applied to the raw data prior to spectral analysis. This process is performed by a FORTRAN program called SPINFIX (complete listing in Appendix II.6) which convolves an entire file of data points with a rectangular window function. The window has height of unity and length equal to the spin period. In the frequency domain this process transforms to multiplying the power spectrum by $T_p^2 \sin^2(\omega T/2)/(\omega T/2)^2$, where T_p is the number of data points in a spin period, T is the spin period in seconds, and ω is the angular frequency. The filtering action of the averaging necessitates some minor changes to SPECTRA. Multiplying the calculated power spectrum by $(\pi fT/T_p)^2$ leaves a spectrum multiplied only by $\sin^2(\pi fT)$ where f is the frequency. This should eliminate strong peaks at multiples of 1/T, the spin frequency. The power spectrum of the data in Figure 4.3 is shown in Figure 4.16. Figure 4.17 shows the power spectrum of the same data after SPINFIX is applied. The FFT length is chosen to extend over at least one spin period. Figure 4.17 shows a dramatic reduction of spectral power in the lower frequency ranges.

4.7 Summary

The analysis described in this chapter may be viewed as a series of refinements toward the ultimate goal of estimating the power spectrum and the spectral index. Irregularities must first be identified and distinguished from noise added by the experimental apparatus. The identification is achieved by the analog processing system developed by Klaus and Smith (1978). This system also provides a rough estimate of the fine structure

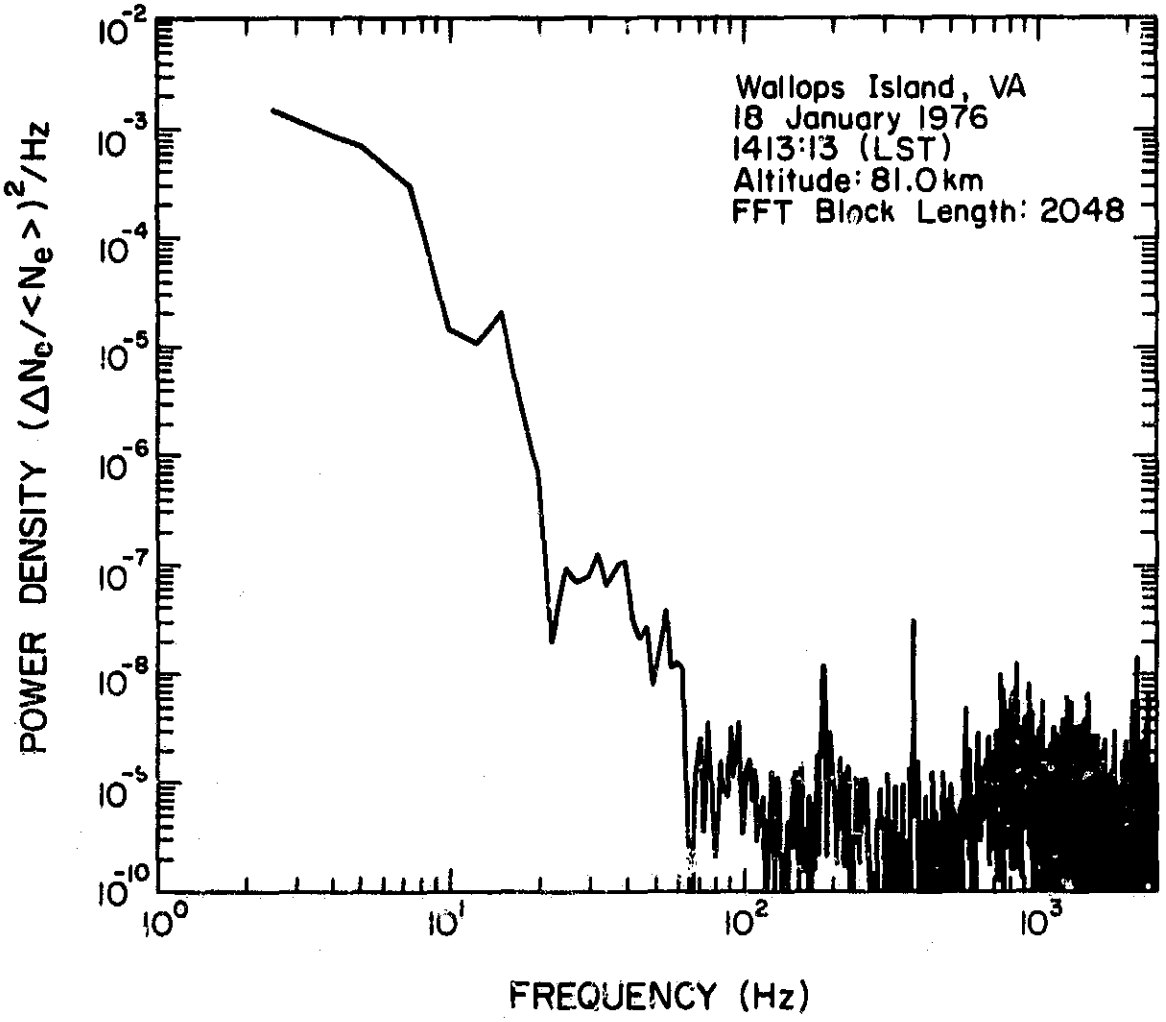

Figure 4.16 Spectrum of spin noise before application of program SPINFIX.

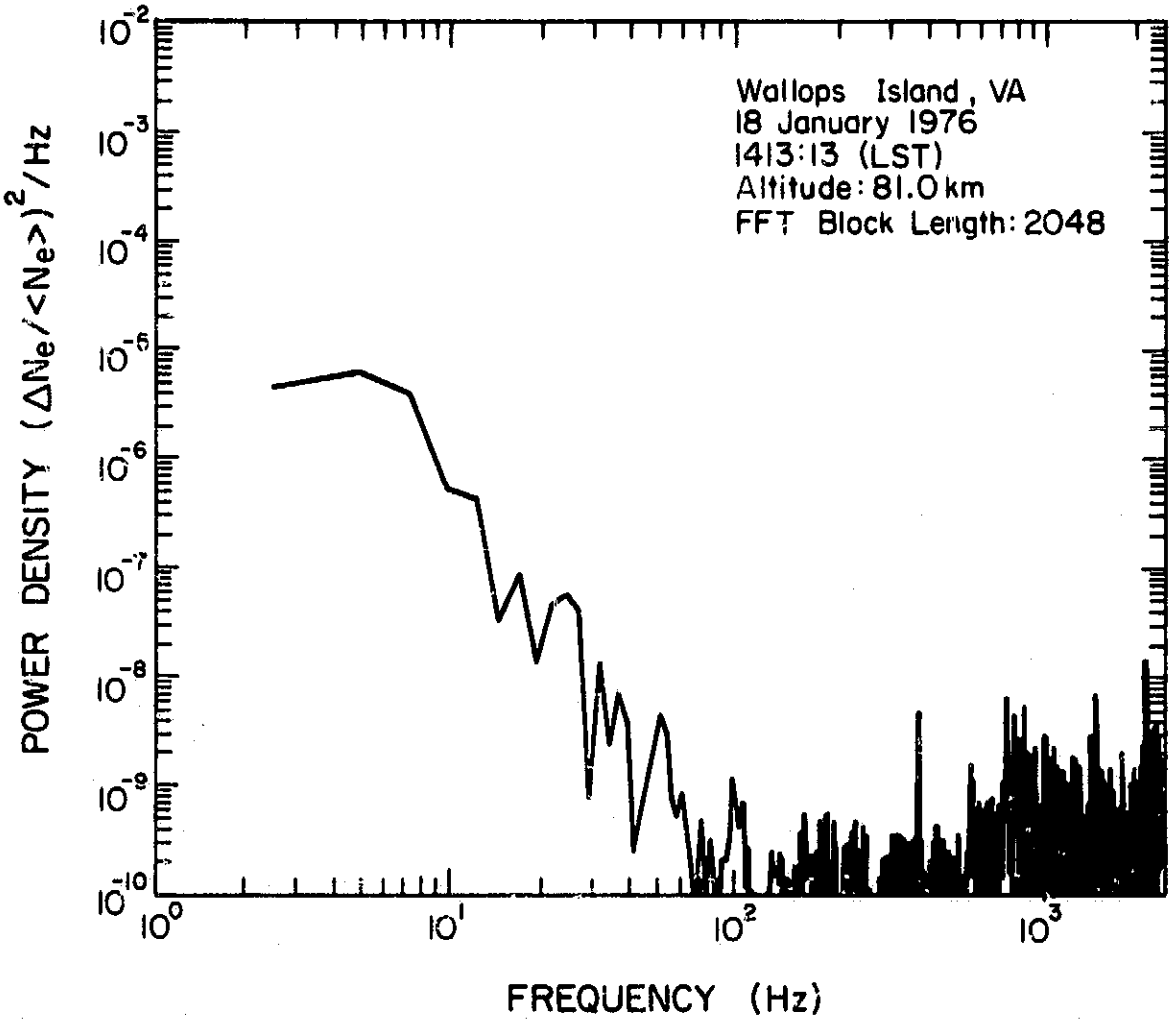

Figure 4.17 Spectrum of spin noise after application of program SPINFIX.

spectrum. Once interesting portions of the signal are identified, the data may be digitized. Detailed plots of the digital data provide the exact locations of irregularities within the data record. These irregularities are then subjected to digital analysis. The resulting spectrum has far better resolution than that afforded by the analog analysis. Smoothing and noise subtraction provide further ways of improving the spectral index estimates.

5. RESULTS

5.1 Introduction

This chapter presents some results of the analysis described in Chapter 4. Fine structure data are examined from the nine daytime rocket flights since 1975 that have carried the fine structure experiment. Possible ionospheric irregularities are found with five of the nine flights, and power spectra of the irregularities are calculated. Many spectra exhibit a wave number range with a spectral index close to -5/3, consistent with the existence of an inertial range of turbulence. The slope and wave number range of the best fit lines to the spectra are tabulated. Of particular interest is the upper wave number extent of the best fit line. This limit is compared to predictions made by Rastogi and Bowhill (1976).

Section 5.2 describes each rocket flight on which irregularities are observed. A particular irregularity from the 28 May 1975 Peru flight is analyzed to illustrate the analysis procedure. Measured parameters of all observed irregularities are tabulated. Section 5.3 discusses the results derived in Section 5.2 and makes comparisons to the spectral model of Hill and Bowhill (1976) and to the inertial range predictions of Rastogi and Bowhill (1976). Section 5.4 presents the conclusion that the observed irregularities are consistent with those expected from atmospheric turbulence.

5.2 Observations of Irregularities

The 28 May 1975 Peru flight was launched from the Punta Lobos rocket range at Chilca, Peru at 15 26 local standard time (LST). The coordinates of the site are 12.5° S and 76.8° W. The prime objective of the flight was to observe the equatorial electrojet. This site is particularly interesting

since the Jicamarca radio observatory is located only 60 km north of the rocket range. The close proximity of the two sites facilitates coincident rocket and radar measurements. More details of the launch operations and flight are available in Klaus and Smith (1978), including comparison of Langmuir probe electron density measurements to incoherent scatter measurements taken at Jicamarca.

The fine structure data from the 28 May 1975 Peru flight, although containing some interference, in general are of exceptional quality. There is no discernible spin contamination since a nose tip probe was used. Analog preprocessing produces the strip chart records shown in Figure 4.5. The data are marred by interference spikes appearing every half second, attributable to an RF resonance probe on the rocket. Two isolated noise spikes occur at 70.3 and 84.8 km. Their source is unknown, but the shortness and strength of the spikes suggest they are due to interference. Not so easily explained are the four fluctuations seen following the large spike at 84.8 km. Examination of the digital record reveals no obvious common features between them. They cannot be attributed to spin since their spacing is not exactly regular or close to the spin period. Aside from these three groups of isolated noise spikes, the only other noise present is the unavoidable noise due to the telemetry system.

The fine structure data reveal the presence of six irregularities between 70 and 90 km. Table 5.1 lists their altitudes and vertical extent. To illustrate the analysis process, the irregularity at 74.9 km is considered here in detail. The top plot in Figure 5.1 shows a portion of the digital record at 74.9 km. This represents the raw fine structure signal without correction for the various filters in the experiment. In particular the observed signal is not corrected for the low frequency

Table 5.1 Parameters of irregularities for nine rocket shots. No irregularities are found with the last four shots listed.

Rocket Flight	Altitude of Center of Irregularity (km)	Irregularity Thickness (km)	Maximum $\Delta N_e / \langle N_e \rangle$ (percent)	$\langle N_e \rangle$ (cm^{-3})	Electron Concentration Gradient (cm^{-3}/km)	Slope of Best Fit Straight Line	Approximate Limits of Spatial Frequency for Best Fit Line (rad/m)
Chilca, Peru 28 May 1975	87.5 77.5 76.3 74.9 74.3	0.67 0.72 0.29 0.48 0.22	12 1.5 1.1 1.9 1.1	9.6×10^2 2.9×10^2 2.6×10^2 2.2×10^2 2.1×10^2	$(1.0 \pm .2) \times 10^3$ 30 ± 5 20 ± 10 30 ± 5 -20 ± 10	-1.8 -1.7 -1.8 -1.7 -1.9	0.022 - 0.19 0.052 - 0.23 0.021 - 0.39 0.041 - 0.42 0.020 - 0.13
(#14.532)	71.8	0.43	0.65	1.1×10^2	30 ± 10	-1.6	0.040 - 1.8
Wallops Island, Virginia 18 January 1976 (#18.169)	82.2 77.6 73.5 70.8	0.44 0.36 0.60 0.49	7.2 4.7 4.9 <1.5	9×10^3 8×10^3 3×10^3 7×10^2	10^2 10^1 10^2 10^2	-2.1 -2.1 -1.7 -2.1	0.036 - 0.25 0.034 - 0.24 0.033 - >2.3 0.032 - 0.59
Wallops Island 12 August 1976 (#18.1006)	83.5	0.66	13	4.3×10^3	$(8 \pm 1) \times 10^2$	-1.9	0.028 - 0.17
Wallops Island 8 January 1977 (#18.1008)	75.9	0.25	<4.1	5.4×10^2	30 ± 10	-1.7	0.029 - 0.40
Peru 27 February 1983 (#31.028)	85.8	1.3	4.9	2.1×10^3	$(7.5 \pm 2.5) \times 10^3$	-1.5	0.010 - 0.17
Ontario 24 February 1979 (#18.1020)							
Ontario 26 February 1979 (#18.1021)							
Ontario 26 February 1979 (#18.1022)							
Peru 12 March 1983 (#31.029)							

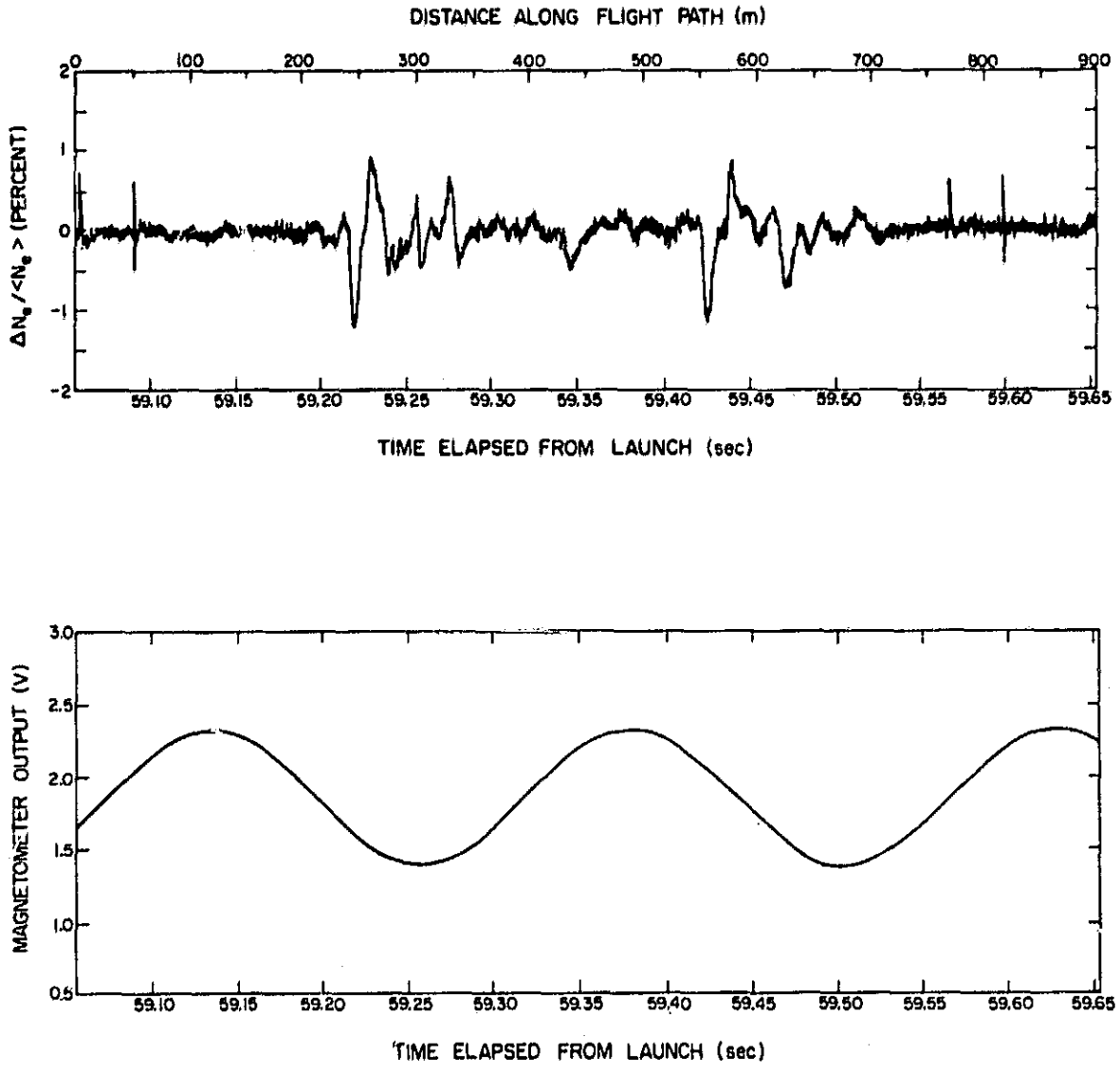

Figure 5.1 Upper plot shows portion of digital record from the 28 May 1975 Peru flight. Launch time at 15 26 (LST). Altitude of the irregularity center is 74.9 km. Lower plot shows the magnetometer output.

attenuation from the ac amplifier. Low frequency components thus appear de-emphasized. The upper independent axis gives relative distance along the flight path while the lower axis shows elapsed time from launch. The center of the irregularity, at 900 m on the distance scale, occurs at 74.9 km altitude. Interpretation of the observed temporal fluctuations as spatial fluctuations with scale sizes read directly from the distance axis requires the assumption of isotropy. With this assumption, a temporal oscillation with frequency f corresponds to a spatial oscillation with wave number k given by

$$k = 2\pi f/v \qquad (5.1)$$

where v is the rocket velocity. Most spectra presented in this chapter, although calculated for temporal frequencies, display a wave number axis with values found from equation (5.1).

The two-sided character of the 74.9 km irregularity suggested by Figure 4.5 shows up quite strongly in Figure 5.1. It might be suspected that the two distinct portions of the irregularity are the results of rocket spin. However, analysis of the irregularity reveals two countering arguments. First, as observed in Figure 4.3, each cycle of the spin modulation should closely resemble the neighboring cycles. This is not the case in the top portion of Figure 5.1. Second, any matching features of the two suspected cycles should be separated exactly by the spin period. A portion of the magnetometer signal coincident with the irregularity is shown in the bottom portion of Figure 5.1. The spin period is measured to be 0.245 seconds. In contrast, the time displacement between the two large dips on the left of each apparent spin cycle in Figure 5.1 is 0.207 seconds.

Two power spectra are estimated, one for each of the two prominent halves of the irregularity. The two power spectra each have an FFT length

of 512 points. The average of the two spectra is shown in Figure 5.2a. The frequency scale is converted to a wave number scale using equation 5.1 with a speed of 1.50×10^3 m/sec. The units on the vertical axis are converted from Hz^{-1} to $(rad/m)^{-1}$. A noise floor due to the telemetry system is seen at approximately 10^{-7} $(rad/m)^{-1}$. This limits the useful wave number range to below 1 rad/m, where the irregularity spectrum crosses the noise floor. To help measure the spectral index, a noise estimate, Figure 5.2b, is subtracted from the averaged spectrum. The difference is shown in Figure 5.2c. The data used in calculating the noise estimate come from a data segment adjacent to the irregularity. The observed noise is attributed to the telemetry system. Since the telemetry noise enters the signal after the ac amplifier, the SPECTRA correction for the high pass filtering boosts the low frequency telemetry noise components above their actual level. This partially accounts for the spectral strength at low frequencies observed in Figure 5.2b. The difference spectrum is smoothed by SPECTRA using the process discussed in Chapter 4. The window multiplication factor is 1.4. The resulting smoothed spectrum is shown in Figure 5.2d.

Three separate regions of the smoothed spectrum may be distinguished. A line may be fitted between the first point on the left and the point at 0.23 rad/m. The best fit line has a slope of -1.7. The second region, between 0.23 and 2.6 rad/m, exhibits a slope of -3.7. The third region is that above 2.6 rad/m. In this region telemetry noise overwhelms the signal and little information may be extracted. The V-shaped dips shown in Figure 5.2d are an artifact of the computer plotting routine, which rounds up off-scale points to the lowest point on the graph. The average of a set of points on the difference spectrum (Figure 5.2c) may be negative and hence off-scale. Negative points are therefore set to the lowest point on the

C-2

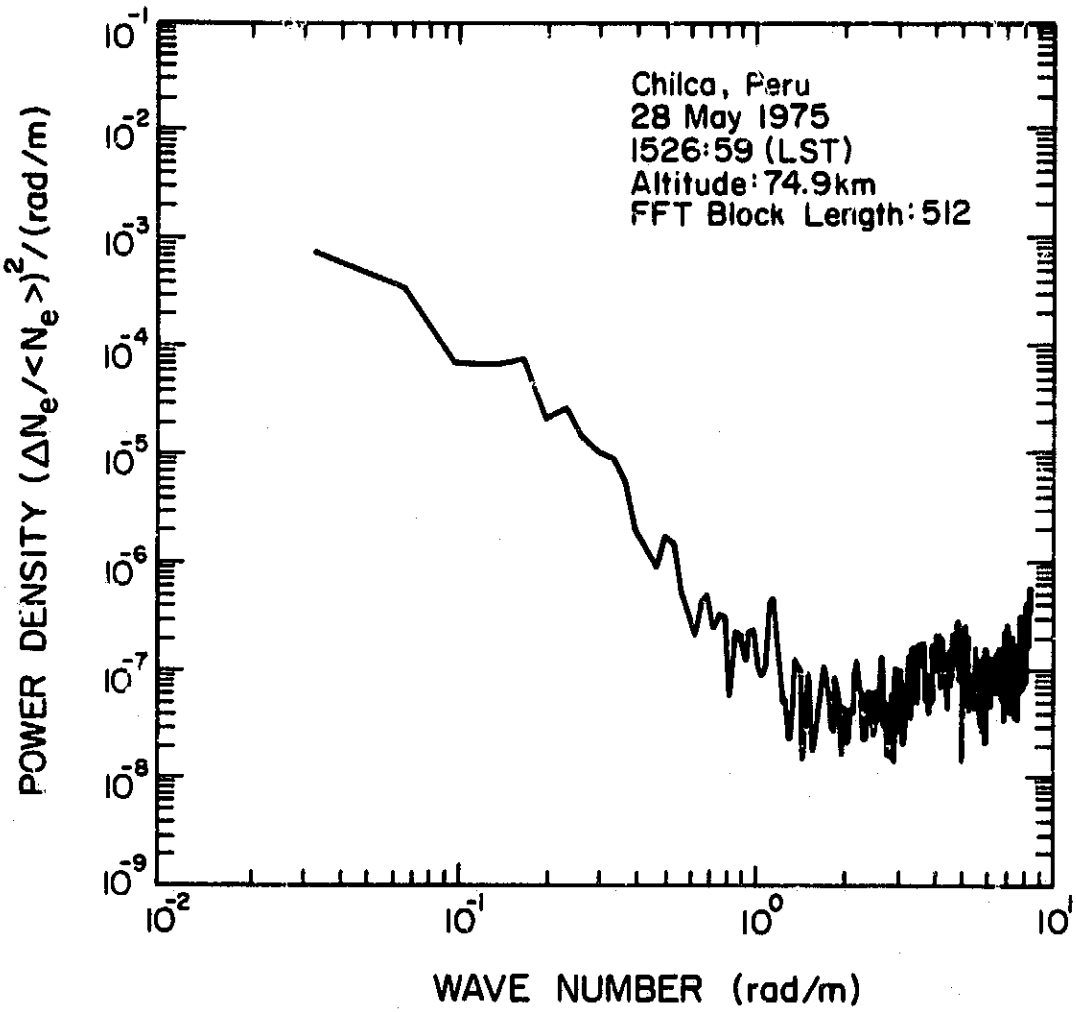

Figure 5.2a Power spectrum estimate of the irregularity shown in Figure 5.1.

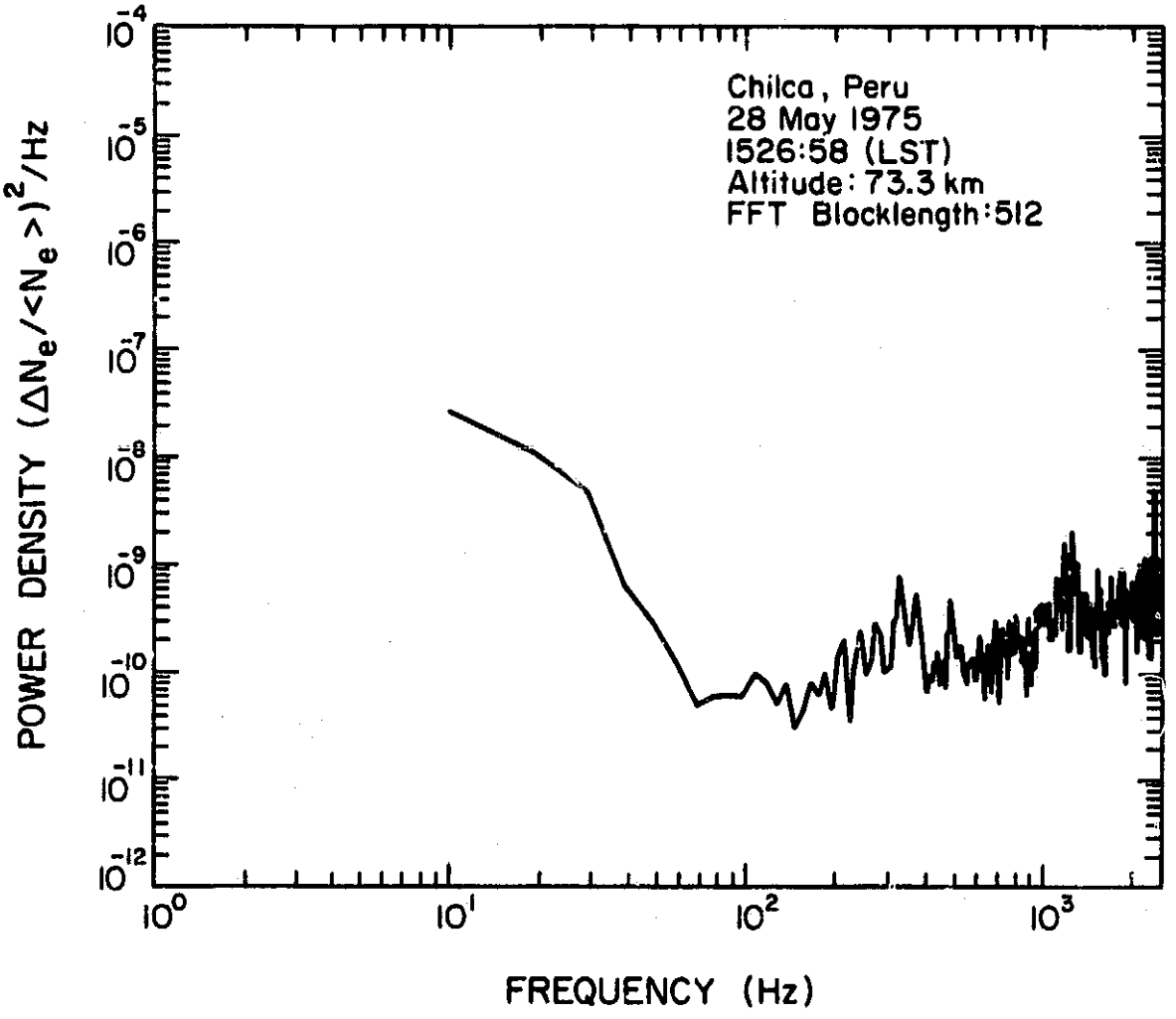

Figure 5.2b Estimated noise power spectrum for the 74.9 km irregularity.

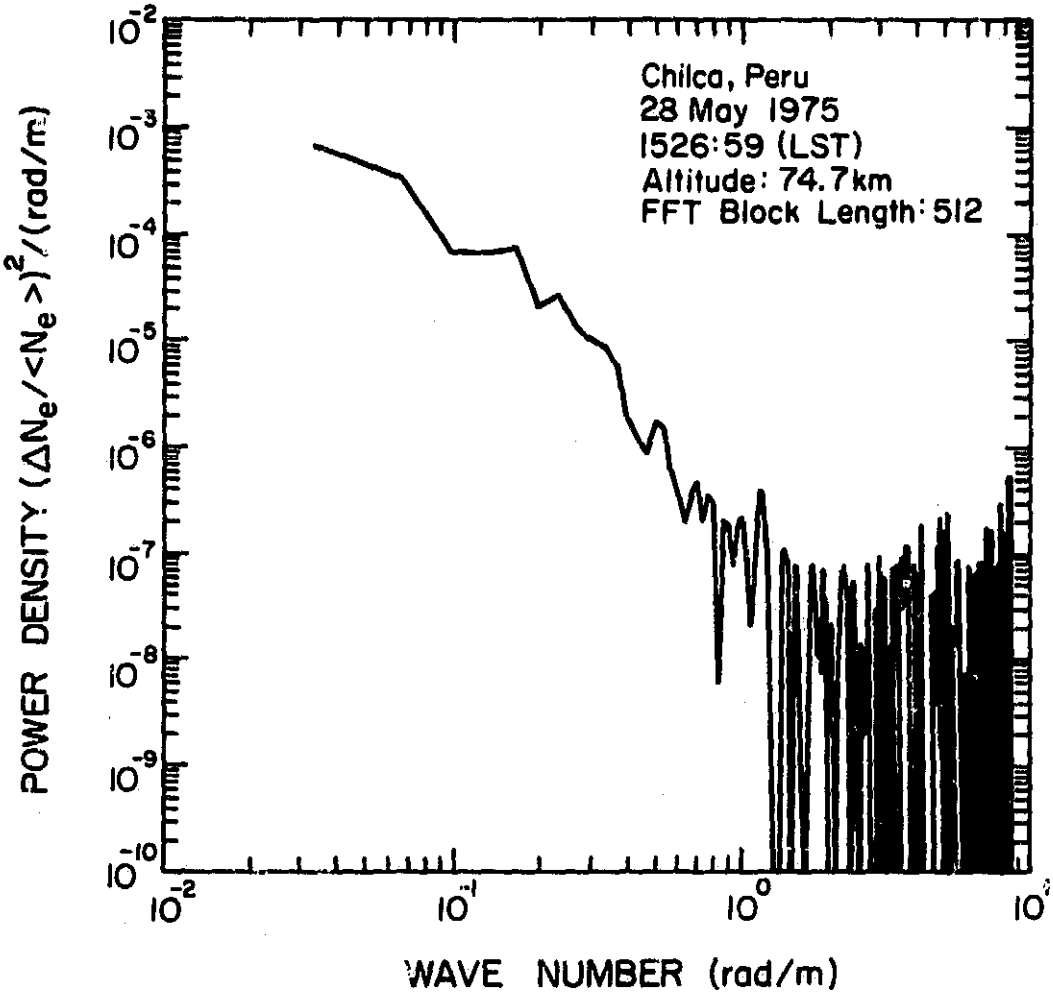

Figure 5.2c Difference between the irregularity power spectrum and the noise power spectrum shown in Figures 5.3a and 5.3b, respectively.

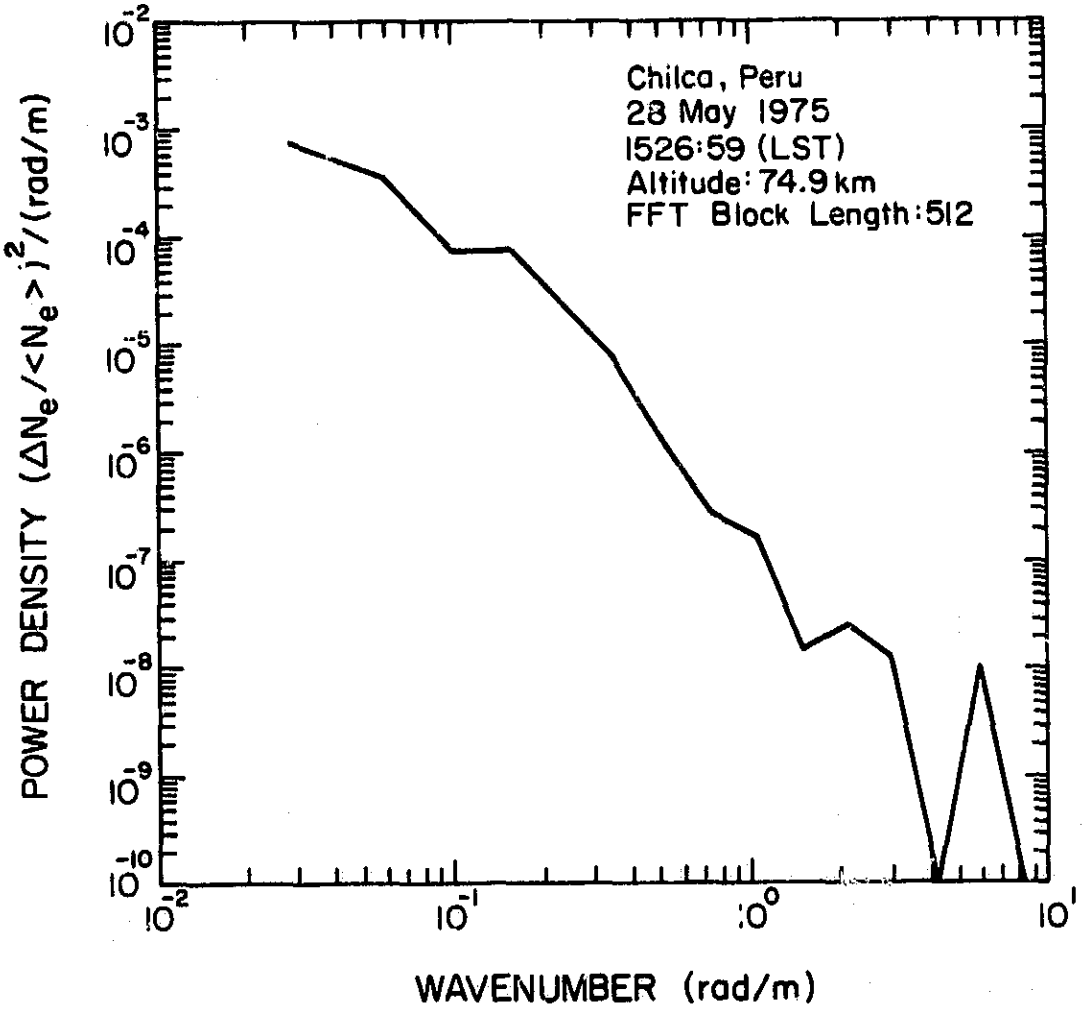

Figure 5.2d Smoothed difference spectrum with window multiplication factor of 1.4.

vertical axis.

Figure 5.3 shows the smoothed power spectum of an irregularity at 87.5 km. The best fit line to the wave number region below 0.19 rad/m has a slope of -1.8. The second steeper slope has a value of -7.5. The total power is much greater than that in the irregularity at 74.7 km. Figure 5.4 shows the electron density profile from the 28 May 1975 Peru flight. Note that the altitude of the 87.5 km irregularity coincides with a large electron density gradient. It might be suspected that the irregularity is merely the response of the ac amplifier to the sudden increase in electron density. However, the data record at times immediately following the irregularity shows very little activity, in spite of the continued presence of the gradient. It is thus reasonable to assume that the source of the irregularity is geophysical and not instrumental.

The results described above are given in Table 5.1, along with the results from other irregularities from the 28 May 1975 Peru flight. The wave number range over which the power law extends is determined from the unsmoothed difference spectra. In most cases the best fit line extends to the lowest wave number on the spectrum. The low limit listed in Table 5.1 thus reflects the lowest wave number for which the FFT is calculated and is a function of the FFT size and the digitizing rate. The high limit listed is the largest wave number at which the spectrum remains on the best fit line.

As mentioned previously, the digitized fine structure signal (e.g., Figure 5.1) is not corrected for the low frequency attenuation from the ac amplifier. To measure the maximum deviation of an irregularity, this attenuation must be accounted for. To correct the observed maximum deviations, the main frequency component of the deviation is estimated and

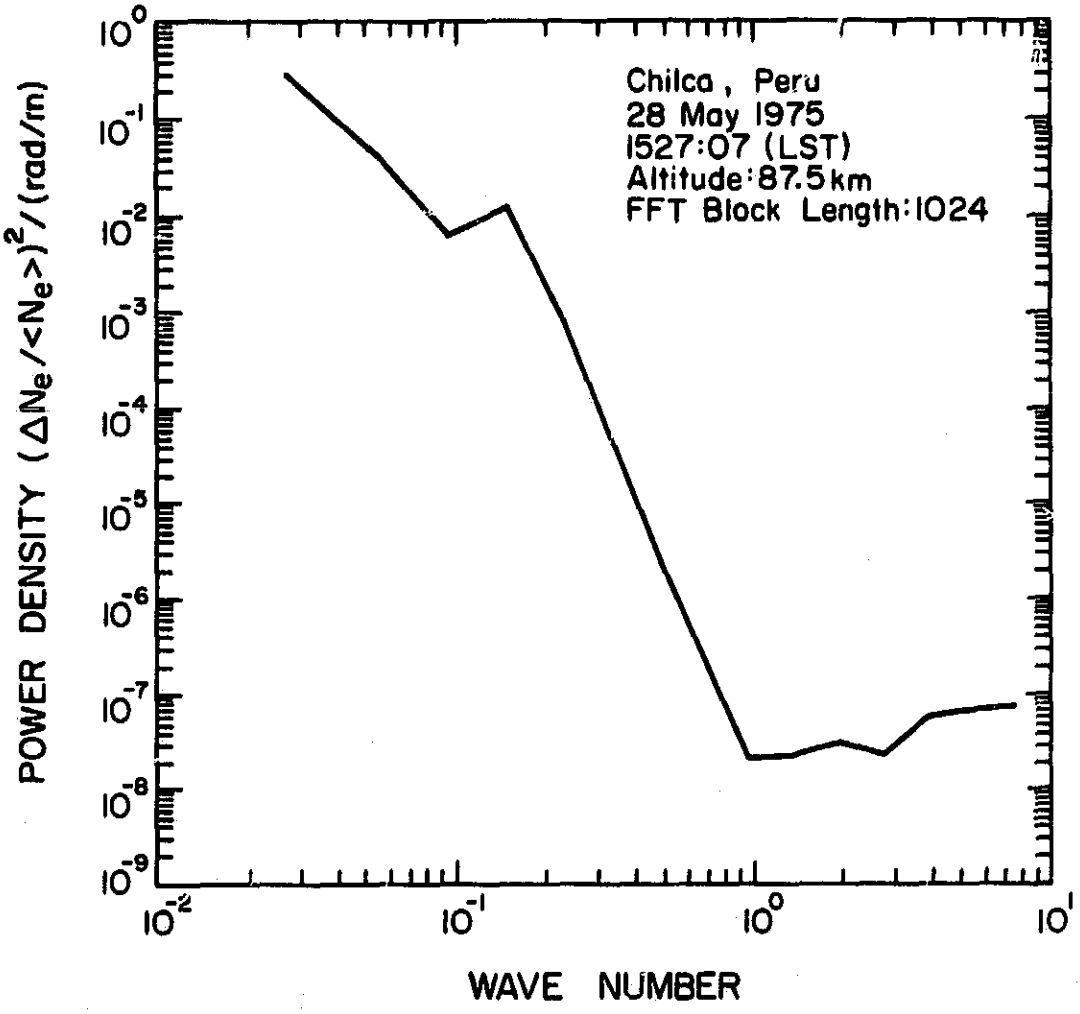

Figure 5.3 Smoothed difference spectrum of the 87.5 km irregularity.

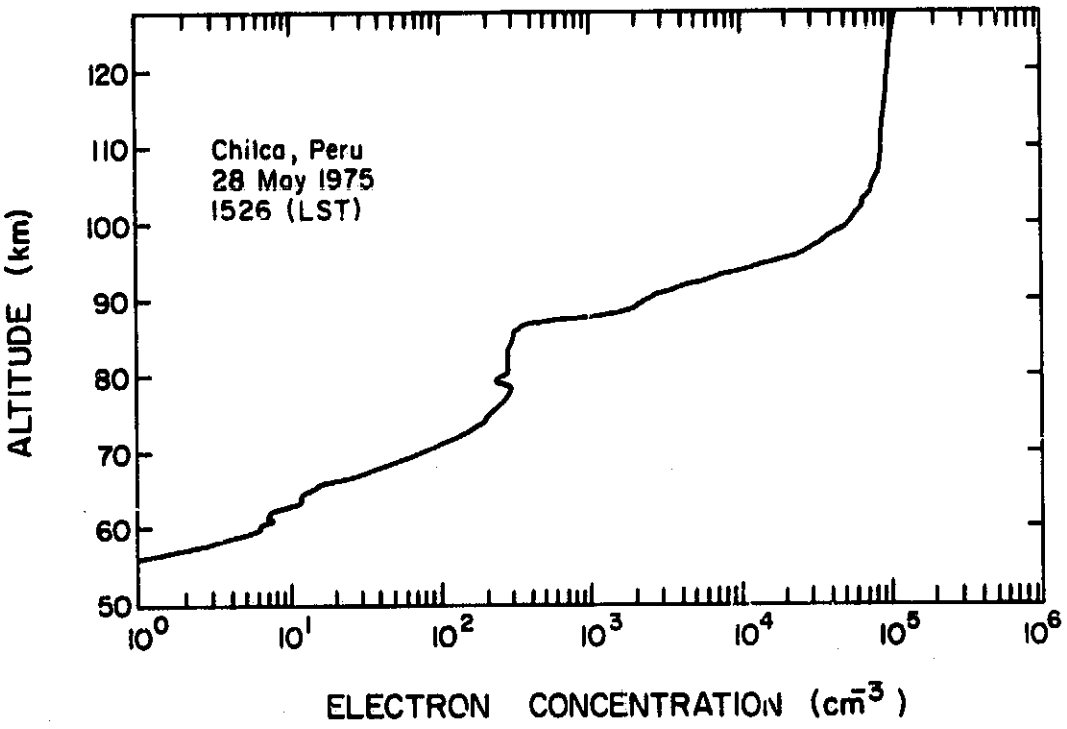

Figure 5.4 Electron concentration profile for the 28 May 1975 Peru flight.

the attenuation calculated. For example, the maximum deviation observed in Figure 5.1 is 1.2%. The main frequency component of the deviation appears to be 44 Hz. With a lower 3 dB frequency of 54 Hz, the amplifier attenuates a 44 Hz signal by 1.6. The corrected deviation is thus 1.6 x 1.2% = 1.9%. All deviations in Table 5.1 represent corrected values.

The 18 January 1976 Wallops Island flight was launched from Wallops Island, Virginia (37.8° N 75.5° W) at 14 12 LST. The primary purpose of the flight was to observe the winter anomaly. The rocket also carried a mass spectrometer prepared by the University of Bern, Switzerland. The placement of the spectrometer beneath the nose cone prevented the use of a nose tip probe configuration. Instead, the probes were placed on booms extended from the sides of the rocket payload. Unfortunately, the nose cone shell detachment to expose the spectrometer malfunctioned during the flight, damaging the telemetry system and the propagation experiment. Thus no calibration between electron density and probe current could be calculated. The probe and fine structure experiments were not damaged. A description of this flight is given in Edwards (1976).

Since no calibration is available for the probe current the electron density can be only roughly estimated. Processed values for the probe current are also unavailable. Fortunately, the raw probe current signal is available on analog tape (IRIG channel 15). Plotting this signal on a strip chart provides a way to measure the probe current, albeit with less accuracy than a digital analysis would yield. To convert the observed current to electron density, an average calibration value from other flights is applied. Using a calibration value of 3×10^9 cm^{-3}/A yields the concentration data shown in Table 5.1. Due to the coarseness of the probe current measurement and the high degree of spin contamination, calculations of the

electron density gradient are unreliable, and only order of magnitude estimates are given. It is possible to observe a large positive gradient in the probe current beginning at 84 km.

The data reveal four ionospheric irregularities. Their altitudes and thicknesses are given in Table 5.1. As observed in Figure 4.3, spin contamination is a serious problem in the fine structure data from the 18 January 1976 Wallops Island flight. To calculate a power spectrum estimate, a number of noise samples are analyzed and their average spectrum subtracted from the irregularity spectrum. The segments of noise and irregularity data have the same phase with respect to the spin contamination. The slope and limits of the best lines fit to the spectra are given in Table 5.1. A smoothed spectrum from the irregularity at 82.2 km is given in Figure 5.5.

The 12 August 1976 Wallops Island flight was launched at 10 54 (LST). The main purpose of the probe experiment on the rocket was to observe sporadic E layers. Details of the probe current analysis are given in Edwards (1977). The fine structure experiment again used a boom probe configuration. The spin contamination was very small. It should be noted that the propagation experiment data on this flight are unreliable above 84 km (Edwards, 1977). This unreliability contributes uncertainty to the electron density calculations above 84 km since the propagation experiment is used to calibrate the probe current.

Only one irregularity is observed in the data, occurring at 83.5 km. A smoothed spectrum from this irregularity is shown in Figure 5.6. This irregularity is superposed upon the steep electron density gradient often observed between 80 and 90 km. The peak fluctuation of the irregularity is unusually high: 13%.

The 8 January 1977 Wallops Island flight was launched at 14 03 (LST).

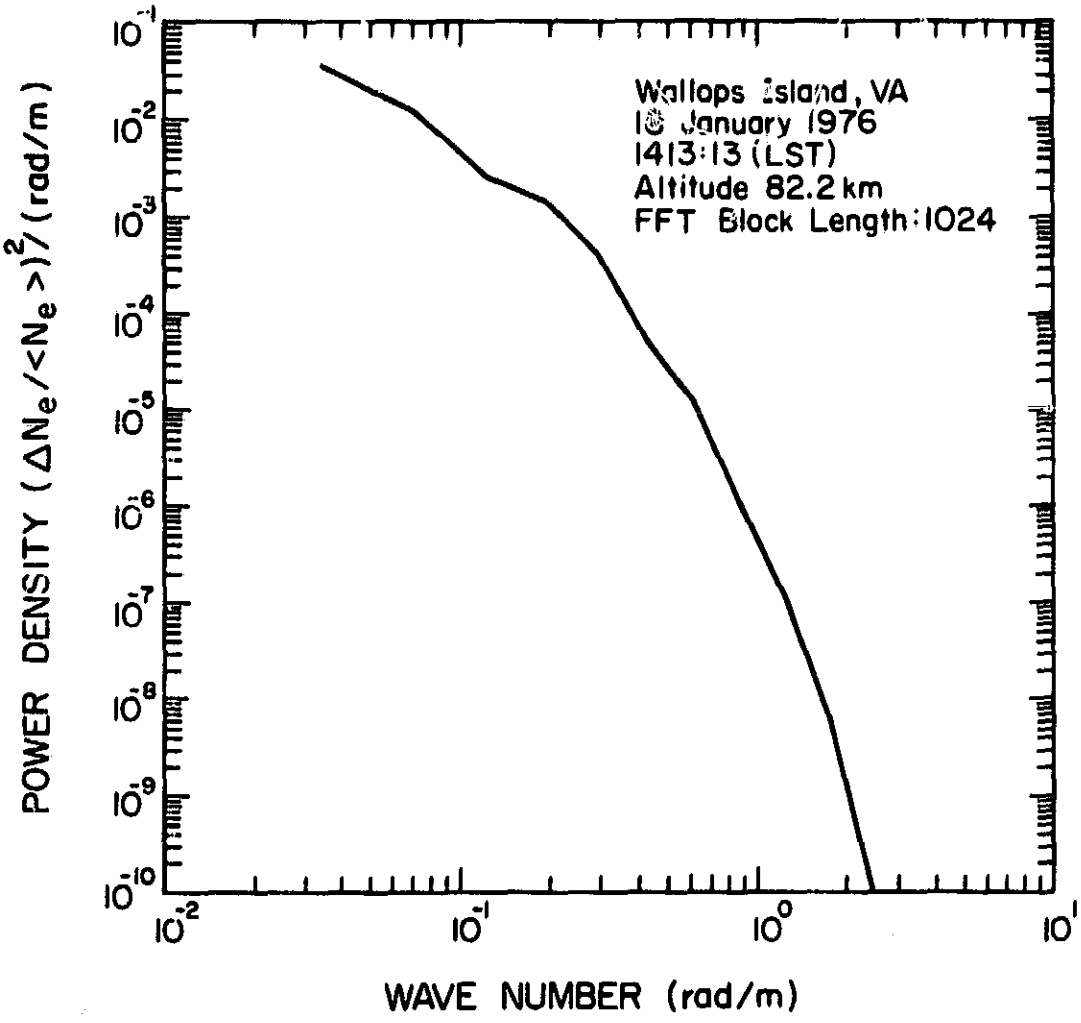

Figure 5.5 Smoothed difference spectrum of the 82.2 km irregularity from the 18 January 1976 Wallops Island flight.

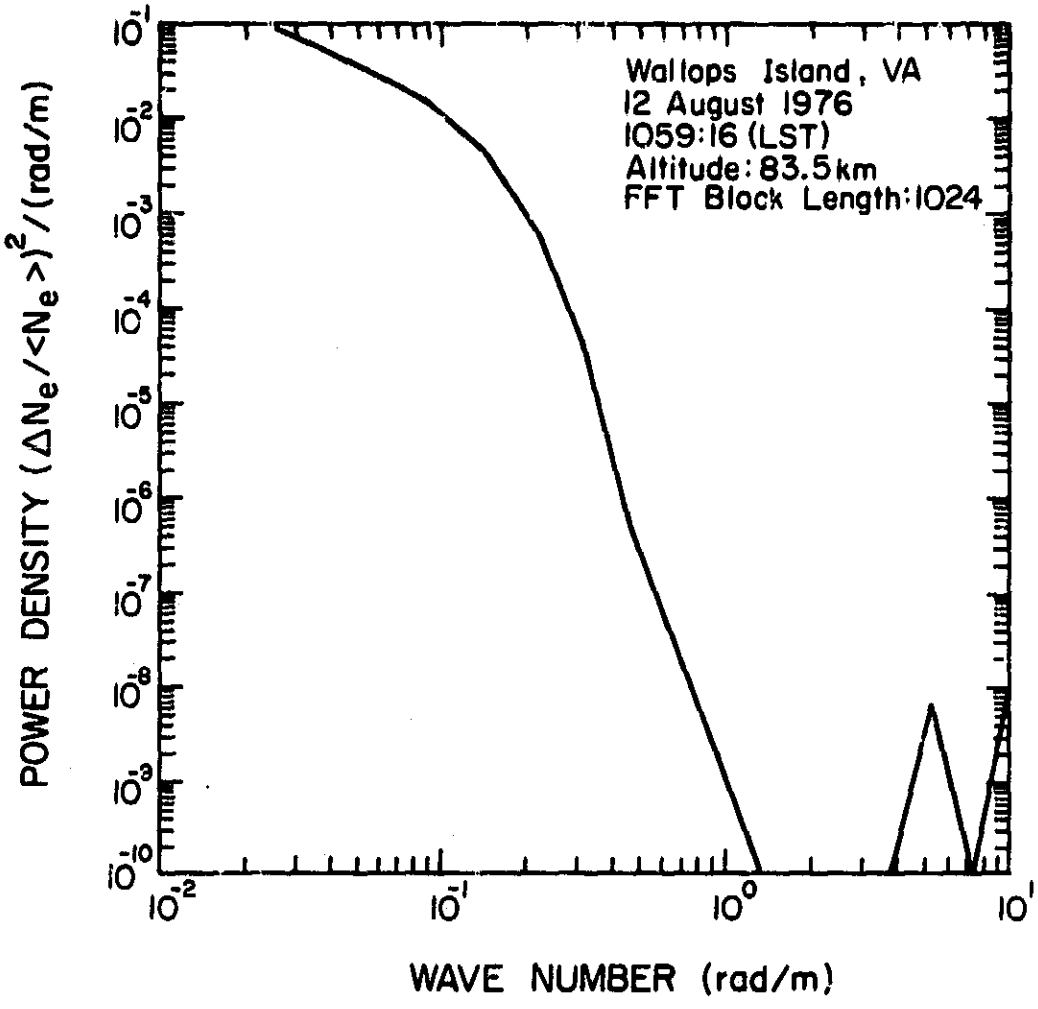

Figure 5.6 Smoothed difference spectrum of the 83.5 km irregularity from the 12 August 1976 Wallops Island flight.

The primary purpose of the flight was to observe the winter anomaly. A description of the flight preparations is given in Edwards (1977). The data suffered from moderate spin contamination.

Only one irregularity was observed. As shown in Table 5.1, the irregularity extended over a relatively short altitude range. Figure 5.7 gives the smoothed spectrum. The large dip at 0.06 rad/m results from the estimated noise spectrum exceeding the estimated signal plus noise spectrum.

The 27 February 1983 Peru flight was launched from the Punta Lobos site at 11 33 (LST). Its principal purpose was to study electron concentration in the equatorial D and E regions. On this flight the fine structure experiment was modified to allow greater gain in the ac amplifier. These changes are documented in Roth (1982a, 1982b). The flight did not carry the mass spectrometer, permitting use of the nose tip probe configuration.

The data reveal one irregularity at 85.8 km, superposed on a steep electron density gradient. This irregularity is thoroughly investigated by Royrvik and Smith (1984) and is compared to simultaneous coherent scatter measurements at Jicamarca. A spectrum of this irregularity is shown in Figure 5.8.

5.3 Discussion of Results

All spectra calculated show a low wave number range over which a power law may be fitted. That the slope of this fitted line usually has a value close to -5/3 (Table 5.1) suggests the presence of an inertial range of turbulence. As a consequence of spectral aliasing, the one-dimensional spectra do not show the spectral decrease expected below the inertial range in the three-dimensional spectra. In the wave number ranges above the suspected inertial range, the measured spectra do not always demonstrate the same behavior. Some show a second power law range, as in Figures 5.2a and

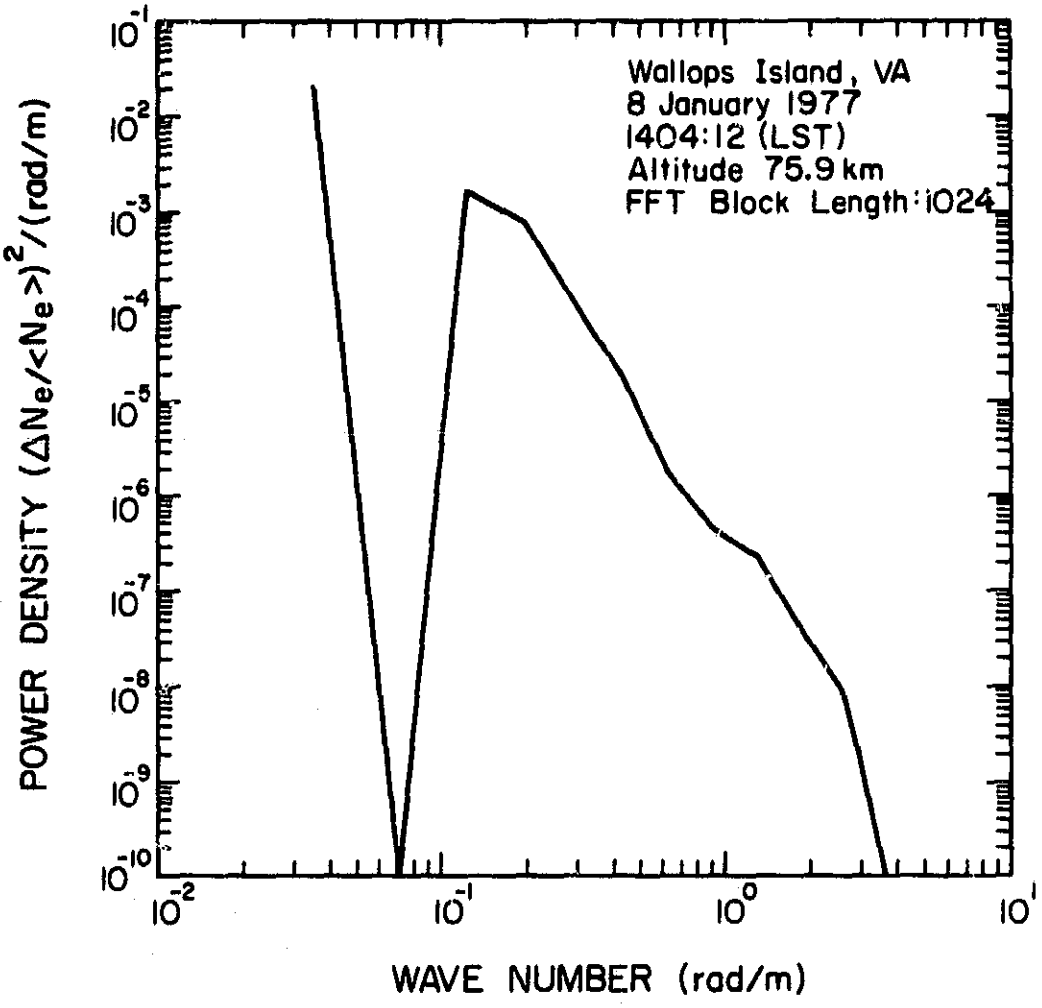

Figure 5.7 Smoothed difference spectrum of the 75.9 km irregularity from the 8 January 1977 Wallops Island flight.

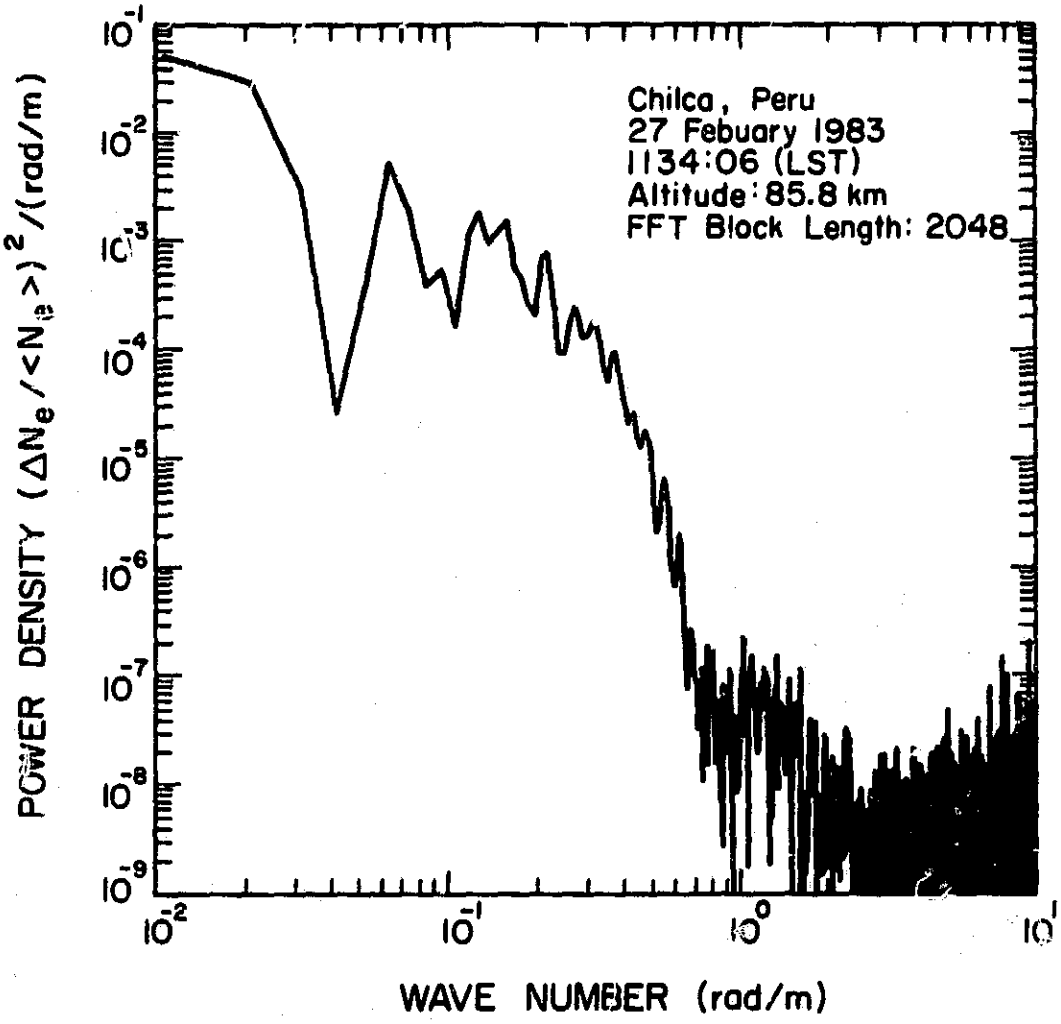

Figure 5.8 Spectrum of the 85.8 km irregularity from the 27 February 1983 Peru flight.

5.3, while others show a more curved decrease in spectral power. In all spectra the telemetry noise floor prevents observation of the upper wave number behavior over any sizable wave number range. It is interesting to note that three of the five flights discussed show irregularities superposed upon the electron density gradients. All three irregularities have quite high maximum $\Delta N_e/\langle N_e \rangle$ values.

Qualitative comparisons may be made with the spectral model of Hill and Bowhill (1976) described in Chapter 3. Figure 3.3 shows the predicted spectra for various values of the parameter ξ, equal to $2\beta(k^*/k_c)^{4/3}$. This parameter should be of the order of unity in the D region. The predicted spectrum for $\xi \simeq 1$ shows no viscous-convective range or power law above the inertial range. No viscous-convective range is found in any of the irregularities observed, in agreement with the model. Figures 5.5, 5.6, 5.7, and 5.8 show a curved decrease as predicted by the spectral model. In contrast to the model, Figures 5.2a and 5.3 show a power law dependence above the apparent inertial range.

The results of Table 5.1 may be compared with predictions by Rastogi and Bowhill (1976) of the wave number extent of the -5/3 power law dependence. For two models of ε, Rastogi and Bowhill (1976) calculate the variation of k_d with altitude. Figures 5.9a and 5.9b, using model 1 and model 2 of ε, respectively, show three wave number ranges. Below k_ν the energy spectrum should vary as $k^{-5/3}$. Above k_i the spectrum is predicted to fall off exponentially. Superposed upon Figures 5.9a and 5.9b are the upper wave number limits given in the last column of Table 5.1. It should be noted that the calculated spectra used in creating Table 5.1 are one-dimensional spectra. As suggested by Figure 3.1, the upper limit of the -5/3 power law reaches a higher wave number in the three-dimensional

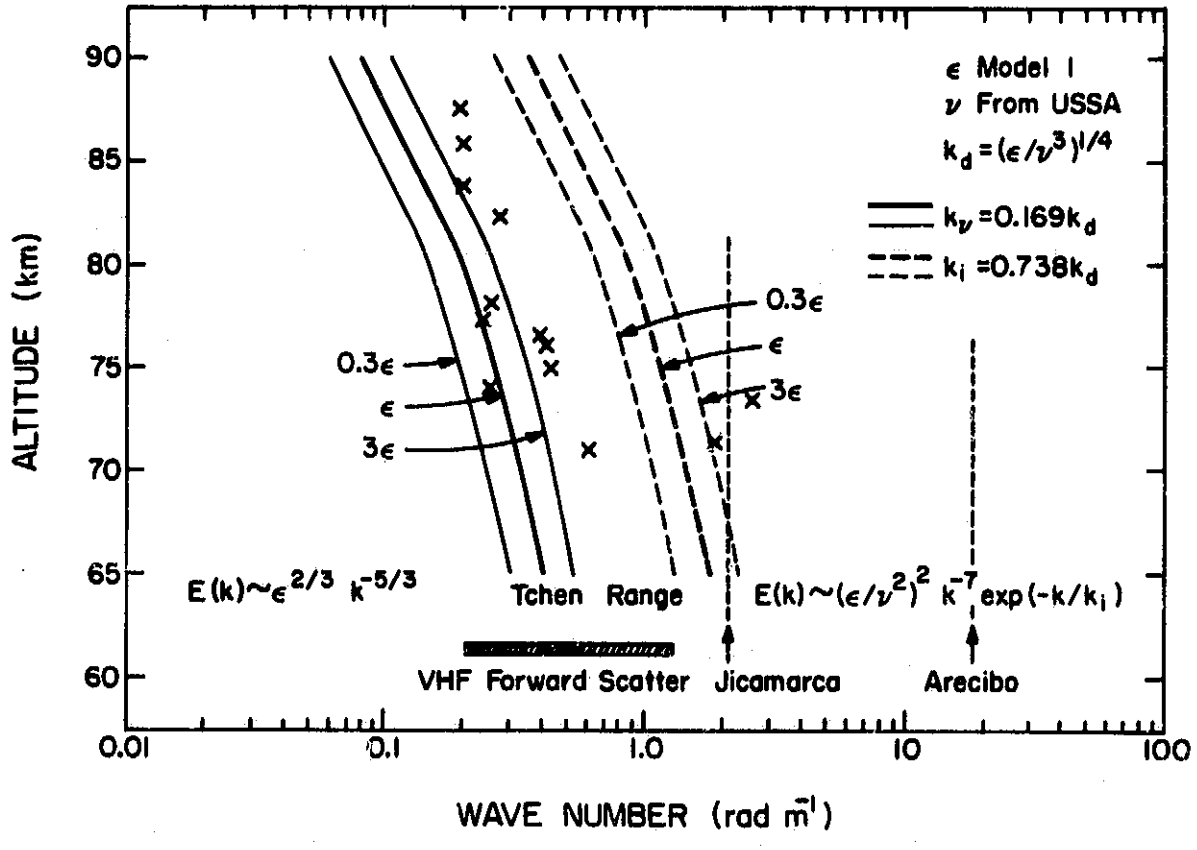

Figure 5.9a Suggested profile of cutoff wave number demarcating range where -5/3 power law holds ($k < k_\nu$). Wave number of Jicamarca (50 MHz) and Arecibo (430 MHz) incoherent scatter radars are shown. The wave number range used for VHF forward scattering is also shown. ε from model 1 (Rastogi and Bowhill, 1976).

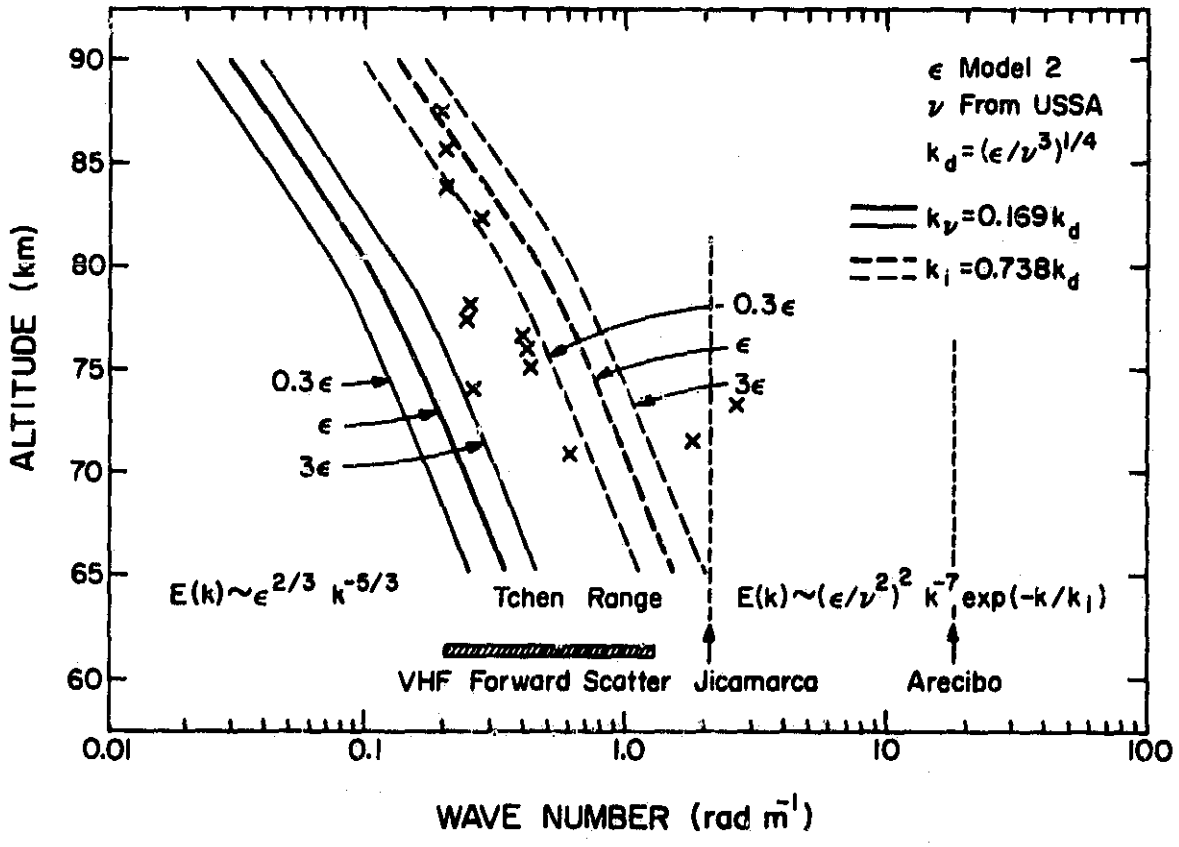

Figure 5.9b Suggested profile of cutoff wave number demarcating range where -5/3 power law holds ($k < k_\nu$). Wave number of Jicamarca (50 MHz) and Arecibo (430 MHz) incoherent scatter radars are shown. The wave number range used for VHF forward scattering is also shown. ε from model 2 (Rastogi and Bowhill, 1976).

scalar spectrum than in the one-dimensional spectrum. The values in Table 5.1 thus underestimate the upper wave number limit of the apparent inertial range. Also, the values plotted in Figures 5.9a and 5.9b are from scalar spectra, as opposed to energy spectra. However, viscous and diffusive effects should be expected to begin at approximately the same wave number since $k_c \approx k_d$ in the mesosphere. It is thus not surprising that the scalar spectrum inertial range extends to the same order of wave number as the energy spectrum as suggested by Figures 5.9a and 5.9b.

5.4 Conclusions

The scalar spectra shown in this chapter demonstrate consistency with theories of homogeneous, isotropic turbulence measured in one dimension. All the spectra show a definite wave number range over which the scalar spectrum varies as a negative power of k. Most theories of turbulence predict an inertial range with a $k^{-5/3}$ dependence. The data in Table 5.1 give spectral slopes close to -5/3, consistent with an inertial range. Above the inertial range, turbulence theory predicts that viscous and diffusive effects cause a precipitous decrease in the spectrum. Due to the small Schmidt number, no viscous-convective range is expected in mesospheric turbulence.

Although not in agreement on the exact form, most turbulence theories predict an exponential decrease in the spectrum above the inertial range. Hill and Bowhill (1976) incorporate these theories into a model for the scalar spectrum. The model is extended to one-dimensional spectra under the assumption of isotropy. Many of the measured spectra agree qualitatively with the shape of the predicted spectrum. To show further consistency with turbulence theory the spectra are compared to predictions by Rastogi and Bowhill (1976). They predict the upper wave number extent of the inertial

range. The measured limits agree approximately to the predictions. Perhaps more importantly, the measured inertial limits decrease with increasing altitude, in agreement with the functional dependence on altitude predicted by Rastogi and Bowhill (1976). The agreement of the measured spectra with the models of Hill and Bowhill (1976) and Rastogi and Bowhill (1976) support the conclusion that the observed ionospheric irregularties are consistent with irregularities expected from atmospheric turbulence.

6. SUMMARY AND SUGGESTIONS FOR FUTURE WORK

6.1 Summary

Mesospheric electron density irregularities are often observed by both radar and rocket studies. These irregularities are suspected to be the result of turbulent advection of ions and electrons. Possible mechanisms for generating atmospheric turbulence include Kelvin-Helmholtz and Rayleigh-Taylor instabilities. Turbulence may be qualitatively described as the cascading of energy from large scales to small scales. At the smallest scales the turbulent energy is dissipated by viscosity (for turbulence in a velocity field), or by molecular diffusivity (for turbulence in a scalar field). Most theoretical studies of turbulence attempt to estimate the spectrum of homogeneous, isotropic turbulence. Physically, such a spectrum gives the turbulent energy per wave number. Most theories predict an inertial range in the spectrum for flows with sufficiently high Reynolds number. The spectrum is expected to vary as $k^{-5/3}$ in the inertial range. The theories do not agree closely in describing the scalar spectrum above the inertial range, although most theories in general predict an exponential decrease with increasing wave number.

Langmuir probes on sounding rockets provide an in situ method of measuring mesospheric electron density irregularities. In the fine structure experiment flown by the University of Illinois, a Langmuir probe is extended from the rocket into the ionosphere. As the rocket passes through an irregularity, the probe current fluctuates in time. With the assumption of isotropy, temporal fluctuations are interpreted as spatial fluctuations measured in one dimension. The measured current from the probe is processed on board the rocket to produce a voltage proportional to $\Delta N_e/\langle N_e \rangle$. The

signal is telemetered to the ground and is stored on an FM analog tape.

Using digital analysis, the power spectra of the irregularities are estimated. The analog data are digitized with a microcomputer based digitizer. The microcomputer stores the digital data on floppy disks. The data are then transferred to a CDC Cyber mainframe computer for spectral analysis. The FORTRAN program SPECTRA estimates the power spectra of the irregularities using an FFT routine available on the Cyber. Further processing subtracts estimates of the background noise spectra and smooths the result of the subtraction. These smoothed spectra help to identify spectral indices and general trends in the spectra.

The measured spectra appear consistent with the predictions of turbulence theory. The observed spectra all exhibit power laws with spectral indices close to -5/3, consistent with an inertial range of turbulence. Comparisons to a spectral model by Hill and Bowhill (1976) and to predictions of inertial range limits by Rastogi and Bowhill (1976) show further consistency with theory.

6.2 Suggestions for Future Work

There are two significant ways by which the fine structure experiment could be improved. Coincident radar measurements would help to establish the existence of a turbulent layer and perhaps help to determine isotropy. Reduction of telemetry noise would increase the upper wave number limit of the turbulence spectrum.

Coincident radar measurements of an irregularity would provide data unattainable from the Langmuir probe experiment. The coherent-scatter radar technique can measure a single component of the scalar spectrum. The advantage of the radar technique is its ability to measure a spectral component that in the rocket data is obscured by telemetry noise. The radar

thus provides insight into the shape of the spectrum at wave numbers above the inertial range. The combination of radar and rocket measurements is used by Royrvik and Smith (1984) to compare measurements of an irregularity from the 27 February 1983 Peru flight with coincident radar measurements at Jicamarca. Radar can also measure aspect sensitivity of an irregularity, an indication of anisotropy. This property cannot be measured by the fine structure experiment. Knowledge of isotropy is essential in allowing comparisons of measured one-dimensional spectra with theories predicting three-dimensional spectra.

Reduction of telemetry noise would increase the highest observable wave number of a measured spectrum. Telemetry noise could be greatly reduced by use of a digital telemetry system. One possible analog noise reduction scheme is described in Roth (1982b). Essentially, the method takes advantage of the relatively large spectral magnitude expected at low frequencies in an irregularity spectrum. The fine structure experiment described by Klaus and Smith (1978) uses an approximately 50 Hz 3 dB point in the ac amplifier high pass filter to prevent saturation of the telemetry system by the low frequencies. Further attenuation of the low frequencies allows the overall gain to be increased, giving a better ratio of signal to telemetry noise. The new system places the 3 dB point at 400 Hz and raises the ac amplifier gain to 400. The power spectra calculated from this new system show an order of magnitude decrease in the telemetry noise floor. Ideally the 3 dB point should occur just below the frequency at which the irregularity spectrum crosses the telemetry noise floor. Inclusion of this system in future rocket flights would raise the highest observable wave number of the calculated spectra.

The above analog noise reduction scheme could be improved by the use of

a more elaborate filter. If instead of a single-pole low pass filter the ac amplifier used a filter more closely matched to the expected irregularity spectrum, then the amplifier gain could be increased further, improving the ratio of signal to telemetry noise. SPECTRA could then easily correct the calculated irregularity spectra for the filter transfer function.

APPENDIX I FREQUENCY RESPONSE OF AN AC AMPLIFIER

To make corrections for the filtering of the ac amplifier used in the fine structure experiment the upper and lower 3 dB points of the frequency response need to be known. Figure I.1 shows a circuit diagram of the amplifier circuit. The logarithmic electrometer driving the ac amplifier has an output impedence of 1 kΩ. Including the electrometer output impedance in series with the 11 kΩ resistor gives an amplifier gain of 100 and upper and lower 3 dB frequencies of 1.7 kHz and 60 Hz, respectively.

The frequency response of three amplifier circuits was measured. To simulate payload conditions the amplifiers were tested after their incorporation into circuit modules used in an actual payload. A Hewlett Packard frequency synthesizer (model 3325A) was used as the input to the ac amplifiers. The frequencies at which the amplifier output was attenuated by $2^{-1/2}$ times the maximum output are given in Table I.1.

The deviation of the measured values from theoretical predictions does not seriously affect the data analysis. The measured lower 3 dB frequencies are in good agreement with the value of 54 Hz found by Klaus and Smith (1978) for the 28 May 1975 Peru flight. Unfortunately, the lower 3 dB frequencies were not measured on the other eight flights studied in this thesis. The lower 3 dB frequency is needed by SPECTRA to correct for the ac amplifier high pass filter. The value 54 Hz is adopted to represent the 3 dB point for all flights. Although the measured upper 3 dB frequencies differ markedly from the expected values, telemetry noise dominates the irregularity spectrum at frequencies of the order of the upper 3 dB frequency. Exact correction for the ac amplifier low pass filtering is thus unimportant. However, should telemetry noise be reduced on future flights

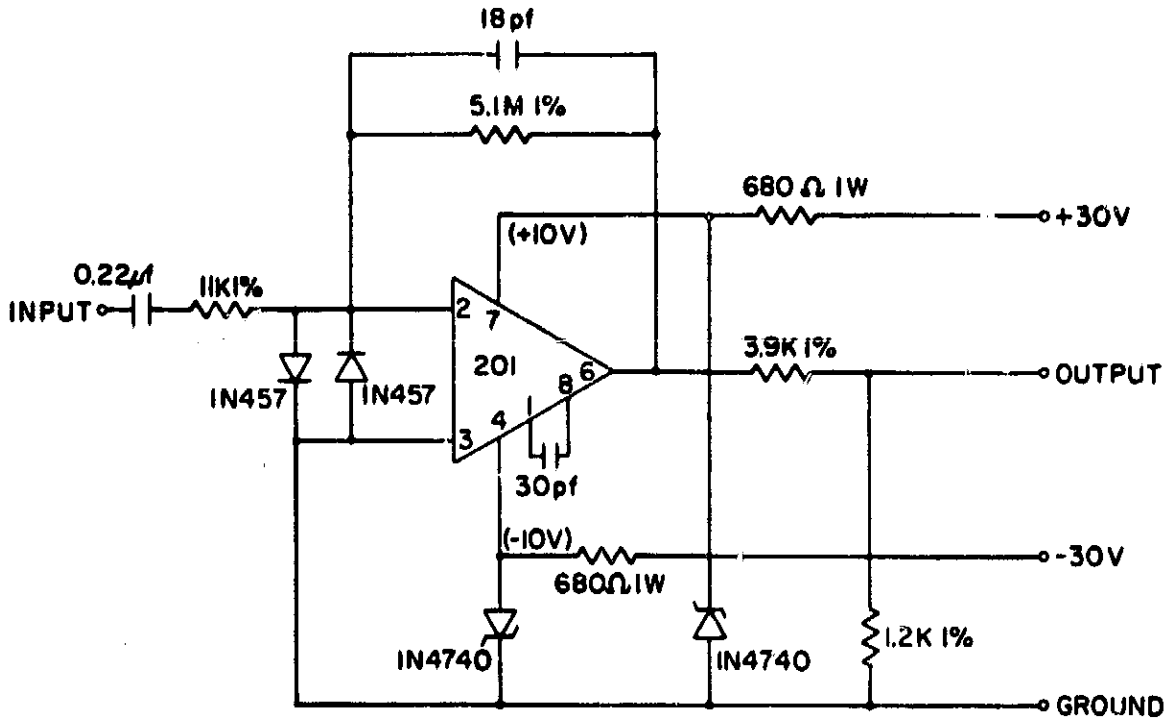

Figure I.1 Circuit diagram of ac amplifier used in fine structure experiment.

Table I.1 Measured frequency response of ac amplifiers.

Amplifier	Lower 3 dB Frequency (Hz)	Upper 3 dB Frequency (Hz)
1	57	806
2	52	1140
3	58	1000

to such a level that the irregularity spectrum is stronger than the high frequency telemetry noise, then pains should be taken to accurately measure the upper 3 dB frequency.

APPENDIX II SOFTWARE LISTINGS

II.1 DIGIAUTOSTART

```
SOURCE FILE: DIGIAUTOSTART
0000:            1 ;THIS PROGRAM TAKES A LARGE NUMBER
0000:            2 ;OF SAMPLES FROM THE A/D CARD AND PUTS THEM IN A BUFFER.  THE STARTING
0000:            3 ;ADDRESS IS GIVEN BY BUFH AND BUFL.  SINCE BASIC MEMORY STARTS AT $9600
0000:            4 ;(WITH DOS LOADED) AND WORKS DOWN, DIGIAUTOSTART SHOULD BE LOADED A WAYS
0000:            5 ;BELOW THAT TO ALLOW FOR A BASIC PROGRAM.  $8000 IS SUGGESTED.  THE PROGRAM
0000:            6 ;PROGRAM DIGITIZER CONTROL TAKES UP ABOUT A PAGE OF MEMORY ($100).  AS IS,
0000:            7 ;THIS PROGRAM RUNS AT A DIGITIZING RATE OF 5 KHZ.  THE JOHN BELL INTERFACE
0000:            8 ;CARD IS IN SLOT 4.  THE A/D SLOT IS NOT FIXED BUT IS CONTROLLED BY CHNL.
0000:            9 ;THIS PROGRAM ALSO ASSUMES A REFERENCE FREQUENCY OR 100 KHZ, OR 10 USEC
0000:           10 ;PER REFERENCE PULSE.  TO CHANGE THE DIGITIZENG RATE THE DGPAUS ASSIGNMENT
0000:           11 ;MUST BE CHANGED.  TO CHANGE THE J.B. CARD SLOT THE BELSLT ASSIGNMENT MUST
0000:           12 ;BE CHANGED.  BOTH CHANGES REQUIRE RECOMPILING.  THE DATA COLLECTION IS
0000:           13 ;IS TRIGGERED BY A POSITIVE TRANSITION ON THE CAi LINE OF THE JOHN BELL CARD.
0000:           14 ;A 1 PULSE PER SECOND SIGNAL IS AVAILABLE FROM THE TIME CODE TRANSLATOR
0000:           15 ;IN THE ROCKET LAB.  THE PROGRAM USES THE JOHN BELL CARD TO COUNT A
0000:           16 ;NUMBER OF EXTERNAL CLOCK CYCLES.  WHEN THE COUNT IS UP, THE J.B. CARD
0000:           17 ;GENERATES AN AN INTERRUPT REQUEST SIGNAL.  THE COMPUTER GETS OUT OF THE
0000:           18 ;WAIT LOOP AND JUMPS TO THE INTERRUPT SERVICE ROUTINE CALLED IHNDLR.
0000:           19 ;THIS PROGRAM IS A MODIFICATION OF A PROGRAM CALLED CLKREAD.  CLKREAD
0000:           20 ;AND OTHER A/D PROGRAMS CAME WITH THE MOUNTAIN HARDWARE D/A A/D CARD.
0000:           21 ;DIGIAUTOSTART BY ROD STOLTZFUS, WRITTEN SEPTEMBER 1984
0000:           22 ;FOR THE AERONOMY LAB AT THE UNIVERSITY OF ILLINOIS.
------ NEXT OBJECT FILE NAME IS DIGIAUTOSTART.OBJ0
8000:           23         ORG  $8000      ;PUT PROGRAM AT LOCATION $8000
8000:78         24 START   SEI              ;CALLED FROM A BASIC PROGRAM, START JUMPS TO
8001:           25 ;                         SUBROUTINE INIT AND INITIALIZES THE PERIPHERAL CARDS.
8001:4C 72 80   26         JMP  INIT
8004:78         27 STOP    SEI              ;RESTORES REGISTERS AND SUCH.
8005:4C E1 80   28         JMP  FINISH
8008:4C 1B 80   29 TICK    JMP  IHNDLR      ;INTERRUPT SERVICE ROUTINE.  THE INTERRUPT
800B:           30 ;                         VECTOR $03FE AND $03FF CONTAINS IHNDLR'S
800B:           31 ;                         ADDRESS NOT TICK'S ADDRESS.
800B:4C 07 81   32 DUMMY   JMP  WAIT        ;A LOOP IN WHICH TO WAIT FOR AN INTERRUPT.
800E:           33 ;*************************************************************
800E:           34 ;DATA STORAGE LOCATIONS: POKED BY A BASIC PROGRAM.
800E:           35 ;*************************************************************
800E:           36 CHNL    DS   1           ;=A/D SLOT# * 16 + A/D CHANNEL NUMBER (0 TO 15).
800F:           37 BUFFER  DS   1           ;HIGH BYTE OF STARTING ADDRESS OF THE BUFFER
8010:           38 ;                         WHICH HOLDS THE DATA.  LOW BYTE ASSUMED TO BE $00.
8010:           39 ;                         THIS ASSUMPTION MAY BE ALTERED BY CHANGING BUFL
8010:           40 ;                         IN THE INIT SUBROUTINE.
8010:           41 COUNT   DS   2           ;NUMBER OF SAMPLES TO BE TAKEN AND STORED.
8012:EA         42         NOP
8013:EA         43         NOP
8014:           44 INTADH  DS   1           ;HIGH BYTE OF IHNDLR ADDR. PROBABLY EQUAL TO THE
8015:           45 ;                         HIGH BYTE OF THE ORG ADDRESS (SEE FIRST LINE).
8015:           46 ;*************************************************************
8015:           47 ;INTERNAL VARIABLES NEXT
8015:           48 ;*************************************************************
8015:00         49 FLAG    DFB  $00         ;NOT USED
8016:00         50 STATUS  DFB  $00         ;NOT USED
8017:00         51 BUFL    DFB  $00
8018:           52 BUFH    DS   1
8019:           53 SAMPLE  DS   1
801A:           54 TMPHLD  DS   1           ;USED FOR TEMPORARILY HOLDING A BYTE.
801B:           55 ;*************************************************************
801B:           56 ;EQUATES
801B:           57 ;*************************************************************
801B:           58 ;THE BASE ADDRESS FOR ALL APPLE SLOTS IS $C000.
801B:           59 ;THE J.B.CARD ADDRESSES START AT C500 WHERE "S" IS THE J.B.'S SLOT NUMBER.
801B:           60 ;THE J.B. CARD USES THE ROM LOCATIONS, NOT THE DEDICATED LOCATIONS, ON
801B:           61 ;THE APPLE I/O MAP.  THE A/D CARD USES THE DEDICATED ADDRESSES SO THE
801B:           62 ;A/D BASE ADDRESS IS $C080.
```

```
0004:           63 BELSLT  EQU  4          ;J.B. CARD IN SLOT 4.
C400:           64 JBBASE  EQU  BELSLT*256+49152 ;THE BASE ADDRESS OF THE J.B. CARD.
C00E:           65 SETINT  EQU  14         ;INTERRUPT ENABLE ADDRESS REGISTER ON THE J.B. CARD.
0009:           66 CLRIRQ  EQU  9          ;J.B. CARD TIMER2 INTERUPT CLEAR AND COUNTER START.
0008:           67 TMADDR  EQU  8          ;LOW BYTE OF TIMER2 LATCH.
8010:           68 CNTL    EQU  COUNT      ;LOW BYTE OF ADDRESS CONTAINING THE NUMBER
801B:           69 ;                         OF SAMPLES TO BE TAKEN.
0002:           70 DDRA    EQU  2          ;DATA DIRECTION REGISTER A ON JOHN BELL CARD.
0003:           71 DDRB    EQU  3          ;DATA DIRECTION REGISTER B ON JOHN BELL CARD.
8011:           72 CNTH    EQU  CNTL+1     ;HIGH BYTE OF SAME ADDRESS.
000B:           73 ACR     EQU  11         ;AUX REGISTER ADDRESS ON J.B. CARD.
C408:           74 T2CL    EQU  JBBASE+TMADDR ;ABSOLUTE ADDRESS OF TIMER 2 COUNTER LOW BYTE.
801B:           75 ;                         WRITING T2CL WRITES TO THE LATCH.  READING T2CL
801B:           76 ;                         READS FROM THE COUNTER LOW BYTE.
C409:           77 T2CH    EQU  JBBASE+CLRIRQ ;ABSOLUTE ADDRESS OF HIGH COUNTER BYTE.
801B:           78 ;                        THERE IS NO TIMER 2 HIGH LATCH BYTE.
000D:           79 IFR     EQU  13         ;INTERRUPT FLAG REGISTER ADDRESS ON J.B. CARD.
C40D:           80 JBIFR   EQU  JBBASE+IFR ;ABSOLUTE ADDRESS OF IFR.
000C:           81 PCR     EQU  12         ;ADDRESS OF PERIPHERAL CONTROL REGISTER.
C40D:           82 JBPCR   EQU  JBBASE+IFR ;ABSOLUTE ADDRESS OF J.B. PCR
0012:           83 DGPAUS  EQU  18         ;THIS CONTROLS THE DIGITIZING PERIOD. SEE IHNDLR.
C402:           84 JBDDRA  EQU  JBBASE+DDRA ;ABSOLUTE ADDRESS OF DATA DIRECTION REGISTER A
C403:           85 JBDDRB  EQU  JBBASE+DDRB ;ABSOLUTE ADDRESS OF DATA DIRECTION REGISTER B
801B:           86 ;
801B:           87 ;*************************************************************
801B:           88 ;    INTERRUPT HANDLER
801B:           89 ;*************************************************************
801B:           90 ;                  THIS ROUTINE IMMEDIATELY RESTARTS THE J.B. CARD
801B:           91 ;                  COUNTDOWN.  IT THEN TAKES A SAMPLE FROM THE A/D CARD,
801B:           92 ;                  FIGURES OUT WHERE THE NEXT FREE BUFFER ADDRESS IS,
801B:           93 ;                  STORES THE SAMPLE THERE, INCREMENTS THE VALUE OF THE
801B:           94 ;                  NEXT FREE BUFFER ADDRESS, AND DECREMENTS THE NUMBER
801B:           95 ;                  OF SAMPLES YET TO BE TAKEN.
801B:           96 ;
801B:           97 ;
801B:A5 45      98 IHNDLR  LDA  $45        ;THE APPLE INTERRUPT RESPONSE
801D:           99 ;                        PUTS THE ACCUMULATOR AT $45.
801D:48        100        PHA
801E:          101 ;                       GET THE ACCUMULATOR FROM $45
801E:          102 ;                       AND PUT IT ON THE STACK.
801E:8A        103        TXA
801F:48        104        PHA
8020:98        105        TYA
8021:48        106        PHA
8022:          107 ;
8022:          108 ;                       RELOAD AND RESET TIMER2 LATCH ON J.B. CARD.
8022:          109 ;
8022:18        110        CLC
8023:AD 08 C4  111        LDA  T2CL       ;LOAD ACCUMULATOR WITH THE LOW COUNTER BYTE,
8026:          112 ;   WHICH BY THIS POINT HAS DECREMENTED BELOW ZERO.
8026:69 12     113        ADC  #DGPAUS    ;ADD 18 TO IT.  SINCE TIMER2 RESTART IS 20 CYCLES
8028:          114 ;                       AWAY AND THE REFERENCE PULSES ARE 10 USEC LONG,
8028:          115 ;                       TWO REFERENCE PULSES WILL HAVE PASSED
8028:          116 ;                       PASSED BY THE TIME TIMER2 IS RESTARTED
8028:8D 08 C4  117        STA  T2CL       ;REMEMBER THAT WRITING T2CL WRITES
802B:          118 ;                       TO THE LATCH NOT THE COUNTER.
802B:          119 ;                        THIS STEP RELOADS THE TIMER LATCH APPROPRIATELY.
802B:A9 00     120        LDA  #00
802D:EA        121        NOP
802E:EA        122        NOP
802F:EA        123        NOP
8030:EA        124        NOP
8031:8D 09 C4  125        STA  T2CH       ;STORE 0 IN THE HIGH COUNTER BYTE, STARTING TIMER2.
8034:AE 0E 80  126        LDX  CHNL
8037:BD 80 C0  127        LDA  $C080,X    ;READ A SAMPLE AND START ON A NEW READING.
803A:EA        128        NOP
803B:EA        129        NOP
803C:EA        130        NOP
803D:EA        131        NOP
803E:EA        132        NOP
803F:BD 80 C0  133        LDA  $C080,X    ;READ SAMPLE STARTED BY PREVIOUS LINE.
8042:8D 19 80  134        STA  SAMPLE     ;STORE THE SAMPLE IN A TEMPORARY LOCATION.
```

```
8045:AD 17 80  135          LDA  BUFL       ;LOAD ACCULMULATOR WITH THE LOW BYTE OF THE
8048:          136 ;                         AVAILABLE BUFFER SPACE.
8048:8D 55 80  137          STA  PATCH+1    ;STORE IT AT ADDRESS PATCH+1.  NOTE THAT THIS
804B:          138 ;                         ALTERS THE PROGRAM ITSELF.
804B:AD 18 80  139          LDA  BUFH       ;LOAD THE HIGH BYTE OF THE BOTTOM OF AVAILABLE
804E:8D 56 80  140          STA  PATCH+2    ;BUFFER SPACE STORE IT AT ADDRESS PATCH+2.
8051:AD 19 80  141          LDA  SAMPLE     ;GET THE STORE SAMPLE OUT OF THE TEMPORARY LOCATION.
8054:8D 00 01  142 PATCH    STA  $0100      ;STORE ACCUMULATOR IN THE ADDRESS GIVEN BY THE
8057:          143 ;                         NEXT TWO BYTES.  THESE ARE THE VALUES PUT IN BY
8057:          144 ;                         THE PREVIOUS "STA PATCH" LINES.
8057:          145 ;                         THE VALUE OF $0100 IS JUST A PLACE HOLDER.
8057:EE 17 80  146          INC  BUFL       ;INCREMENT THE LOW BYTE OF THE ADDRESS OF THE
805A:          147 ;                         LOWEST AVAILABLE BUFFER SPACE TO
805A:          148 ;                         GET READY FOR THE NEXT SAMPLE.
805A:D0 03     149          BNE  DECCNT     ;IF BUFL WAS INCREMENTED TO ZERO BUFH MUST
805C:          150 ;                         BE INCREMENTED ONE TO TAKE CARE OF THE CARRY.
805C:EE 18 80  151          INC  BUFH
805F:CE 10 80  152 DECCNT   DEC  CNTL       ;DECREMENT THE NUMBER OF SAMPLES YET TO BE TAKEN.
8062:D0 08     153          BNE  LEAVE      ;IF CNTL WAS NOT DECREMENTED TO ZERO
8064:          154 ;                         THEN LEAVE IHNDLR.
8064:AD 11 80  155          LDA  CNTH       ;OTHERWISE CHECK CNTH TO SEE IF IT IS ZERO.
8067:          156 ;                         IF CNTH IS ZERO THEN ALL
8067:          157 ;                         REQUIRED SAMPLES HAVE BEEN TAKEN
8067:F0 7D     158          BEQ  EXIT       ;IF ALL REQUIRED SAMPLES ARE IN
8069:          159 ;                         EXIT FROM THE DIGITIZER.
8069:CE 11 80  160          DEC  CNTH       ;IF CNTH WAS NOT ZERO, DECREMENT IT SINCE
806C:          161 ;                         CNTL WENT THROUGH ZERO.
806C:68        162 LEAVE    PLA
806D:A8        163          TAY
806E:68        164          PLA
806F:AA        165          TAX
8070:68        166          PLA
8071:40        167          RTI
8072:          168 ;*****************************************************************
8072:          169 ;
8072:          170 ; INITIALIZE INTERRUPTS, ETC.
8072:          171 ;
8072:          172 ;*****************************************************************
8072:48        173 INIT     PHA
8073:8A        174          TXA
8074:48        175          PHA
8075:98        176          TYA
8076:48        177          PHA
8077:AD 11 80  178          LDA  CNTH       ;MAKE SURE THAT AT LEAST ONE SAMPLE WILL BE TAKEN.
807A:D0 08     179          BNE  OKAY
807C:AD 10 80  180          LDA  CNTL
807F:D0 03     181          BNE  OKAY
8081:EE 10 80  182          INC  CNTL       ;IF NOT FORCE AT LEAST ONE SAMPLE TO BE TAKEN.
8084:AD 0F 80  183 OKAY     LDA  BUFFER     ;LOAD AND STORE HIGH BYTE OF DATA BUFFER
8087:8D 18 80  184          STA  BUFH       ;AT BUFH.
808A:A9 00     185          LDA  #$00       ;LOW BYTE OF DATA BUFFER IS ASSUMED TO BE ZERO.
808C:8D 17 80  186          STA  BUFL
808F:A9 1B     187          LDA  #IHNDLR    ;PUT LOW BYTE OF IHNDLR ADDR INTO ACC.
8091:8D FE 03  188          STA  $3FE       ;STORE AT LOW BYTE OF INTERRUPT VECTOR.
8094:AD 14 80  189          LDA  INTADH     ;PUT HIGH BYTE INTO ACCUMULATOR.
8097:          190 ;                         FOR INFO ON INTADH SEE
8097:          191 ;                         "DATA STORAGE LOCATIONS" SECTION.
8097:8D FF 03  192          STA  $3FF       ;STORE AT THE INTERRUPT VECTOR HIGH BYTE.
809A:          193 ;
809A:          194 ;
809A:          195 ;
809A:          196 ;SELECT TIMER2 FUNCTION ON J.B. CARD BY SETTING UP THE AUX. CTRL. REG.
809A:          197 ;SET UP THE INTERRUPT ENABLE REGISTER TO ALLOW ONLY TIMER2 INTERRUPTS.
809A:A2 0B     198          LDX  #ACR       ;J.B. ADDRESS OF AUXILIARY CONTROL REGISTER.
809C:A9 20     199          LDA  #$20       ;TO BE WRITTEN TO THE AUX CONTROL REGISTER.
809E:9D 00 C4  200          STA  JBBASE,X   ;SELECTS TIMER2 EXTERMAL COUNT MODE.
80A1:A2 0E     201          LDX  #SETINT    ;J.B. ADDRESS OF THE INTERRUPT ENABLE REGISTER.
80A3:A9 A0     202          LDA  #$A0       ;CODE TO ENABLE TIMER2 INTERRUPT.
80A5:9D 00 C4  203          STA  JBBASE,X   ;STORE CODE IN INTERRUPT ENABLE REGISTER.
80A8:A9 5F     204          LDA  #$5F       ;CODE WHICH DISABLES ALL OTHER INTERRUPTS.
80AA:9D 00 C4  205          STA  JBBASE,X   ;DISABLE ALL OTHER J.B. INTERRUPTS.
```

```
80AD:A9 00      206         LDA  #00
80AF:8D 03 C4   207         STA  JBDDRB    ;CONFIGURE DATA I/O REGISTER B LINES AS INPUTS.
80B2:           208 ;
80B2:           209 ;
80B2:           210 ;FINISH UP INITIALIZATION UPON RECEIVING A POSITIVE TRANSITION ON LINE CA1.
80B2:           211 ;FIRST CLEAR THE IFR.  THEN SET UP THE PERIPHERAL CONTROL REGISTER TO
80B2:           212 ;SET THE CA1 INTERRUPT FLAG ON A NEGATIVE CA1 TRANSITION. THEN SIT IN A
80B2:           213 ;WAIT LOOP,MONITORING THE IFR.ONCE A FLAG IS SET START THE COUNTER AND
80B2:           214 ; START DIGITIZING.
80B2:           215 ;NOTE THAT THE CA1 INTERRUPT ENABLE BIT IS !!NOT!! SET.
80B2:           216 ;IT IS ONLY NECESSARY TO DETECT IFR BEING SET.
80B2:           217 ;DO NOT WANT INTERRUPT SEQUENCE TO START.
80B2:A2 0D      218         LDX  #IFR
80B4:A9 FF      219         LDA  #$FF
80B6:9D 00 C4   220         STA  JBBASE,X  ;CLEAR THE IFR.
80B9:A2 0C      221         LDX  #PCR
80BB:A9 00      222         LDA  #00       ;INTERRUPT SET ON A NEGATIVE TRANSITION ON CA1.
80BD:9D 00 C4   223         STA  JBBASE,X  ;WRITE TO PCR.
80C0:           224 ;
80C0:AD 0D C4   225 STRTDG  LDA  JBIFR
80C3:F0 FB      226         BEQ  STRTDG    ;IF IFR IS CLEAR, STARTING SIGNAL HAS
80C5:           227 ;                       NOT YET BEEN RECEIVED.
80C5:           228 ;                       IF IFR NOT CLEAR THEN CONTINUE TO AWAIT TRIGGER.
80C5:           229 ;
80C5:A2 0D      230         LDX  #IFR      ;CLEAR THE IFR
80C7:A9 FF      231         LDA  #$FF
80C9:9D 00 C4   232         STA  JBBASE,X
80CC:           233 ;
80CC:           234 ;LOAD UP TIMER2 LATCH
80CC:           235 ;
80CC:           236 ;
80CC:A2 08      237         LDX  #TM2ADR
80CE:A5 12      238         LDA  DGPAUS
80D0:9D 00 C4   239         STA  JBBASE,X
80D3:A2 09      240         LDX  #CLRIRQ
80D5:A9 00      241         LDA  #$00
80D7:9D 00 C4   242         STA  JBBASE,X  ;START COUNTER ON TIMER2.
80DA:           243 ;
80DA:           244 ; RESTORE REGISTERS
80DA:           245 ;SINCE THE J.B. COUNTER IS RUNNING AT THIS POINT,  THE FOLLOWING STEPS
80DA:           246 ;SHOULD NOT TAKE LONGER THAN THE TOTAL TIME COUNTED DOWN BY THE J.B. CARD.
80DA:           247 ;
80DA:68         248         PLA
80DB:A8         249         TAY
80DC:68         250         PLA
80DD:AA         251         TAX
80DE:68         252         PLA
80DF:58         253         CLI
80E0:60         254         RTS
80E1:           255 ;*************************************************************
80E1:           256 ;   FINISH UP AND DISABLE J.B. CARD.
80E1:           257 ;*************************************************************
80E1:           258 ;
80E1:48         259 FINISH  PHA             ;SAVE THE REGISTERS
80E2:8A         260         TXA
80E3:48         261         PHA
80E4:98         262         TYA
80E5:48         263         PHA
80E6:           264 ;      CAUTION!!!!!
80E6:           265 ;THE FOLLOWING ROUTINE IS REACHED BY A JUMP FROM IHNDLR.  EXIT'S PURPOSE
80E6:           266 ;IS TO RETURN TO THE BASIC PROGRAM FROM THE CALL TO THE WAIT LOOP.
80E6:           267 ;TO DO THIS THE ADDRESS OF THE
80E6:           268 ;WAIT LOOP, PLACED ON THE TOP OF THE STACK BY THE INTERRUPT,
80E6:           269 ;MUST BE SKIPPED OVER, BRINGING UP THE ADDRESS OF THE BASIC STATEMENT
80E6:           270 ;AFTER THE CALL TO THE WAIT LOOP.
80E6:A9 7F      271 EXIT    LDA  #$7F
80E8:A2 0E      272         LDX  #SETINT    ;DISABLE J.B. INTERRUPTS.
80EA:9D 00 C4   273         STA  JBBASE,X
80ED:A9 65      274         LDA  #$65       ;THESE FOUR STEPS RESTORE THE
80EF:           275 ;                       ORIGINAL INTERRUPT VECTOR
80EF:8D FE 03   276         STA  $3FE
```

```
80F2:A9 FF      277          LDA  #$FF
80F4:8D FF 03   278          STA  $3FF
80F7:68         279          PLA              ;RESTORE THE
80F8:A8         280          TAY
80F9:68         281          PLA              ;REGISTERS.
80FA:AA         282          TAX
80FB:68         283          PLA
80FC:8D 1A 80   284          STA  TMPHLD      ;SAVE ACCUMULATOR TEMPORARILY
80FF:28         285          PLP              ;TAKE PROCESSOR STATUS BYTE FROM STACK.
8100:           286 ;                         THIS MIMICKS
8100:           287 ;                          THE RTI INSTRUCTION WITHOUT RETURNING TO THE
9100:           288 ;                        INTERRUPT CALL
8100:68         289          PLA              ;WASTE THE RETURN-TO-WAIT-FROM-INTERRUPT ADDRESSES.
8101:68         290          PLA
8102:AD 1A 80   291          LDA  TMPHLD      ;GET ACCUMULATOR FROM TEMPORARY HOLDING SPOT.
8105:58         292          CLI
8106:60         293          RTS              ;RETURN TO BASIC PROGRAM, NOT TO WAIT LOOP
8107:58         294 WAIT     CLI
8108:EA         295 BACK     NOP
8109:4C 08 81   296          JMP  BACK
810C:           297 ;
810C:           298 ;
810C:           299 ;
```

II.2 TEXTIFY

```
40  REM     PROGRAM TEXTIFY. RODNEY STOLTZFUS, FEB.1 1984.
50  REM   THIS PROGRAM CONVERTS A BINARY FILE TO A TEXT FILE
51  REM     WITH THE FORMAT XYZXYZXYZ WHERE XYZ IS A THREE PLACE DECIMAL
      INTEGER.
52  REM     THE USER SUPPLIES THE STARTING ADDRESS OF THE BINAY FILE IN
      APPLE MEMORY.
53  REM     THE RECORDS OF THE GENERATED TEXT FILE HAVE 20 THREE DIGIT
      NUMBERS.
100 D$ =  CHR$ (4)
110  INPUT "AT WHAT ADDRESS DOES THE BINARY DATA START IN MEMORY?";START
120  INPUT "HOW MANY BYTES TO BE CONVERTED? SHOULD BE A MULTIPLE OF 20.";
     LNG
130  INPUT "NUMBER OF FILE (#) ? (FILE NAME IS ROCKET TEXT#)";N$
190  PRINT "RUNNING..."
200  PRINT D$"OPEN ROCKET TEXT";N$
300  PRINT D$"WRITE ROCKET TEXT";N$
410  REM  START GIVES THE ADDRESS OF THE FIRST BYTE TO BE TRANSMITTED.
500  FOR J = 1 TO (LNG / 20)
550 C$ = ""
600  FOR I = 1 TO 20
610  REM   ADD 1000 TO EACH NUMBER TO GIVE EACH NUMBER THE SAME LENGTH.
700 X = 1000 +  PEEK (START + (J - 1) * 20 + (I - 1))
750  REM  BUILD STRING WITH RIGHT 3 CHARACTERS OF THE OFFSET DATA
800 C$ = C$ +  RIGHT$ (( STR$ (X)),3)
900  NEXT I
910  PRINT C$
920 Y =  FRE (0)
1000  NEXT J
1100  PRINT D$"CLOSE ROCKET TEXT";N$
1110  PRINT "FINISHED: DATA ON DISK"
1200  END
```

II.3 APL2CDC

```
      PROGRAM APL2CDC(INPUT,OUTPUT,APLFIL,APLOUT,TAPE1=INPUT,
     +       TAPE2=OUTPUT,TAPE3=APLFIL,TAPE4=APLOUT)
C
C      THIS PROGRAM CONVERTS AN ICE FILE TO A FILE CAPABLE OF
C      BEING READ BY THE PROGRAM SPECTRA AND OTHERS WITH THE
C      SAME FORMAT NEED.  THE ICE FILE CONVERTED IS TRANSFERRED
C      FROM THE APPLE (SEE APPLE PROGRAM TEXTIFY FOR FORMAT).
C      THE APPLE FILE IS CALLED ROCKET TEXT.
C      THIS PROGRAM ASSUMES A 5KHZ DIGITIZING RATE AND A .05 SECOND
C      RECORD LENGTH.  TO CHANGE THIS, CHANGE THE LENGTH OF THE ARRAYS.
C      AND FIX THE TIME SPACING BETWEEN RECORDS    (I.E. CHANGE RECPRD,
C      THE TIME PERIOD OF ONE RECORD)
C      THE OUTPUT RECORDS HAVE THE FORMAT  [F/DATA/F/F/F] WHERE F IS
C      FILLER (I.E. IS ONLY TAKING UP SPACE) AND DATA IS THE DATUM.
C      THIS FIVE POINT SEQUENCE IS CALLED A FRAME AND THERE ARE 250
C      FRAMES PER .05 SECOND RECORD.
C      TEXTIFY AND APL2CDC WERE CREATED BY RODNEY STOLTZFUS
C      DECEMBER,1983
C       AS OF FEB. 3, 1984 THE FORMAT OF THE APPLE FILE IS 20
C      3 DIGIT NUMBERS PER TEXT LINE.  THIS CAUSES PROBLEMS AS THE
C      APL2CDC   OUTPUT SHOULD BE IN BLOCKS OF 250.  THE SOLUTION IS
C      TO READ IN 500 POINTS AT A TIME AND PRINT OUT 2 ARRAYS AT
C      ONE PASS THROUGH SUBROUTINE REFORM.  ESSENTIALLY THIS MEANS
C      THAT THE NUMBER OF INPUT POINTS SHOULD BE A MULTIPLE OF 500
C      RATHER THAN 250.
C
C
C**********************************************************************
C
C      V A R I A B L E   D I C T I O N A R Y
C
C
C   IARRAY:  HOLDS THE INTEGER DATA BEFORE TRANSMITTING.  IARRAY
C            IS EQUIVALENT TO ARRAY(2 TO 1251).
C
C   ARRAY :  HOLDS THE IARRAY AND THE TIME CODE.  THE TIME CODE IS
C            IN ARRAY(1).
C
C   DATNUM:  IS THE TOTAL NUMBER OF DATA POINTS IN THE FILE
C
C   DATA  :  IS AN ARRAY THAT HOLDS 500 PIECES OF RAW DATA.
C
C   I,J,K :  GENERAL PURPOSE COUNTERS.
C
C   BLOCKS:  GIVES THE NUMBER OF 250 POINT BLOCKS IN THE INPUT FILE.
C
C   RECPRD:  GIVES THE TIME DURATION OF ONE RECORD.
C
C**********************************************************************
C
      INTEGER DATA(500),I,J,K,DATNUM,BLOCKS,J19
      REAL TIME
C
C
      PRINT*,"WHAT IS THE UNIVERSAL TIME OF THE FIRST RECORD?"
      READ*,TIME
      PRINT*,"HOW MANY DATA POINTS ARE IN THE INPUT FILE?"
      PRINT*,"(MUST BE MULTIPLE OF 500. SEE  OPENING PROGRAM COMMENTS)"
      READ*,DATNUM
C
C   READ IN THE DATA IN DOUBLE BLOCKS
C
      BLOCKS=DATNUM/250
      DO 110 I=1,BLOCKS,2
        DO 100 J=1,500,20
          J19=J+19
          READ (3,900) (DATA(K),K=J,J19)
 100    CONTINUE
C
C   INSERT THE FILLER DATA AND THE TIME CODE FOR TWO BLOCKS.
```

```
C   WRITE THEM OUT TO TAPE4 (SEE PROGRAM STATEMENT).
C
      CALL REFORM(DATA,I,TIME)
 110  CONTINUE
 900  FORMAT(2013)
      STOP
      END
C
C   SUBROUTINE REFORM INSERTS THE EXTRA DATA POINTS,PUTS ON
C   THE TIME MARK, PUTS THE DATA INTO ARRAY, AND WRITES OUT ARRAY.
C   IT PUTS OUT TWO ARRAYS IN A PASS.
C
      SUBROUTINE REFORM(DATA,RECNUM,TIME)
      REAL ARRAY(1251),TIME,RECPRD
      INTEGER RECNUM,DATA(500),IARRAY(1250),K
      EQUIVALENCE (ARRAY(2),IARRAY(1))
C
C   PUT IN EXTRA GARBAGE DATA POINTS
C
C
C   SET THE RECORD DURATION TIME.  FOR 5KHZ IT SHOULD BE .05 SECONDS.
C
      RECPRD=.05
      DO 210 K=1,2
      DO 200 J=1,250
        IARRAY((J-1)*5+1)=9999
        IARRAY(((J-1)*5)+2)=DATA(J+250*(K-1))
        IARRAY(((J-1)*5)+3)=9999
        IARRAY(((J-1)*5)+4)=9999
        IARRAY(((J-1)*5)+5)=9999
 200  CONTINUE
C
C   THE NEXT STATEMENT ATTACHES A TIME CODE RELATIVE TO TIME.
C   WITH A RECPRD SECOND RECORD LENGTH, EACH AFFIXED TIME CODE SHOULD
C   BE RECPRD SECONDS GREATER THAN THE PRIVIOUS ONE.
C   (RECNUM-1) IS USED SINCE THE NTH RECORD SHOULD HAVE A TIME CODE
C   OF (N-1)*RECPRD.  THE (K-1) IS USED SINCE SUBROUTINE REFORM PUTS
C   OUT 2 RECORDS, ONE AT K=1 AND ONE AT K=2.
C
      ARRAY(1)=TIME+(FLOAT((RECNUM-1)+(K-1))*RECPRD)
      WRITE(4) ARRAY
 210  CONTINUE
      RETURN
      END
```

II.4 SPECTRA

```
C   PROGRAM SPECTRA IS AN INTER-ACTIVE ROUTINE WHICH ALLOWS THE
C   COMPUTATION OF POWER SPECTRA TO BE USED IN THE CALCULATION
C   OF FINE STRUCTURE IRREGULARITIES.  THE FINE STRUCTURE DATA
C   FILE TO BE ANALYZED IS ENTERED THROUGH DEVICE 3.  THE USER
C   IS THEN PROMPTED TO PROVIDE INFORMATION REGARDING THE DATA
C   AND THE ANALYSIS.  A LINEAR FIT MAY ALSO BE PERFORMED ON
C   THE DATA AND THE SPECTRAL INDEX CALCULATED.  THE USER MAY
C   STORE VALUES OF THE SPECTRAL INDEX AND MAGNITUDE IN ARRAY
C   INDEX.  PROGRAM SPINDEX MAY THEN BE USED TO PLOT THE
C   SPECTRAL INDEX AND MAGNITUDE AS A FUNCTION OF ALTITUDE.
C      PRIOR TO EXECUTION OF SPECTRA, THE USER MUST PROVIDE
C   CERTAIN PARAMETERS.   THESE PARAMETERS ARE
C         1) GAIN  --  THIS IS THE GAIN OF THE EXPERIMENT.
C         2) CHANNEL  --  THIS REFERS TO THE CHANNEL NUMBER
C                         OF THE REQUIRED DATA AS STORED ON
C                         A CDC FORMAT TAPE.
C         3) MINMAG  --  THIS IS THE LOWER BOUNDARY ON THE
C                        PLOTTING AXIS.
C         4) BANDCAL  --  THIS IS THE ARRAY WHICH CONTAINS
C                         THE DATA CALIBRATIONS AS DETERMINED
C                         FROM PROGRAM CWALCAL.
C         5) LOLIMIT  --  LOLIMIT IS THE LOWER BOUND ON THE
C                         FREQUENCY OF DATA POINTS TO BE INCLUDED
C                         IN THE LEAST SQUARES FIT.
C         6) HILIMIT  --  HILIMIT IS THE UPPER BOUND ON THE
C                         FREQUENCY OF DATA POINTS TO BE INCLUDED
C                         IN THE LEAST SQUARES FIT.
C         7) FC  --  THIS IS THE UPPER 3DB FREQUENCY OF THE
C                    TELEMETRY LOW PASS FILTER.
C         8) FAC --  THIS IS THE UPPER 3DB FREQUENCY OF THE
C                    AC AMPLIFIER.
C         9) FLE --  THIS IS THE UPPER 3DB FREQUENCY OF THE
C                    LOGARITHMIC ELECTROMETER.
C        10) BBAND  --  THIS IS THE NUMBER OF THE BROADBAND
C                       AMPLIFIER OUTPUT BEING PROCESSED.  (TO
C                       BYPASS DEEMPH, SET BBAND .EQ. 0)
C   THESE VALUES ARE ENTERED UNDER THE TITLE "EXPERIMENT
C   PARAMETERS" IN THE PROGRAM. (WRITTEN BY BRUCE TOMEI, 1983).
C
C     THIS VERSION OF SPECTRA IS MODIFIED FROM THE ORIGINAL VERSION
C         BY BRUCE TOMEI.  AN ATTEMPT HAS BEEN MADE TO DOCUMENT
C         MAJOR CHANGES.  DEBUGGING OF THE ORIGINAL IS NOT
          RECORDED.  THERE IS AN EXTENDED
C         PLOTTER ROUTINE ALLOWING INCLUSION OF THE ROCKET SHOT
C         NUMBER, THE LAUNCH TIME (IN UNIVERSAL TIME), THE NUMBER
C         OF SECONDS INTO THE LAUNCH AT WHICH SPECTRA ARE DESIRED,
C         THE ROCKET SPEED AT THAT TIME, THE ALTITUDE, THE ROCKET
C         ANGLE OFF VERTICAL, THE FFT BLOCK LENGTH, THE SEGMENT
C         OVERLAP, THE DIGITIZATION RATE, THE ROCKET SPIN RATE,
C         AND THE GAIN OF THE EXPERIMENT.
C     NEW VARIABLES AND CONSTANTS ARE: SHOTNUM,ALTITUD, AND ROCKSPD.
C         THIS VERSION OF SPECTRA DOES NOT ASK FOR THE ANGLE,
C         OR THE SPIN RATE OF THE ROCKET.
C         RODNEY STOLTZFUS.  10/11/83
C
C     ANOTHER MODIFICATION:
C         SPECTRA USED TO PLOT A STRING OF SEQUENTIAL PLOTS.  YOU COULD
C         PLOT AS MANY AS YOU WISHED OUT OF THE AVAILABLE SEGMENTS.
C         HOWEVER, YOU COULD NOT PICK OUT INDIVIDUAL PLOTS.  FOR EXAMPLE,
C         YOU COULD NOT PLOT ONLY THE FIFTH SEGMENT; YOU HAD TO
C         PLOT SEGMENTS 1,2,3,4, AND 5.
C     THE MODIFICATION ALLOWS YOU TO CHOOSE ANY AVAILABLE PLOT OR
C         PLOTS.  THE COMPUTED AVERAGE IS OVER THESE SELECTED
C         PLOTS RATHER THAN OVER THE WHOLE RANGE OF SEGMENTS.
C         THIS ADMITTEDLY CONSTRAINS THE AVERAGE PLOT TO COVER ONLY
C         THOSE SPECTRA WHICH ARE ACTUALLY PRINTED.  YOU MUST PLOT
C         ALL SPECTRA YOU WISH TO HAVE INCLUDED IN THE AVERAGE.
C     THIS MODIFICATION IS PERFORMED BY PUTTING THE DESIRED PLOT NUMBERS
C         IN AN ARRAY CALLED PLOTS.  YOU CAN INCLUDE UP TO 99 PLOTS.
C         SUBROUTINE SELECT HANDLES THE CONSTRUCTION OF THE ARRAY CALLED
C         PLOTS.
C         2/16/84       RODNEY STOLTZFUS
```

```
C
C     MODIFICATION:  SPECTRA NOW HAS THE ABILITY TO SAVE AVERAGE
C          PLOTS FOR LATER PROCESSING.  YOU CAN PUT AN AVERAGE PLOT
C          INTO MEMORY LOCATIONS (CALLED PLOT BAYS) AND GO BACK TO
C          CREATE MORE AVERAGE PLOTS.
C
C     PROCESSING INCLUDES AVERAGING TWO PLOTS, TAKING THE DIFFERENCE
C          OF TWO PLOTS, PERFORMING AN INCREMENTED WINDOW AVERAGE,
C          AND PLOTTING THE FINAL RESULT.
C     THERE ARE CURRENTLY TWO PLOT BAYS PLUS A WORKING BAY IN WHICH
C          PROCESSED DATA IS KEPT.  IF NECESSARY, MORE BAYS CAN BE
C          IMPLEMENTED BY DECLARING NEW ARRAYS AND ADJUSTING THE
C          SUBROUTINE CALLS.
C     A PLOT BAY CONTAINS THREE ARRAYS: THE FREQUENCIES OF THE FFT,
C          THE CORRESPONDING MAGNITUDES, AND ASSOCIATED PARAMETERS.
C          THE PARAMETERS ARE THE TIME OF THE PLOT, THE SIZE OF THE
C          DATA ARRAYS, AND THE FFT SIZE.
C
C     NOTE: DEPENDING ON THE NUMBER OF PLOT BAYS, THE PROGRAM MAY
C          REQUIRE MORE CENTRAL MEMORY THAN IS USUALLY GIVEN TO
C          A RESEARCH ACCOUNT.  IF THE PROGRAM WILL NOT RUN AT
C          NORMAL TIMES, YOU MAY NEED TO HAVE YOUR CENTRAL MEMORY
C          LIMITS EXPANDED.
C          3/12/84
C
C
C
C        SPECTRA WAS WRITTEN BY BRUCE TOMEI, 1983.
C
C          SPECTRA REQUIRES THE FOLLOWING EXTERNAL INFORMATION:
C          THE IMSL LIBRARY       (ACCESSED BY GRAB,IMSL)
C          THE GCS LIBRARY        (ACCESSED BY GRAB,GCS(TEXT,3D) )
C          AN INPUT FILE IN STANDARD ROCKET FILE FORMAT
C
C
      PROGRAM SPECTRA (INPUT,OUTPUT,DATA11,INDEX,TAPE1=INPUT,
     *                 TAPE2=OUTPUT,TAPE3=DATA11,TAPE4=INDEX)
      INTEGER N,K,M,OVLP,WINDONO,DISPLAY,OPTION,CHANNEL,IHRS,IMIN,S,
     *        NUMBER,FIT1,FIT2,REPEAT,M2,BAND,DIGRATE,JJ,PLOTS(100),
     *        TOTAL,QUES,PLTSIZE,FFTSIZE
      REAL DATA(4096),MAG(2049),MAGAVE(2049),FREQ(2049),X(4096),
     *     BANDCAL(5),MAXMAG,MAXFREQ,LTIME,STIME,SMPTIME,SECS,GAIN,
     *     MINMAG,KREAL,SLOPE,YINT,HILIMIT,LOLIMIT,PC,FAC,FLE,SHOTNUM,
     *     ALTITUD,ROCKSPD,SAVMAG1(1025),SAVMAG2(1025),
     *     WORKMAG(1025),SAVFRQ1(1025),SAVFRQ2(1025),
     *     WORKFRQ(1025),PARAMS1(10),PARAMS2(10),
     *     WKPARMS(10),AVPARMS(10)
      COMPLEX Z(2049)
      EXTERNAL CABS
      DATA Z,DATA,MAG,MAGAVE,X,FREQ,SAVMAG1,SAVMAG2,WORKMAG,
     *     SAVFRQ1,SAVFRQ2,WORKFRQ,PARAMS1,PARAMS2,
     *     WKPARMS,AVPARMS/2049*((0.0,0.0)),4096*(0.0),
     *     2049*(0.0),2049*(0.0),4096*(0.0),2049*(0.0),
     *     1025*(0.0),1025*(0.0),1025*(0.0),
     *     1025*(0.0),1025*(0.0),1025*(0.0),10*(0.0),
     *     10*(0.0),10*(0.0),10*(0.0)/
C
C    REMINDER TO CHECK EXPERIMENT PARAMETERS.
C
      PRINT*,"REMINDER:MAKE SURE YOU HAVE SET THE EXPERIMENT"
      PRINT*,"PARAMETERS CORRECTLY (I.E. GAIN,BANDCAL,ETC. )"
      PRINT*,"       "
C
C   ENTER USER-SPECIFIED VARIABLES
C
      PRINT*,"ENTER THE LAUNCH TIME.  (HH MM SEC.)"
      READ*,IHRS,IMIN,SECS
      LTIME=FLOAT(IHRS*3600+IMIN*60)+SECS
   10 PRINT*,"ENTER THE DESIRED STARTING TIME.  (SECONDS AFTER LAUNCH)"
      READ*,STIME
      IF(REPEAT .EQ. 1)GOTO 50
      PRINT*,"ENTER THE NUMBER OF DATA POINTS."
```

```
      READ*,N
      PRINT*,"ENTER THE SEGMENT LENGTH (MUST BE AN EVEN INTEGER)"
      READ*,L
      PRINT*,"       NUMBER OF SEGMENTS          OVERLAP"
      S=N/L
      PRINT4,S,0
      IF(S .EQ. 1) GOTO 40
      DO 100 I=2,L
        KREAL=FLOAT(N-(I-1))/FLOAT(L-(I-1))
        IF(KREAL-AINT(KREAL))100,20
 20   K=IFIX(KREAL)
      PRINT4,K,I-1
  4   FORMAT(13X,I4,19X,I4)
100   CONTINUE
 40   PRINT*,"ENTER THE NUMBER OF SEGMENTS "
      PRINT*,"THE DATA SHOULD BE DIVIDED INTO"
      READ*,K
      OVLP=(L*K-N)/(K-1)
      PRINT*,'ENTER THE DESIRED WINDOW.    1-RECTANGULAR"
      PRINT*,"                             2-BARTLETT"
      PRINT*,"                             3-HANNING"
      PRINT*,"                             4-HAMMING"
      PRINT*,"                             5-BLACKMAN"
      PRINT*,"                             6-BLACKMAN-HARRIS"
      READ*,WINDOWNO
      PRINT*,"ENTER THE FFT BLOCK LENGTH  (MUST BE A POWER OF 2)"
      READ*,M
      M2=M/2+1
      PRINT*,"ENTER THE DESIRED PLOT.      1-LINEAR"
      PRINT*,"                             2-LOGARITHMIC"
      PRINT*,"                             3-NO PLOT"
      READ*,OPTION
      FIT2=2
      DISPLAY=2
      FIT1=1
      PRINT*,"DO YOU WISH TO PLOT INDIVIDUAL PERIODOGRAMS?    1-YES"
      PRINT*,"                                                2-NO"
      READ*,DISPLAY
C
C   THE FOLLOWING ALLOWS THE USER TO SELECT INDIVIDUAL PLOTS TO
C   BE PLOTTED (AND INCLUDED IN THE AVERAGE).  PLOTS(100)
C   HOLDS THE RESPONSE TO THE QUESTION.
C   MODIFICATION TO ORIGINAL SPECTRA PROGRAM.  SEE INITIAL PROGRAM
C   COMMENTS OR COMMENTS FOR SUBROUTINE SELECT.  2/16/84
C
      PRINT*,"DO YOU WISH TO DISPLAY AND AVERAGE ONLY CERTAIN PLOTS?"
      PRINT*,"                1-YES, I ONLY WANT SOME OF THE SEGMENTS"
      PRINT*,"                2-NO, I WANT ALL SEGMENTS AVERAGED"
      READ*,PLOTS(100)
C
C   CALL SUBROUTINE SELECT. THIS WILL PUT THE DESIRED PLOT NUMBERS
C   INTO THE ARRAY CALLED PLOTS.  YOU CAN INCLUDE UP TO 99 PLOTS.
C
      CALL SELECT(PLOTS,NUMBER,K,TOTAL)
      PRINT*,"PERFORM LINEAR FIT TO INDIVIDUAL PERIODOGRAMS?    1--YES"
      PRINT*,"                                                  2--NO"
      READ*,FIT2
 30   PRINT*,"PERFORM LINEAR FIT TO AVERAGED PERIODOGRAM?   1--YES"
      PRINT*,"                                              2--NO"
      READ*,FIT1
      PRINT*,"WHAT IS THE NUMBER OF THE ROCKET SHOT?"
      READ*,SHOTNUM
C      PRINT*,"WHAT IS THE ALTITUDE FOR THIS ANALYSIS?"
C      READ*,ALTITUD
C      PRINT*,"WHAT IS THE ROCKET SPEED AT THIS ALTITUDE?"
C      READ*,ROCKSPD
      PRINT*,"WHAT IS THE DIGITIZING RATE OF THE DATA?"
      READ*,DIGRATE
 70   PRINT*,"ANY CHANGES?              1-YES"
      PRINT*,"                          2-NO"
      READ*,S
      IF(S .EQ. 1)GOTO 10
C
```

```
C   EXPERIMENT PARAMETERS
C
      GAIN=35.000
      CHANNEL=2
      MINMAG=0.000000000001
      BANDCAL(1)=-115.50
      BANDCAL(2)=5.0600
      BANDCAL(3)=127.000
      BANDCAL(4)=248.000
      BANDCAL(5)=370.000
      PRINT*,"DO YOU WANT TO CHANGE THE BANDCALS?  1-YES"
      PRINT*,"                                     2-NO"
      READ*,QUES
      IF (QUES .EQ. 2) GOTO 75
      PRINT*,"ENTER THE BANDCALS AS YOU ARE ASKED:"
      PRINT*,"BANDCAL(1)?"
      READ*,BANDCAL(1)
      PRINT*,"BANDCAL(2)?"
      READ*,BANDCAL(2)
      PRINT*,"BANDCAL(3)?"
      READ*,BANDCAL(3)
      PRINT*,"BANDCAL(4)?"
      READ*,BANDCAL(4)
      PRINT*,"BANDCAL(5)?"
      READ*,BANDCAL(5)
 75   LOLIMIT=100.0
      HILIMIT=2500.0
      FC=1050.0
      FAC=1880.0
      FLE=2500.0
C
C   BBAND = 2 IF YOU WANT TO SELECT YOUR OWN LOWER 3DB DEEMPHASIS
C   POINT.
C
      BBAND=2
C
C   BEGIN PROCESSING
C
  50  REWIND 3
      CALL LOAD(DATA,N,CHANNEL,LTIME,STIME,SMPTIME)
      CALL CALIB(DATA,N,BANDCAL,GAIN)
      CALL SPECTRM(DATA,MAG,MAGAVE,FREQ,X,Z,N,K,M,M2,L,OVLP,WINDONO,
     *             SMPTIME,OPTION,DISPLAY,NUMBER,MINMAG,FIT2,FIT1,
     *             LOLIMIT,HILIMIT,FC,FAC,FLE,BBAND,LTIME,STIME,SHOTNUM,
     *             DIGRATE,TOTAL,PLOTS)
      CALL FILTCAV(MAGAVE,FREQ,M2,FC,FAC,FLE)
      CALL DEEMPH(MAGAVE,FREQ,M2,BBAND)
      CALL MAXMIN(MAGAVE,FREQ,MAXMAG,MAXFREQ,M,M2)
      JJ=0
C   SETTING JJ=0 WILL CAUSE 0 TO BE PRINTED ON THE AVERAGE
C   PLOT.
      CALL PLOTTER(MAGAVE,FREQ,M,M2,MAXMAG,MINMAG,MAXFREQ,OPTION,
     *        SLOPE,YINT,FIT1,LOLIMIT,HILIMIT,STIME,SHOTNUM,
     *        ALTITUD,ROCKSPD,IHRS,IMIN,SECS,DIGRATE,OVLP,GAIN,JJ)
      PRINT*,"DO YOU WISH TO STORE THE SPECTRAL INDEX?     1--YES"
      PRINT*,"                                             2--NO"
      READ*,S
      IF(S .EQ. 2)GOTO 60
      CALL STORE(SLOPE,YINT,LTIME,STIME,SMPTIME,N)
C
C
  60  PRINT*,"ARE YOU FINISHED?              1-YES"
      PRINT*,"                               2-NO"
      READ*,S
      IF(S .EQ. 1)STOP
C
C  ***************************************************************
C     THE FOLLOWING SECTION ALLOWS FURTHER ANALYSIS OF SPECTRA.
C  SPECIFICALLY IT ALLOWS THE USER TO SAVE THE AVERAGE PLOT MADE BY
C  SUBROUTINE SPECTRM, AND ALLOWS THE USER TO CREATE MORE SPECTRA.
C  THE SPECTRA ARE SAVED IN ARRAYS SAVMAG1 AND SAVMAG2.
C  EACH ARRAY CAN HOLD UP TO 1025 POINTS (CORRESPONDING TO A 2048
C  POINT FFT.
```

```
C  FREQUENCIES ASSOCIATED WITH THE SAVED MAGNITIUDES ARE IN ARRAYS
C  SAVFRQ1 AND SAVFRQ2. CERTAIN PLOT PARAMETERS ARE STORED IN
C  PARAMS1 AND PARAMS2.  THE ORDER OF STORAGE IS TIME, NUMBER OF POINTS,
C  AND FFT SIZE.
C      IN ADDITION TO THESE THREE ARRAYS THERE IS A WORKING PLOT CALLED
C  WORKMAG.  WORKFRQ AND WKPARMS STORE THE FREQUENCIES AND THE
C  ASSOCIATED FREQUENCIES AND PARAMETERS.
C
C     FIRST, STORE THE AVERAGE PLOT IN ONE OF THE PLOT BAYS.  ALSO SET UP
C  AN ARRAY AVPARAM.
C
      PRINT*,"DO YOU WISH TO STORE THE LAST AVERAGE PLOT? 1-YES"
      PRINT*,"                                            2-NO"
      READ*,QUES
      IF (QUES .EQ. 2) GOTO 100
      AVPARMS(1)=STIME
      AVPARMS(2)=M2
      AVPARMS(3)=M
C
C    DISPLAY WHICH PLOTS ARE WHERE
C
      CALL PRTSTAT(PARAMS1,PARAMS2,WKPARMS)
      PRINT*,"IN WHICH BAY DO YOU WISH TO STORE THE AVERAGE PLOT"
      PRINT*,"                                          1-BAY#1"
      PRINT*,"                                          2-BAY#2"
      PRINT*,"                                          3-DON'T STORE"
      READ*,QUES
C
C   USE SUBROUTINE TRNSPLT TO SWITCH THE AVERAGE PLOT INTO A PLOT BAY.
C
      IF (QUES .EQ. 1) CALL TRNSPLT(MAGAVE,FREQ,AVPARMS,SAVMAG1,SAVFRQ1,
     *  PARAMS1)
      IF (QUES .EQ. 2) CALL TRNSPLT(MAGAVE,FREQ,AVPARMS,SAVMAG2,SAVFRQ2,
     *  PARAMS2)
 100  CALL PRTSTAT(PARAMS1,PARAMS2,WKPARMS)

      PRINT*,"DO YOU WISH TO CONTINUE TO PROCESSING?  1-YES "
      PRINT*,"                                        2-NO, GO BACK
      PRINT*,"                                        FOR MORE SPECTRA
      PRINT*,"                                        3-QUIT SPECTRA"
      READ*,QUES
      IF (QUES .EQ. 2)GOTO 110
      IF (QUES .EQ. 3) STOP
C
C      BEGIN PROCESSING
C   ASK THE USER WHICH PROCESS IS DESIRED.  THE SUBROUTINE MENU
C   ASKS THIS AND RETURNS WITH A NUMBER IN QUES.
C
 105  CALL MENU(QUES)
C
C   ANY SUBROUTINE WITH "SET" IN IT MERELY SETS UP A CALL TO THE
C   ACTAUL MATHEMATICAL ROUTINE DESIRED.
C
      IF(QUES .EQ. 1)CALL DIFFSET(SAVMAG1,SAVFRQ1,PARAMS1,SAVMAG2,
     *                    SAVFRQ2,PARAMS2,WORKMAG,WORKFRQ,WKPARMS)

      IF(QUES .EQ. 2)CALL WNDOSET(SAVMAG1,SAVFRQ1,PARAMS1,SAVMAG2,
     *                    SAVFRQ2,PARAMS2,
     *                    WORKMAG,WORKFRQ,WKPARMS)

      IF(QUES .EQ. 3)CALL TRNSSET(SAVMAG1,SAVFRQ1,PARAMS1,SAVMAG2,
     *                    SAVFRQ2,PARAMS2,
     *                    WORKMAG,WORKFRQ,WKPARMS)

      IF(QUES .EQ. 4)CALL AVRGSET(SAVMAG1,SAVFRQ1,PARAMS1,SAVMAG2,
     *                    SAVFRQ2,PARAMS2,WORKMAG,WORKFRQ,WKPARMS)


      IF(QUES .EQ. 5)CALL PRTSTAT(PARAMS1,PARAMS2,WKPARMS)

      FFTSIZE=IFIX(WKPARMS(3))
      PLTSIZE=IFIX(WKPARMS(2))
```

```
      IF(QUES .EQ. 6)CALL PLOTTER(WORKMAG,WORKFRQ,FPTSIZE,
     *                    PLTSIZE,MAXMAG,MINMAG,MAXFREQ,
     *                    OPTION,SLOPE,YINT,FIT1,LOLIMIT,HILIMIT,
     *                    WKPARMS(1),SHOTNUM,ALTITUD,ROCKSPD,IHRS,
     *                    IMIN,SECS,DIGRATE,OVLP,GAIN,JJ)


      IF(QUES .EQ. 8) CALL COPYSET(SAVMAG1,SAVFRQ1,PARAMS1,
     *                             SAVMAG2,SAVFRQ2,PARAMS2,
     *                             WORKMAG,WORKFRQ,WKPARMS)

      IF(QUES .GT. 8)CALL PRNTERR(3)
C
C   IF QUES WAS NOT EQUAL TO 7, GO BACK TO THE MENU.
C
      IF (QUES .NE. 7) GOTO 105


C
C   GO BACK TO THE BEGINNING OF SPECTRA FOR MORE PLOTS
C
 110  PRINT*,"ARE YOU FINISHED?                    1-YES"
      PRINT*,"                                     2-NO"
      READ*,QUES
      IF (QUES .EQ. 1) STOP
      PRINT*,"GO BACK TO MAKE MORE PLOTS."
      PRINT*,"DIFFERENT TIME,SAME ANALYSIS?        1-YES"
      PRINT*,"                                     2-NO"
      READ*,QUES
      REPEAT=0
      IF (QUES .EQ. 1) REPEAT=1
      GOTO 10

      STOP
      END
C
C   SUBROUTINE LOAD READS A SPECIFIED CHANNEL ON A
C   PDP2CDC CONVERTED TAPE AND STORES THIS DATA IN ARRAY
C   DATA.  THE NUMBER OF DATA POINTS TO BE READ AND THE
C   TIME CORRESPONDING TO THE FIRST DATA POINT ARE ENTERED
C   BY THE USER.  IF THE STARTING TIME ENTERED DOES NOT
C   CORRESPOND TO A SPECIFIC DATA POINT, THE FIRST DATA
C   POINT OF THE DESIRED CHANNEL FOLLOWING THE GIVEN
C   STARTING TIME WILL BE THE FIRST TO BE READ.  FOLLOWING
C   IS A LIST OF THE SUBROUTINE VARIABLES.
C   (NOTE -- THE NUMBER IN PARENTHESES IN THE READ STATEMENT
C   SPECIFIES THE DEVICE TO BE READ.  THIS SHOULD BE MODIFIED
C   IN ACCORDANCE WITH THE USER'S PROGRAM STATEMENT.)
C
C     DATA    =ARRAY CONTAINING THE CHANNEL SAMPLES.
C     N       =NUMBER OF SAMPLES TO BE READ.
C     LTIME   =LAUNCH TIME IN UNIVERSAL TIME (IN SECONDS).
C     STIME   =TIME CORRESPONDING TO THE FIRST SAMPLE TO BE
C              READ (IN SECONDS FROM LAUNCH).
C     PTIME   =TIME CORRESPONDING TO FIRST SAMPLE IN A RECORD.
C     SMPTIME =CHANNEL SAMPLING PERIOD.
C     TIME    =TIME OF DATA POINT IN UNIVERSAL TIME (LTIME+
C              STIME).
C     FRAME   =THE FRAME NUMBER (A FRAME IS A SET OF FIVE DATA POINTS).
C     CHANNEL =THE DESIRED CHANNEL TO BE READ.
C     POINT   =THE DATA POINT CORRESPONDING TO TIME
C     IPOINT  =THE LARGEST INTEGER LESS THAN OR EQUAL TO POINT.
C     STPOINT =THE FIRST DATA POINT TO BE READ (STARTING POINT).
C
C

      SUBROUTINE LOAD (DATA,N,CHANNEL,LTIME,STIME,SMPTIME)
      REAL DATA(N),ARRAY(1251),LTIME,STIME,TIME,SMPTIME,PTIME,POINT,
     *       TIME11
      INTEGER IARRAY(1250),IPOINT,STPOINT,CHANNEL
      EQUIVALENCE(ARRAY(2),IARRAY(1))
      TIME=LTIME+STIME
      READ(3) ARRAY
```

```
      PTIME=ARRAY(1)
      READ(3) ARRAY
      SMPTIME=(ARRAY(1)-PTIME)/250.000000
      REWIND 3
C
C   LOCATE THE PROPER RECORD
C
 10   READ(3) ARRAY
C   TIMEL1 IS THE TIME OF THE RECORD PREVIOUS TO THE DESIRED ONE.
C   THE .0001 IS USED TO PREVENT ROUND OFF ERRORS.
      TIMEL1 = TIME-(SMPTIME*250.0000) + .0001
      IF (ARRAY(1) .GT. TIMEL1) GOTO 20
      GOTO 10
20    POINT=(TIME-ARRAY(1))/(SMPTIME/5.0)+1.0
      IPOINT=POINT
      IF(POINT-FLOAT(IPOINT) .LT. 0.000001) GOTO 30
      IPOINT=IPOINT+1
      IF(IPOINT .LE. 1250) GOTO 30
      READ(3) ARRAY
      IPOINT=1
  30  FRAME=(IPOINT-1)/5+1
      STPOINT=(FRAME-1)*5+CHANNEL
      IF(IPOINT .LE. STPOINT) GOTO 40
      STPOINT=STPOINT+5
      IF(STPOINT .LE. 1250) GOTO 40
      READ(3) ARRAY
      STPOINT=CHANNEL
C
C   READ IN THE DATA
C
  40  DO 100 I=1,N
        DATA(I)=FLOAT(IARRAY(STPOINT))
      STPOINT=STPOINT+5
      IF(STPOINT .LE. 1250) GOTO 100
      READ(3) ARRAY
      STPOINT=CHANNEL
 100  CONTINUE
      RETURN
      END
C
C
C
C
C
C   SUBROUTINE CALIB PERFORMS THE NECESSARY
C   CALIBRATIONS SO THAT THE DATA IS REPRESENTATIVE
C   OF THE OUTPUT FROM THE EXPERIMENT.  THESE
C   CALIBRATIONS INCLUDE ADJUSTMENTS FOR EXPERIMENT
C   GAIN, DIGITIZER GAIN, SIGNAL OFFSETS, AND
C   DISCRIMINATOR NON-LINEARITIES.  THE NON-LINEARITIES
C   ARE REMOVED WITH A CALIBRATION CURVE OBTAINED BY
C   A PIECEWISE-LINEAR FIT TO THE CALIBRATION VALUES
C   (BANDCAL(5)).
C
C
      SUBROUTINE CALIB (DATA,N,BANDCAL,GAIN)
      REAL DATA(N),BANDCAL(5),GAIN
      INTEGER N
      DO 100 I=1,N
        IF(DATA(I) .GT. BANDCAL(2)) GOTO 10
        DATA(I)=((1.25/(BANDCAL(2)-BANDCAL(1)))*DATA(I)
     *          -(1.25*BANDCAL(1)/(BANDCAL(2)-BANDCAL(1)))-2.5)/GAIN
        GOTO 100
  10    IF(DATA(I) .GT. BANDCAL(3)) GOTO 20
        DATA(I)=((1.25/(BANDCAL(3)-BANDCAL(2)))*DATA(I)
     *          -(1.25*BANDCAL(2)/(BANDCAL(3)-BANDCAL(2)))-1.25)/GAIN
        GOTO 100
  20    IF(DATA(I) .GT. BANDCAL(4)) GOTO 30
        DATA(I)=((1.25/(BANDCAL(4)-BANDCAL(3)))*DATA(I)
     *          -(1.25*BANDCAL(3)/(BANDCAL(4)-BANDCAL(3))))/GAIN
        GOTO 100
  30    DATA(I)=((1.25/(BANDCAL(5)-BANDCAL(4)))*DATA(I)
     *          -(1.25*BANDCAL(4)/(BANDCAL(5)-BANDCAL(4)))+1.25)/GAIN
```

```
 100  CONTINUE
      RETURN
      END
C
C
C
C
C
C   SUBROUTINE SPECTRM SEGMENTS THE DATA, REMOVES THE MEAN,
C   WINDOWS THE DATA, COMPUTES THE PERIODOGRAM, UPDATES AN
C   AVERAGE OF THE PERIODOGRAMS, AND THEN DISPLAYS THE
C   INDIVIDUAL PERIODOGRAMS.  AN AVERAGED PERIODOGRAM IS
C   OBTAINED UPON RETURN FROM THE SUBROUTINE.
C
C
      SUBROUTINE SPECTRM(DATA,MAG,MAGAVE,FREQ,X,Z,N,K,M,M2,L,OVLP,
     *                   WINDONO,SMPTIME,OPTION,DISPLAY,NUMBER,MINMAG,
     *                   FIT2,FIT1,LOLIMIT,HILIMIT,FC,FAC,FLE,BBAND,
     *                   LTIME,STIME,SHOTNUM,DIGRATE,TOTAL,PLOTS)
      INTEGER N,K,M,M2,OVLP,D,L,WINDONO,IWK(12),DISPLAY,OPTION,
     *     NUMBER,S,BBAND,V,FIT1,FIT2,PLOTS(100),TOTAL,PRESPLT,DIGRATE
      REAL DATA(N),MAG(M2),MAGAVE(M2),FREQ(M2),X(M),MEAN,WK(1),
     *     SMPTIME,MAXMAG,MINMAG,MAXFREQ,LOLIMIT,HILIMIT,FC,FAC,FLE,
     *     LTIME,STIME,SLOPE,YINT
      COMPLEX Z(M2)
C
C   INITIALIZE ARRAYS
C
      DO 100 I=1,M2
        MAGAVE(I)=0.0
        Z(I)=((0.0,0.0))
 100  CONTINUE
      DO 700 I=1,M
        X(I)=0.0
 700  CONTINUE
      D=(N-OVLP)/K
      S=1
      PRESPLT=1
C
C
C   BEGIN SPECTRAL ESTIMATION
C
      PRINT*,PLOTS(1),PLOTS(2),PLOTS(3),PLOTS(100)
C
      DO 200 J=1,K
C
C   THE ARRAY PLOTS CONTAINS THE PLOT NUMBERS DESIRED BY THE USER.
C   THE FOLLOWING STEP CHECKS WHETHER THE DESIRED PLOT NUMBER (CON-
C   TAINED IN PLOTS(PRESPLT) ) MATCHES THE J'TH PLOT ABOUT TO
C   BE CALCULATED BY THE "DO 200" LOOP.  IF THERE IS A MATCH THE
C   LOOP IS EXECUTED AND PRESPLT IS INCREMENTED.  IF THERE IS NO
C   MATCH THE LOOP IS SKIPPED ( J BEING AUTOMATICALLY INCREMENTED)
C   AND AGAIN THE STEP SEES IF PLOTS(PRESPLT) = J.
C   A MODIFICATION BY ROD STOLTZFUS, 2/16/84
C
      PRINT*,PLOTS(PRESPLT),J
      IF (PLOTS(PRESPLT) .NE. J) GOTO 200
      PRESPLT=PRESPLT+1

C
C   READ IN THE APPROPRIATE DATA SEGMENT.
C
      DO 300 I=1,L
        X(I)=DATA(I+(J-1)*D)
 300  CONTINUE
C
C   MEAN REMOVAL
C
      MEAN=0.0
      DO 400 I=1,L
        MEAN=MEAN+(X(I)-MEAN)/FLOAT(I)
```

```
 400  CONTINUE
      DO 500 I=1,L
        X(I)=X(I)-MEAN
 500  CONTINUE
C
C   APPLY WINDOW TO DATA.
C
      CALL WINDOW(X,L,M,WINDOWO)
C
C   COMPUTE PERIODOGRAM
C
C   FOR MORE INFORMATION ON FFTRC SEE THE IMSL DOCUMENTATION.
C
      CALL FFTRC(X,M,Z,IWK,WK)
C     DO 800 I=1,M2          (OPTIONAL)
C       Z(I)=CONJG(Z(I))     (OPTIONAL)
C800  CONTINUE               (OPTIONAL)
      DO 600 I=1,M2
        MAG(I)=(2.0*SMPTIME/FLOAT(L))*(CABS(Z(I)))**2
        FREQ(I)=(I-1)/(FLOAT(M)*SMPTIME)
 600  CONTINUE
C
C   AVERAGE PERIODOGRAMS
C
      DO 900 I=1,M2
        MAGAVE(I)=(1.0/FLOAT(TOTAL))*MAG(I)+MAGAVE(I)
 900  CONTINUE
C
C   DISPLAY INDIVIDUAL PERIODOGRAM
C
      IF(DISPLAY .EQ. 2)GOTO 200
      IF(S .GT. NUMBER)GOTO 200
      CALL FILTCAL(MAG,FREQ,M2,FC,FAC,FLE)
      CALL DEEMPH(MAG,FREQ,M2,BBAND)
      CALL MAXMIN(MAG,FREQ,MAXMAG,MAXFREQ,M,M2)
      CALL PLOTTER(MAG,FREQ,M,M2,MAXMAG,MINMAG,MAXFREQ,OPTION,SLOPE,
     *             YINT,FIT2,LOLIMIT,HILIMIT,STIME,SROTNUM,ALTITUD,
     *             ROCKSPD,IHRS,IMIN,SECS,DIGRATE,OVLP,GAIN,J)
      IF(FIT2 .EQ. 2)GOTO 10
      PRINT*,"DO YOU WISH TO STORE THE SPECTRAL INDEX?   1—YES"
      PRINT*,"                                           2—NO"
      READ*,V
      IF(V .EQ. 1)CALL STORE(SLOPE,YINT,LTIME,STIME,SMPTIME,N)
  10  S=S+1
 200  CONTINUE
C
C       RECONSTRUCT ARRAY FREQ( ) SINCE SUBROUTINE PLOTTER DESTROYS IT.
C       FOLLOWING LOOP ADDED ON B. TOMEI'S SUGGESTION. 10/24/83
C
      DO 999 I=1,M2
        FREQ(I)=(I-1)/(FLOAT(M)*SMPTIME)
 999  CONTINUE
      RETURN
      END
C
C
C
C
C
C   SUBROUTINE MAXMIN CALCULATES THE VALUES OF MAXMAG, MAXMIN,
C   AND MAXFREQ AND ROUNDS THEM TO APPROPRIATE VALUES FOR AXES
C   PLOTTING.
C
C
      SUBROUTINE MAXMIN(MAG,FREQ,MAXMAG,MAXFREQ,M,M2)
      INTEGER M,M2
      REAL MAG(M2),FREQ(M2),MAXMAG,MAXFREQ
      MAXMAG=0.0
      MAXFREQ=FREQ(M2)
      DO 100 I=1,M2
        IF(MAG(I) .GT. MAXMAG) MAXMAG=MAG(I)
```

```
  100  CONTINUE
       CALL LIMITS(MAXMAG)
       RETURN
       END
C
C
C
C
C
C  SUBROUTINE FILTCAL PERFORMS A CALIBRATION TO THE SPECTRUM
C   IN ORDER TO COMPENSATE FOR THE ROLLOFF EFFECTS OF THE
C   TELEMETRY FILTER, THE AC AMPLIFIER, AND THE LOGARITHMIC
C   ELECTROMETER.  THE TELEMETRY FILTER IS MODELED AS AN
C   IDEAL 3-POLE LOW PASS FILTER (SEE ZIMMERMAN,1980).  THE
C   AC AMPLIFIER AND LOG ELECTROMETER ROLLOFFS ARE MODELLED
C   AS SINGLE POLE LOW PASS FILTERS.  THE INPUT PARAMETERS
C   ARE
C         FC  --  THE UPPER 3DB FREQUENCY OF THE TELEMETRY FILTER.
C        FAC  --  THE UPPER 3DB FREQUENCY OF THE AC AMPLIFIER.
C        FEL  --  THE UPPER 3DB FREQUENCY OF THE LOG ELECTROMETER.
C   HC,HAC,HEL ARE THE MAGNITUDES SQUARED OF THE TRANSFER FUNCTIONS
C   CORRESPONDING TO THE RESPECTIVE FILTER.
C
C
      SUBROUTINE FILTCAL(MAG,FREQ,M2,FC,FAC,FLE)
      INTEGER M2
      REAL MAG(M2),FREQ(M2),OMEGA,PI,WC,WAC,WLE
      PI=3.14159265
      WC=2.0*PI*FC
      WAC=2.0*PI*FAC
      WLE=2.0*PI*FLE
      DO 100 I=1,M2
        OMEGA=2.0*PI*FREQ(I)
        HC=7.75338*WC**6/(((2.10199*WC**2-OMEGA**2)**2
     *     +4.40165*(WC*OMEGA)**2)*(1.75480*WC**2
     *     +OMEGA**2))
        HAC=WAC**2/(WAC**2+OMEGA**2)
        HLE=WLE**2/(WLE**2+OMEGA**2)
        MAG(I)=MAG(I)/(HC*HAC*HLE)
  100 CONTINUE
      RETURN
      END
C
C
C
C
C
C   SUBROUTINE DEEMPH PERFORMS DE-EMPHASIS ON THE SPECTRUM
C   OBTAINED FROM THE FINE STRUCTURE EXPERIMENT. THE PRE-EMPHASIS
C   FILTER IS MODELED AS A SINGLE-POLE HIGH PASS FILTER WITH
C   CUTOFF FREQUENCY EQUAL TO THAT OF THE BROADBAND AMPLIFIER.
C   THE DE-EMPHASIS FILTER IS THEN OBTAINED BY TAKING THE INVERSE
C   OF THE PRE-EMPHASIS FILTER TRANSFER FUNCTION.  DE-EMPHASIS
C   IS REQUIRED FOR PAYLOADS 31.028, 31.029, AND ANY OTHER
C   PAYLOADS WITH THE SAME EXPERIMENT CONFIGURATION.  THE
C   PARAMETERS ARE
C      1) BBAND  --  THIS NUMBER REFERS TO THE NUMBER OF THE
C                    BROADBAND AMPLIFIER WHOSE OUTPUT IS UNDER
C                    ANALYSIS.  FOR BBAND .EQ. 0, DE-EMPHASIS
C                    IS BYPASSED.
C      2) WC  --  THIS IS THE LOWER 3DB CUTOFF FREQUENCY OF THE
C                 BROADBAND AMPLIFIER.
C      3) HDE -- THIS IS THE MAGNITUDE SQUARED OF THE DE-EMPHASIS
C                FILTER TRANSFER FUNCTION.
C
C
      SUBROUTINE DEEMPH(MAG,FREQ,M2,BBAND)
      INTEGER M2,BBAND,L
      REAL MAG(M2),FREQ(M2),PI,OMEGA,WC,HDE
      PI=3.14159265
      IF(BBAND .EQ. 0)RETURN
```

```
C
C   PERFORM DE-EMPHASIS
C
      WC=2.0*PI*400.0
      IF(BBAND .EQ. 2) WC=2.0*PI*53.9
      DO 100 I=2,M2
        OMEGA=2.0*PI*FREQ(I)
        HDE=(OMEGA**2+WC**2)/OMEGA**2
        MAG(I)=HDE*MAG(I)
 100  CONTINUE
      RETURN
      END
C
C
C
C
C
C   SUBROUTINE PLOTTER PLOTS THE POWER DENSITY VERSUS
C   FREQUENCY OR SCALE SIZE  IN LINEAR OR LOGARITHMIC FORM.
C   A LINEAR FIT MAY ALSO BE PERFORMED ON THE LOGARITHMIC PLOT.
C
C****
C   NOTE THAT THIS SUBROUTINE WILL ROUND OFF POINTS WHICH ARE OFF
C   THE PLOTTING SURFACE.  THUS THE ROUTINE IS A BIT DESTRUCTIVE.
C   A LOCAL COPY OF THE MAGNITUDE ARRAY COULD BE BE MADE IF ABSOLUTE
C   INTEGRITY OF THE DATA IS REQUIRED.
C
C   IF CURVE FITTING IS CHOSEN, THE INPUT MAGNITUDE INFORMATION IS
C   TOTALLY DESTROYED IN PROVIDING INFORMATION TO THE LINE FITTING
C   SUBROUTINE.
C****
C
C
C
      SUBROUTINE PLOTTER (MAG,FREQ,M,M2,MAXMAG,MINMAG,MAXFREQ,OPTION,
     *                    SLOPE,YINT,FIT,LOLIMIT,HILIMIT,STIME,SHOTNUM,
     *                    ALTITUD,ROCKSPD,IHRS,IMIN,SECS,DIGRATE,OVLP,
     *                    GAIN,PLOTNUM)
      INTEGER M,M2,OPTION,FIT,J,IHRS,IMIN,OVLP,DIGRATE,PLOTNUM
      REAL MAG(M2),FREQ(M2),MAXMAG,MINMAG,MAXFREQ,YINT,SLOPE,
     *     LOLIMIT,HILIMIT,X1(3),Y1(3),STIME,TIME,ALTITUD,ROCKSPD,
     *     SECS,GAIN,SHOTNUM,REALK,REALM,RELOVLP,REALDIG,LOCMAG(2049)
C
C
C
C****
C  SUBROUTINE PLOTTER ADJUSTS THE DATA TO FIT INTO THE LEGAL BOUNDS
C  OF THE REQUESTED PLOT.  FOR EXAMPLE, IT CHANGES ANYTHING <
C  MINMAG TO MINMAG.  TO PRESERVE THE ORIGINAL DATA THE ORIGINAL
C  DATA IS SAVED IN MAG.
C****
C
      DO 5 I=1,M2
        LOCMAG(I)=MAG(I)
  5   CONTINUE
C
C   INITIALIZE PLOTTING PARAMETERS
C
C
      CALL USTART
C       THE FOLLOWING DISPLAY CAPABILITY WAS ADDED BY RODNEY
C            STOLTZFUS. 10/09/83.
C       TO USE, REMOVE THE C'S AT THE BEGINNING OF THE LINES.
C      ALSO MAKE SURE APPROPRIATE PARAMETERS ARE PASSED INTO SUBROUTINE
C      PLOTTER AND SPCTRM.
      CALL UWRITE(52.,98.,"ROCKET SHOT     ;")
C      CALL UWRITE(52.,95.,"LAUNCH TIME     ;")
      CALL UWRITE(52.,95.,"PLOT NUMBER;")
      CALL UWRITE(52.,92.,"SEC AFTER LAUNCH;")
C      CALL UWRITE(52.,89.,"SPEED           ;")
C      CALL UWRITE(52.,86.,"ALTITUDE        ;")
C      CALL UWRITE(52.,83.,"ROCKET ANGLE    ;")
      CALL UWRITE(52.,80.,"FFT BLOCK LENGTH;")
      CALL UWRITE(52.,77.,"SEGMENT OVERLAP;")
```

```
C      CALL UWRITE(52.,75.,"DIGITIZING RATE ;")
C      CALL UWRITE(52.,72.,"ROCKET SPIN RATE;")
C      CALL UWRITE(52.,69.,"GAIN            ;")
       CALL UPSET("PRECISION",6.)
       CALL USET("REAL")
       CALL UWRITE(84.,98.,SHOTNUM)
C      CALL UWRITE(84.,72.,SPINRAT)
C      CALL UWRITE(84.,83.,ANGLE)
C      CALL UWRITE(84.,86.,ALTITUD)
C      CALL UWRITE(84.,89.,ROCKSPD)
C
C     STIME IS THE TIME AFTER LAUNCH
C      WHEN STIME IS PASSED TO SUBROUTINE PLOTTER IT CONTAINS THE
C      TIME OF THE FIRST PLOT.  IN PLOTTER, A LOCAL COPY CALLED TIME
C      IS USED FOR LOCAL HANDLING.
C     IF PLOTNUM IS 0 THE AVERAGE PLOT IS BEING REQUESTED.  THUS
C      CORRECT TIME S.T. IT IS THE FIRST PLOT'S TIME (I.E. STIME).
C      THE FOLLOWING FORMULA ASSUMES FFT LENGTH = SEGMENT LENGTH.
C
       TIME=STIME+((FLOAT(PLOTNUM-1))*(FLOAT(M-OVLP))/(FLOAT(DIGRATE)))
       IF(PLOTNUM .EQ. 0) TIME=STIME


       CALL UWRITE(84.,92.,TIME)
C      CALL UWRITE(96.,95.,SECS)
C      CALL UWRITE(84.,69.,GAIN)
C      CALL USET("INTEGER")
C
C     MUST MAKE ALL VARIABLES REAL TO BE PASSED WHEN PLOTTING.
C
C
       CALL UWRITE(84.,95.,FLOAT(PLOTNUM))
C      CALL UWRITE(84.,95.,FLOAT(IHRS))
C      CALL UWRITE(90.,95.,FLOAT(IMIN))
C      CALL UWRITE(84.,72.,FLOAT(DIGRATE))
       CALL UWRITE(84.,77.,FLOAT(OVLP))
       CALL UWRITE(84.,80.,FLOAT(M))
       CALL USET("TEXT")
C
C    END DISPLAY MODIFICATIONS BY R.S.
C
C
       CALL USET("XBOTHLABEL")
       CALL USET("YBOTHLABEL")
       CALL USET("OWNSCALE")
       CALL UPSET("XLABEL"," ;")
       CALL UPSET("YLABEL"," ;")
       CALL UPSET("TERMINATOR",";")
       CALL UPSET("VERTICAL",3.0)
       CALL UPSET("HORIZONTAL",2.0)
       CALL USET("SOFTWARE")
       CALL UDAREA(0.0,7.0,0.0,5.7)
       CALL UPRINT(40.0,2.0,"FREQUENCY  (HZ);")
       CALL UMOVE(4.0,0.0)
       CALL UROTAT(90.0)
       CALL UPRINT(25.0,0.0,"POWER DENSITY   (DELTA N/N) /HZ;")
       CALL UPRINT(79.0,1.5,"2;")
       CALL USET("HARDWARE")
       CALL USET("SYSTEM")
C
C    THE FOLLOWING THREE STATEMENTS MAY BE USED TO
C    SUPERCEDE THE OUTPUT OF SUBROUTINE MAXMIN.  IF
C    THIS IS DESIRED, REMOVE THE COMMENT MARKERS.
C
C      MINMAG=10E-12       (OPTIONAL)
       MAXMAG=10E-4
C      MAXFREQ=1000.0      (OPTIONAL)
C
       CALL UWINDO(0.0,MAXFREQ,0.0,MAXMAG)
       IF(OPTION .EQ. 2)GOTO 10
C
C    PERFORM LINEAR PLOTTING
C
```

```
      CALL UPLOT1(FREQ,MAG,FLOAT(M2))
      GOTO 20
C
C   PERFORM LOGARITHMIC PLOTTING
C
  10  CALL UWINDO(1.0,MAXFREQ,MINMAG,MAXMAG)
      CALL USET("XYLOGARITHMIC")
      CALL USET("LOGXAXIS")
      CALL USET("LOGYAXIS")
      J=0
      DO 100 I=1,M2
        IF(MAG(I) .LE. MINMAG) MAG(I)=MINMAG
        IF(FREQ(I) .LE. MAXFREQ) J=J+1
 100  CONTINUE
      FREQ(1)=0.01
      CALL UPLOT1(FREQ,MAG,FLOAT(J))
      CALL UFLUSH
      CALL UPAUSE
C
C   RESTORE THE MAG USING THE SAVED LOCMAG.
C
      DO 195 I=1,M2
        MAG(I)=LOCMAG(I)
 195  CONTINUE
C
C
C   PERFORM LINEAR LEAST-SQUARES FIT IF FIT .NE. 2.
C
C
      IF(FIT .EQ. 2)RETURN
      FREQ(1)=0.0
C
C   FLAG DATA POINTS WITH MAGNITUDE EQUAL TO ZERO
C   OR WITH FREQUENCY OUT OF LIMITS.
C
C ***** ORIGINALLY B. TOMEI HAD .EQ. IN THE SECOND PAIR OF FOLLOWING
C***** CONDITIONALS.  THEY HAVE BEEN CHANGED TO .LE.
C***** R.S. 3/11/84
C
      DO 200 I=2,M2
        IF(FREQ(I) .LT. LOLIMIT)FREQ(I)=0.0
        IF(FREQ(I) .GT. HILIMIT)FREQ(I)=0.0
        IF(MAG(I) .LE. MINMAG)FREQ(I)=0.0
        IF(MAG(I) .LE. 0.0)FREQ(I)=0.0
  200  CONTINUE
C
C   REMOVE FLAGGED DATA POINTS AND COMPRESS DATA
C     ****FLAGGED POINTS ARE THOSE WITH FREQUENCY LESS
C     ****THAN 0.1.  IF THE PLOT'S LOWEST FREQUENCY IS
C     ****LESS THAN 0.1 CHANGE THE CONDITIONAL WHICH
C     ****WHICH REMOVES THE DATA POINT
C
C
      J=1
      DO 300 I=1,M2
        IF(FREQ(I) .LE. 0.0)GOTO 300
        MAG(J)=ALOG10(MAG(I))
        FREQ(J)=ALOG10(FREQ(I))
        J=J+1
  300 CONTINUE
C
C   PERFORM LINEAR FIT
C
      CALL ULINFT(FREQ,MAG,FLOAT(J-1),SLOPE,YINT)
C
C   GENERATE FITTED CURVE (THREE POINTS ONLY)
C
      X1(1)=LOLIMIT
      Y1(1)=(10.0**YINT)*(X1(1)**SLOPE)
      X1(2)=(LOLIMIT+HILIMIT)/2.0
      Y1(2)=(10.0**YINT)*(X1(2)**SLOPE)
      X1(3)=HILIMIT
      Y1(3)=(10.0**YINT)*(X1(3)**SLOPE)
```

```
C
C   PLOT FITTED LINE
C
      CALL USET("LINE")
      CALL USET("OLDSCALE")
      CALL UPLOT1(X1,Y1,3.0)
   20 CALL UFLUSH
      CALL UPAUSE
      CALL UERASE
C
C      RESTORE ARRAY MAG USING THE SAVED DATA IN LOCMAG
C
      DO 25 I=1,M2
        MAG(I)=LOCMAG(I)
   25 CONTINUE

      CALL UEND
      RETURN
      END
C
C
C
C
C
C   SUBROUTINE STORE STORES THE SPECTRAL INDEX DATA IN ARRAY
C   INDEX IN THE FOLLOWING FORMAT-  TIME,SPECTRAL INDEX,
C   MAGNITUDE.  ARRAY INDEX THEN SERVES AS THE INPUT ARRAY
C   FOR PROGRAM SPINDEX.
C
C
      SUBROUTINE STORE (SLOPE,YINT,LTIME,STIME,SMPTIME,N)
      INTEGER N
      REAL SLOPE,YINT,LTIME,STIME,SMPTIME,AVTIME
      AVTIME=(LTIME+STIME)+(FLOAT(N)*SMPTIME)/2.0
      WRITE(4,11) AVTIME,SLOPE,(10.0**YINT)
   11 FORMAT(1X,F9.2,1X,F10.5,1X,E13.6)
      RETURN
      END
C
C
C
C
C
C   SUBROUTINE WINDOW APPLIES A SPECIFIED WINDOW TO THE DATA
C   SEGMENT X.  THE WINDOW IS SPECIFIED BY WINDONO.  THE
C   WINDOWED DATA IS ALSO NORMALIZED BY THE INCOHERENT
C   POWER GAIN OF THE WINDOW (IPG).
C
C
      SUBROUTINE WINDOW (X,L,M,WINDONO)
      INTEGER L,J,R,WINDONO,M
      REAL X(M),PI,IPG
      PI=3.141592653
      GOTO(10,20,30,40,50,60)WINDONO
C
C   RECTANGULAR WINDOW
C
   10 RETURN
C
C   BARTLETT WINDOW
C
   20 J=L/2
      R=J+1
      IPG=0.0
      DO 100 I=1,J
        WEIGHT=FLOAT(I-1)/FLOAT(J)
        X(I)=X(I)*WEIGHT
        IPG=WEIGHT**2+IPG
  100 CONTINUE
      DO 200 I=R,L
        WEIGHT=FLOAT(L-I+1)/FLOAT(J)
        X(I)=X(I)*WEIGHT
        IPG=WEIGHT**2+IPG
```

```
 200  CONTINUE
      IPG=IPG/FLOAT(L)
      DO 201 I=1,L
        X(I)=X(I)/SQRT(IPG)
 201  CONTINUE
      RETURN
C
C   HANNING WINDOW
C
  30  IPG=0.375
      DO 300 I=1,L
        WEIGHT=0.5*(1.0-COS(2.0*PI*(I-1)/L))
        X(I)=X(I)*WEIGHT/SQRT(IPG)
 300  CONTINUE
      RETURN
C
C   HAMMING WINDOW
C
  40  IPG=0.3974
      DO 400 I=1,L
        WEIGHT=0.54-0.46*COS(2.0*PI*(I-1)/L)
        X(I)=X(I)*WEIGHT/SQRT(IPG)
 400  CONTINUE
      RETURN
C
C   BLACKMAN WINDOW
C
  50  IPG=0.3046
      DO 500 I=1,L
        WEIGHT=0.42-0.5*COS(2.0*PI*(I-1)/L)+0.08*COS(4.0*PI*(I-1)/L)
        X(I)=X(I)*WEIGHT/SQRT(IPG)
 500  CONTINUE
      RETURN
C
C   BLACKMAN-HARRIS WINDOW (4-TERM)
C
  60  IPG=0.289672277
      DO 600 I=1,L
        WEIGHT=0.40217-0.49703*COS(2.0*PI*FLOAT(I-1)/L)
     *         +0.09392*COS(4.0*PI*FLOAT(I-1)/L)
     *         -0.00183*COS(6.0*PI*FLOAT(I-1)/L)
        X(I)=X(I)*WEIGHT/SQRT(IPG)
 600  CONTINUE
      RETURN
      END
C
C
C
C
C
C   SUBROUTINE LIMITS ROUNDS THE VALUE OF MAX FOR EASE IN AXES
C   PLOTTING.  FOR 10**(N+1) > MAX > 10**N ,(N GREATER THAN OR
C   EQUAL TO 1.0), LIMITS ROUNDS THE VALUE OF MAX UP TO THE
C   NEXT (N-1)TH POWER OF TEN.  FOR 10**-(N-1) > MAX > 10**-N ,
C   (N LESS THAN 1.0), LIMITS ROUNDS THE VALUE OF MAX UP TO
C   THE NEXT -(N+1)TH POWER OF TEN.
C
C
      SUBROUTINE LIMITS (MAX)
      REAL Z,Y,FACTOR,MAX,DELTA
      IF(MAX .GE. 10.) GOTO 10
      DO 100 I=1,15
        Z=10.0**(I-14)
 100  IF(MAX .GT. Z)FACTOR=10.0**(I-14)
      Y=(AINT(10.0*MAX/FACTOR))/10.0
      MAX=FACTOR*(Y+.1)
      RETURN
  10  DO 200 I=1,8
        Z=10.0**I
 200  IF(MAX .GT. Z)FACTOR=10.0**(I-1)
      DELTA=0.0
      IF(AMOD(MAX,FACTOR) .GE. 0.0001)DELTA=1.0
```

```
      MAX=FACTOR*(AINT(MAX/FACTOR)+DELTA)
      RETURN
      END
C
C
C
C
C
C
C     SUBROUTINE SELECT ASKS FOR THE PLOT NUMBERS DESIRED.  IF THE
C     USER ONLY WANTS TO SEE PLOTS 3 AND 12, THE USER ENTERS THESE
C     NUMBERS.  THE PLOT NUMBERS MUST BE ENTERED IN ORDER, I.E. PLOT
C     12 CANNOT BE REQUESTED BEFORE PLOT 3.  THE SUBROUTINE VERIFIES
C     THE SEQUENTIALLNESS OF THE DATA.
C     THE SUBROUTINE ALSO RETURNS NUMBER WHICH TELLS THE HIGHEST PLOT
C     NUMBER REQUESTED.  THIS VALUE IS NEEDED FOR OTHER SUBROUTINES.
C     VARIABLE TOTAL CONTAINS THE TOTAL NUMBER OF INDIVIDUAL PLOTS
C     BEING REQUESTED.
C
C     THE VARIABLE K CONTAINS THE NUMBER OF SEGMENTS THE DATA WILL
C   BE DIVIDED INTO.  IT IS THE MAXIMUM NUMBER OF PLOTS PERMITTED.
C
C
C     PLOTS(100) CONTAINS 1 IF INDIVIDUAL PLOTS ARE DESIRED, 2
C     IF ALL SEGMENTS ARE TO BE PLOTTED.  IN THE LATTER CASE,
C     PLOTS WILL CONTAIN 1 TO K.
C
      SUBROUTINE SELECT(PLOTS,NUMBER,K,TOTAL)
      INTEGER PLOTS(100),NUMBER,K,TOTAL,VER

C
C     INITIALIZE
C
   50 NUMBER=0
      PRINT*,"GOT TO SELECT ROUTINE"
C
C     CHECK IF THE USER WISHES ALL POSSIBLE SEGMENTS OR JUST A FEW.
C     PLOTS(100) IS 1 IF SELECTED PLOTTING IS DESIRED, 2 IF ALL ARE
C     WANTED.
C
      IF (PLOTS(100) .NE. 1) GOTO 400
C
      PRINT*,"ENTER THE TOTAL NUMBER OF DESIRED PLOTS"
      READ*,TOTAL
      IF (TOTAL .EQ. K) GOTO 400
      PRINT*,"ENTER THE DESIRED PLOT NUMBERS, ONE AT A TIME, AND"
      PRINT*,"IN ORDER AS YOU ARE QUERIED."
C
C     PUT  THE PLOT NUMBERS INTO PLOTS.  FIND THE HIGHEST PLOT
C     NUMBER AND PUT IT IN NUMBER.
C
      DO 100 I=1,TOTAL
        PRINT*,"PLOT NUMBER?"
        READ*,PLOTS(I)
        NUMBER=PLOTS(I)
  100 CONTINUE
C
C     VERIFY THAT THE PLOT NUMBERS ARE IN ORDER.
C
      VER=0
      DO 200 I=1,TOTAL
        IF (PLOTS(I) .LE. VER) GOTO 300
        VER=PLOTS(I)
  200 CONTINUE
C
C     IF THE PROGRAM GETS HERE, VERIFICATION IS COMPLETE AND THE
C     SUBROUTINE CAN RETURN TO WHERE IT WAS CALLED FROM.
C
      RETURN
C
C     VERIFICATION ERROR COMES HERE.
C
```

```
  300 PRINT*,"***PLOT NUMBERS ARE NOT SEQUENTIAL.  TRY AGAIN."
      PRINT*,"***REMEMBER, IF YOU WANT ALL THE PLOTS, RESPOND"
      PRINT*,"TO THE NEXT QUESTION WITH ",K
      GOTO 50

C
C     IF ALL PLOTS ARE DESIRED, PUT IN ALL POSSIBLE PLOT NUMBERS,
C     THAT IS, 1 TO K.
C
  400 NUMBER=K
      TOTAL=K
      DO 500 I=1,K
      PLOTS(I)=I
  500 CONTINUE
      RETURN
      END



C
C   THE FOLLOWING SUBROUTINES WERE ADDED MARCH,1984.
C


      SUBROUTINE MENU(QUES)

      INTEGER QUES
C
C  THIS SUBROUTINE EXPLAINS THE VARIOUS PROCESSES WHICH CAN BE
C  APPLIED TO STORED PLOTS.  THE USER CHOOSES, SETTING QUES
C  TO 1-8.
C
      PRINT*,"*****************************************"
      PRINT*," "
      PRINT*," "
      PRINT*,"1) SUBTRACT PLOT #1 FROM #2.  THE PLOTS MUST BE OF THE"
      PRINT*,"SAME SIZE.  THE RESULTING PLOT IS PLACED IN THE "
      PRINT*,"WORK PLOT."
      PRINT*," "
      PRINT*,"2) MAKE AN INCREMENTED WINDOW AVERAGE OF THE WORK "
      PRINT*,"PLOT.  THE RESULT IS PLACED IN THE WORKPLOT."
      PRINT*," "
      PRINT*,"3) TRADE THE CONTENTS OF TWO PLOT BAYS.  THE PLOTS"
      PRINT*,"NEED NOT BE OF THE SAME SIZE."
      PRINT*," "
      PRINT*,"4) AVERAGE PLOTS #1 AND #2 TOGETHER.  THE RESULT "
      PRINT*,"IS PLACED IN THE WORK PLOT."
      PRINT*," "
      PRINT*,"5) SHOW THE TIME, SIZE, AND FFT SIZE OF PLOT BAYS"
      PRINT*," "
      PRINT*,"6) PRINT OUT THE WORK PLOT ONTO THE SCREEN."
      PRINT*," "
      PRINT*,"7) GO BACK FOR MORE PLOTS OR QUIT THE PROGRAM."
      PRINT*," "
      PRINT*,"8) COPY A STORAGE BAY TO THE WORK BAY."
      PRINT*," "
      PRINT*," "
      PRINT*,"*****************************************************"
      PRINT*," "
      PRINT*,"TYPE IN YOUR CHOICE"
      READ*,QUES
      PRINT*," "
      PRINT*," "
      RETURN
      END
```

```
      SUBROUTINE DIFFSET(SAVMAG1,SAVFRQ1,PARAMS1,SAVMAG2,SAVFRQ2,
     *                   PARAMS2,WORKMAG,WORKFRQ,WKPARMS)
C
C   THIS SUBROUTINE SUBTRACTS PLOT#1 FROM PLOT#2.  THE TWO PLOTS MUST
C   BE OF THE SAME SIZE.  THE RESULTING SPECTRUM IS PUT IN WORKMAG.
C
      INTEGER QUES
      REAL SAVMAG1(1025),SAVMAG2(1025),SAVFRQ1(1025),
     *     SAVFRQ2(1025),WORKMAG(1025),WORKFRQ(1025),
     *     PARAMS1(10),PARAMS2(10),WKPARMS(10)
      PRINT*,"THIS ROUTINE SUBTRACTS PLOT#1 FROM PLOT#2. THE PLOTS"
      PRINT*,"MUST BE OF EQUAL SIZE.  THE RESULTING PLOT IS"
      PRINT*,"PLACED IN THE WORK PLOT"
      CALL PRTSTAT(PARAMS1,PARAMS2,WKPARMS)
      PRINT*,"DO YOU NEED TO SWITCH PLOTS 1 AND 2?  1-YES"
      PRINT*,"                                      2-NO"
      PRINT*,"                                      3-ABORT ROUTINE"
      READ*,QUES
      IF (QUES .EQ. 3) RETURN
      IF (QUES .EQ. 1) CALL TRNSPLT(SAVMAG1,SAVFRQ1,PARAMS1,SAVMAG2,
     *                              SAVFRQ2,PARAMS2)
      CALL DIFFRNC(SAVMAG1,SAVFRQ1,PARAMS1,SAVMAG2,SAVFRQ2,PARAMS2,
     *             WORKMAG,WORKFRQ,WKPARMS)
      RETURN
      END



      SUBROUTINE WNDOSET(SAVMAG1,SAVFRQ1,PARAMS1,SAVMAG2,SAVFRQ2,
     *                   PARAMS2,WORKMAG,
     *                   WORKFRQ,WKPARMS)

      REAL SAVMAG1(1025),SAVMAG2(1025),SAVFRQ1(1025),SAVFRQ2(1025),
     *     PARAMS1(10),PARAMS2(10),WORKMAG(1025),WORKFRQ(1025),
     *     WKPARMS(10)
      INTEGER QUES
C
C     THE FOLLOWING DOES AN INCREMENTED WINDOW AVERAGE OF THE WORK PLOT.
C   THE RESULT IS PUT IN WORK PLOT ALSO.
C
    PRINT*,"THIS ROUTINE COMPUTES AN INCREMENTED WINDOW AVERAGE OF THE "
    PRINT*,"WORK PLOT.  THE RESULT IS ALOS PUT INTO THE WORK PLOT."
    PRINT*,"DO YOU NEED TO PUT A SAVED PLOT INTO THE WORK PLOT."
    PRINT*,"                                          1-YES,BAY#1"
    PRINT*,"                                          2-YES,BAY#2"
    PRINT*,"                                          4-NO"
    PRINT*,"                                          5=ABORT"
    READ*,QUES
    IF(QUES .EQ. 1) CALL TRNSPLT(SAVMAG1,SAVFRQ1,PARAMS1,WORKMAG,
   *                             WORKFRQ,WKPARMS)
    IF(QUES .EQ. 2) CALL TRNSPLT(SAVMAG2,SAVFRQ2,PARAMS2,WORKMAG,
   *                             WORKFRQ,WKPARMS)
    IF(QUES .EQ. 5) RETURN
    CALL WNDOAVE(WORKMAG,WORKFRQ,WKPARMS)
    RETURN
    END



    SUBROUTINE TRNSSET(SAVMAG1,SAVFRQ1,PARAMS1,SAVMAG2,SAVFRQ2,
   *                   PARAMS2,WORKMAG,
   *                   WORKFRQ,WKPARMS)

    REAL SAVMAG1(1025),SAVMAG2(1025),SAVFRQ1(1025),SAVFRQ2(1025),
   *     WORKMAG(1025),WORKFRQ(1025),PARAMS1(10),PARAMS2(10),
   *     WKPARMS(10)
    INTEGER QUES
```

```
C
C   SWITCH PLOTS AROUND
C
      PRINT*,"THIS ROUTINE TRADES PLOTS BETWEEN A SPECIFIED PLOT"
      PRINT*,"BAY AND THE WORK PLOT."
      PRINT*,"WHICH PLOT DO YOU WISH TO TRADE WITH THE WORK PLOT"
      PRINT*,"                              (  4-NO SWITCHING )"
      READ*,QUES
      IF (QUES .EQ. 1) CALL TRNSPLT(SAVMAG1,SAVFRQ1,PARAMS1,WORKMAG,
     *                              WORKFRQ,WKPARMS)
      IF (QUES .EQ. 2) CALL TRNSPLT(SAVMAG2,SAVFRQ2,PARAMS2,WORKMAG,
     *                              WORKFRQ,WKPARMS)
      CALL PRTSTAT(PARAMS1,PARAMS2,WKPARMS)
      RETURN
      END


      SUBROUTINE COPYSET(SAVMAG1,SAVFRQ1,PARAMS1,SAVMAG2,SAVFRQ2,
     *                   PARAMS2,WORKMAG,WORKFRQ,WKPARMS)

C   THIS ROUTINE COPIES A STORAGE BAY TO THE WORK BAY.  NOTE THAT
C   THIS WILL DESTROY WHATEVER IS IN THE WORK BAY PREVIOUS TO THE
C   CALL.  TO COPY THE WORK BAY TO A STORAGE BAY, TRADE THE WORK
C   BAY WITH THE DESIRED STORAGE BAY, AND THEN DO THE COPYING.
C
      INTEGER QUES
      REAL SAVMAG1(1025),SAVMAG2(1025),WORKMAG(1025),
     *     SAVFRQ2(1025),WORKFRQ(1025),PARAMS1(10),PARAMS2(10),
     *     WKPARMS(10)

      PRINT*,"COPIES A STORAGE BAY TO THE WORK BAY"
      PRINT*," "
      PRINT*,"WHICH STORAGE BAY DO YOU WISH TO COPY?"
      PRINT*,"                              1-BAY#1"
      PRINT*,"                              2-BAY#2"
      PRINT*,"                              3-ABORT ROUTINE"
      READ*,QUES
      IF (QUES .EQ. 1) CALL COPY(SAVMAG1,SAVFRQ1,PARAMS1,WORKMAG,
     *                           WORKFRQ,WKPARMS)
      IF (QUES .EQ. 2) CALL COPY(SAVMAG2,SAVFRQ2,PARAMS2,WORKMAG,
     *                           WORKFRQ,WKPARMS)
      IF (QUES .EQ. 3) RETURN
      RETURN
      END


      SUBROUTINE AVRGSET(SAVMAG1,SAVFRQ1,PARAMS1,SAVMAG2,SAVFRQ2,
     *                   PARAMS2,WORKMAG,WORKFRQ,WKPARMS)
      REAL WORKMAG(1025),WORKFRQ(1025),SAVMAG1(1025),SAVMAG2(1025),
     *     SAVFRQ1(1025),SAVFRQ2(1025)
      INTEGER WKPARMS(10),PARAMS1(10),PARAMS2(10),QUES,ERR
      PRINT*,"AVERAGES PLOT BAYS 1 AND 2.      1-CONTINUE"
      PRINT*,"                                 2-ABORT ROUTINE"
      READ*,QUES
      IF (QUES .EQ. 2) RETURN
C
C   MAKE SURE BAYS 1 AND 2 ARE OF THE SAME SIZE
C
      ERR=0
      CALL SIZEERR(PARAMS1,PARAMS2,2,ERR)
      IF(ERR .NE. 1) RETURN
C
C     PERFORM AVERAGING
C
      CALL AVERAGE(SAVMAG1,SAVFRQ1,PARAMS1,SAVMAG2,SAVFRQ2,
     *             PARAMS2,WORKMAG,WORKFRQ,WKPARMS)
      RETURN
      END
```

```
      SUBROUTINE DIFFRNC(LOCMAG1,LOCFRQ1,LOCPAR1,LOCMAG2,LOCFRQ2,
     *                   LOCPAR2,WORKMAG,WORKFRQ,WKPARMS)

      INTEGER I,ERR,K
      REAL LOCMAG1(1025),LOCFRQ1(1025),LOCMAG2(1025),LOCFRQ2(1025),
     *     WORKMAG(1025),WORKFRQ(1025),LOCPAR1(10),LOCPAR2(10),
     *     WKPARMS(10)
C
C   CHECK TO SEE THAT THE TWO ARRAYS HAVE SAME SIZE.
C
      ERR=0
      CALL SIZEERR(LOCPAR1,LOCPAR2,1,ERR)
      IF (ERR .NE. 1) RETURN
C
C   TAKE THE DIFFERENCE
C
      K=IFIX(LOCPAR1(2) + .1)

      DO 100 I=1,K
        WORKMAG(I)=LOCMAG2(I)-LOCMAG1(I)
        WORKFRQ(I)=LOCFRQ1(I)
  100 CONTINUE
C
C   PUT LOCPAR1 INTO WKPARMS, I.E. EXCHANGE PARAMETERS
C
      WKPARMS(1)=0.0
      WKPARMS(2)=LOCPAR1(2)
      WKPARMS(3)=LOCPAR1(3)
      RETURN
      END



      SUBROUTINE WNDOAVE(WORKMAG,WORKFRQ,WKPARMS)

      INTEGER TOTLFRQ,K1,N,BINS,ENDCNT
      REAL WNDOSIZ,POWRLAW,WNDOFRQ(1025),F1,HLDARRY(1025),
     *     WORKMAG(1025),WORKFRQ(1025),MULTSIZ,WKPARMS(10)

      PRINT*,"THIS ROUTINE COMPUTES A WINDOWED AVERAGE OF A"
      PRINT*,"PLOT IN THE WORK PLOT."
      PRINT*,"THE RESULTING PLOT IS PUT IN THE WORK PLOT."
      PRINT*,"IT WILL HAVE A DIFFERENT SIZE THAN THE INPUT"
      PRINT*,"PLOT."
      PRINT*,"THE FIRST FREQUENCY OF THE INPUT PLOT IS ",WORKFRQ(2)
      PRINT*,"WHAT SHOULD THE FIRST WINDOW FREQUENCY BE?"
C
C   WNDOFRQ(1) SHOULD BE 0.0 ,  CORRESPONDING TO WORKFRQ'S FIRST
C   FREQUENCY BEING 0.0.
C
      READ*,WNDOFRQ(2)
      WNDOFRQ(1)=0.0
      PRINT*," "
      WNDOSIZ=WNDOFRQ(2)
      PRINT*," "
      PRINT*,"HOW MANY WINDOWS DO YOU WANT?"
      READ*,TOTLFRQ
      PRINT*," "
      PRINT*,"WHAT SHOULD THE MULTIPLICATIVE WINDOW INCREMENT BE?"
      PRINT*,"(SHOULD BE GREATER THAN 1)"
      READ*,MULTSIZ
      PRINT*," "
      PRINT*,"TO WHAT POWER LAW DO YOU WISH TO FIT THE SPECTRUM?"
      PRINT*,"(SHOULD BE A NEGATIVE NUMBER)"
      READ*,POWRLAW
      PRINT*,"  "
C
C   VALIDATE POWRLAW AND MULTSIZ
C
      IF (POWRLAW .GT. 0.0) CALL PENTERR(1)
      IF (POWRLAW .GT. 0.0) RETURN
```

```
      IF (MULTSIZ .LT. 1.0) CALL PRNTERR(2)
      IF (MULTSIZ .LT. 1.0) RETURN
C
C   SET UP AN ARRAY OF THE LOWER FREQUENCIES OF EACH WIDOW
C   THE FIRST TWO FREQUENCIES WERE DETERMINED BY WNDOSIZ AND "
C   THE USER SPECIFIED FIRST FREQUENCY.
C
C
      DO 50 I=3,TOTLFRQ
        WNDOFRQ(I)=(WNDOFRQ(I-1)-WNDOFRQ(I-2))*MULTSIZ+WNDOFRQ(I-1)
   50 CONTINUE
C
C   NOW SEARCH THROUGH THE WORKFRQ, FIND ALL POINTS THAT FALL IN
C   A BIN, AVERAGE THEM, AND PLACE EACH AVERAGE SUCCESSIVELY IN
C   THE WORKMAG.  IF NO FREQUENCIES FALL IN A BIN, PUT ZERO IN THE
C   PROPER WORKMAG SLOT.
C
C   THIS MIGHT PLACE ZERO IN THE FIRST BIN AND IN THE UPPER BINS
C   IF TOTLFRQ TAKES THE SEARCH ABOVE THE HIGHEST FREQUENCY IN
C   THE WORKFRQ ARRAY.
C
C   THERE IS ONE LESS BIN THAN THERE ARE WINDOW FREQUENCIES.
C   SO BINS=TOTLFRQ-1.
      BINS=TOTLFRQ-1
C
C   LOOK THROUGH ALL BINS FOR APPROPRIATE POINTS
C   ALSO WATCH FOR EMPTY BINS.  AFTER 2 EMPTY BINS IT CAN BE ASSUMED
C   THAT NO FREQUECIES EXIST IN THE HIGHER BINS.  COUNT THESE WITH ENDCNT.
C   EVERY TIME WE GET A BIN WITH AT LEAST ONE COUNT, RESET THE
C   ENDCNT TO 0
C
      K1=IFIX(WKPARMS(2) + .1)
      ENDCNT=0
      DO 300 I=1,BINS
        N=0
        ADDUP=0.0
        DO 200 J=1,K1
C
C       WNDOFRQ(I) IS THE LOWER FREQUENCY OF THE I'TH BIN, AND
C       WNDOFRQ(I+1) IS THE UPPER FREQUENCY OF THE I'TH BIN
C
          IF((WORKFRQ(J) .GT. WNDOFRQ(I)) .AND. (WORKFRQ(J) .LT.
     *    WNDOFRQ(I+1))) 110,200
  110     N=N+1
          ADDUP=ADDUP+WORKMAG(J)
  200   CONTINUE
C
C       AT THIS POINT, N=0 MEANS NO POINTS WERE FOUND.
C       ADJUST ENDCNT ACCORDINGLY.
C
        IF(N .EQ. 0) HLDARRY(I)=0.0
        IF(N .NE. 0) ENDCNT=0
        IF(N .EQ. 0) ENDCNT=ENDCNT+1
        IF(ENDCNT .EQ. 2) WKPARMS(2)=FLOAT(I)
        IF(N .NE. 0) HLDARRY(I)=ADDUP/(FLOAT(N))
  300 CONTINUE
C
C   CHECK IF THE DATA BINS WERE NOT ENOUGH TO COVER THE INPUT
C   DATA.  DO THIS BY CHECKING FOR ENDCNT LESS THAN 2.  IF THIS
C   IS THE CASE THEN WKPARMS(2) SHOULD BE SET TO BINS.
C   IN ANY CASE PRINT OUT HOW MANY BINS WERE ACTUALLY USED.
C
      IF (ENDCNT .LT. 2) WKPARMS(2)=FLOAT(BINS)
      PRINT*,"THERE ARE ",WKPARMS(2)," FREQUENCY BINS IN THE"
      PRINT*,"INCREMENTED WINDOW AVERAGE SPECTRUM."
C
C   NOW WE HAVE A COLLECTION OF AVERAGE MAGNITUDES FOR A SET OF BINS.
C   TO PROPERLY ASSIGN EACH VALUE TO A PARTICULAR FREQUENCY IN
C   A BIN WE  MUST ACCOUNT FOR THE POWER LAW WEIGHTING.
C
      DO 400 I=2,BINS
        F1=WNDOFRQ(I)-WNDOFRQ(I-1)
```

```
      WORKFRQ(I)=(((WNDOFRQ(I)*(MULTSIZ+1.0)-MULTSIZ*WNDOFRQ(I-1))**
     *           (POWRLAW+1.0)-WNDOFRQ(I)**(POWRLAW+1.0))/
     *           ((POWRLAW+1.0)*MULTSIZ*(F1)))**(1.0/POWRLAW)
  400 CONTINUE

C
C   NOW PUT THE TEMPORARY HOLDING ARRAY (HLDARRY) INTO THE
C   WORKMAG ARRAY.
C
      K1=IFIX(WKPARMS(2) + .1)
      DO 350 I=1,K1
        WORKMAG(I)=HLDARRY(I)
  350 CONTINUE
C
C   CHANGE THE PARAMETERS IN WKPARMS
C   WKPARMS(3) THE FFT SIZE IS THE SAME.
C
      WKPARMS(1)=0.0
      RETURN
      END



C
C      THE FOLLOWING SUBROUTINE MOVES ONE WORK BAY TO ANOTHER
C

      SUBROUTINE TRNSPLT(LOCMAG1,LOCFRQ1,LOCPAR1,LOCMAG2,LOCFRQ2,
     *                   LOCPAR2)

      REAL LOCMAG1(1025),LOCMAG2(1025),LOCFRQ1(1025),
     *     LOCFRQ2(1025),LOCPAR1(1025),LOCPAR2(1025),
     *     SAVEMAG,SAVEFRQ,SAVEPAR
      INTEGER I,J,K,MAXSIZE
C
C   FIND WHICH OF THE TWO ARRAYS IS LARGER AND USE THE INTEGER
C   VALUE IN THE LOOP.
C
      MAXSIZE=IFIX(LOCPAR1(2) + .1)
      IF (LOCPAR2(2) .GT. LOCPAR1(2)) MAXSIZE=IFIX(LOCPAR2(2)+.1)
C
C   SWITCH ELEMENTS OF THE TWO ARRAY SETS
C
      DO 200 I=1,MAXSIZE
        SAVEMAG=LOCMAG1(I)
        LOCMAG1(I)=LOCMAG2(I)
        LOCMAG2(I)=SAVEMAG
        SAVEFRQ=LOCFRQ1(I)
        LOCFRQ1(I)=LOCFRQ2(I)
        LOCFRQ2(I)=SAVEFRQ
  200 CONTINUE
      DO 300 I=1,10
        SAVEPAR=LOCPAR1(I)
        LOCPAR1(I)=LOCPAR2(I)
        LOCPAR2(I)=SAVEPAR
  300 CONTINUE
      RETURN
      END

      SUBROUTINE COPY(LOCMAG1,LOCFRQ1,LOCPAR1,LOCMAG2,LOCFRQ2,
     *                LOCPAR2)

C
C     THIS ROUTINE COPIES LOCAL BAY#1 TO LOCAL BAY#2.  THE CONTENTS
C     OF BAY#2 ARE DESTROYED.
C
      INTEGER I,SIZE
      REAL LOCMAG1(1025),LOCMAG2(1025),LOCFRQ1(1025),
     *     LOCFRQ2(1025),LOCPAR1(10),LOCPAR2(10)

      SIZE=IFIX(LOCPAR1(2) + .1)
```

```
      DO 200 I=1,SIZE
        LOCMAG2(I)=LOCMAG1(I)
        LOCFRQ2(I)=LOCFRQ1(I)
 200  CONTINUE

      DO 300 I=1,10
        LOCPAR2(I)=LOCPAR1(I)
 300  CONTINUE

      RETURN
      END

C
C   SUBROUTINE PRTSTAT GIVES THE PLOT BAYS AND THEIR SIZES
C
      SUBROUTINE PRTSTAT(PARAMS1,PARAMS2,WKPARMS)

      REAL PARAMS1(10),PARAMS2(10),WKPARMS(10)
      INTEGER I,J,K

      PRINT*,"PLOT BAY    TIME    SIZE (POINTS)    FFT SIZE"
      PRINT*,"*********************************************"
      PRINT*," "
      WRITE(2,900) 1,PARAMS1(1),PARAMS1(2),PARAMS1(3)
      WRITE(2,900) 2,PARAMS2(1),PARAMS2(2),PARAMS2(3)
      WRITE(2,1000) WKPARMS(1),WKPARMS(2),WKPARMS(3)
  900 FORMAT(I1,11X,F6.3,2X,F5.0,13X,F5.0)
 1000 FORMAT(9HWORK PLOT,3X,F6.3,2X,F5.0,13X,F5.0)
      RETURN
      END



C
C   SUBROUTINE AVERAGE TAKES THE AVERAGE OF TWO PLOTS.
C
      SUBROUTINE AVERAGE(LOCMAG1,LOCFRQ1,LOCPAR1,LOCMAG2,
     *           LOCFRQ2,LOCPAR2,WORKMAG,WORKFRQ,WKPARMS)

      REAL LOCMAG1(1025),LOCMAG2(1025),WORKMAG(1025),LOCFRQ1(1025),
     *     LOCFRQ2(1025),WORKFRQ(1025),LOCPAR1(10),LOCPAR2(10),
     *     WKPARMS(10),ADDUP
      INTEGER I,J,POINTS

      POINTS=IFIX(LOCPAR1(2) + .1)
      DO 100 I=1,POINTS
        WORKMAG(I)=(LOCMAG1(I)+LOCMAG2(I))/2.0
        WORKFRQ(I)=LOCFRQ1(I)
 100  CONTINUE
C
C   PUT PARAMETERS INTO THE WORK PARAMETERS
C
      WKPARMS(1)=0.0
      WKPARMS(2)=LOCPAR1(2)
      WKPARMS(3)=LOCPAR1(3)
      RETURN
      END
C
C   THE FOLLOWING TWO ROUTINES DEAL WITH ERRORS
C
      SUBROUTINE PRNTERR(I)
      INTEGER I
      GOTO(10,20,30)I
 10   PRINT*," "
      PRINT*,"*** POWER LAW MUST BE A NEGATIVE NUMBER***"
      PRINT*," "
      RETURN
 20   PRINT*," "
      PRINT*,"***THE MULTIPLICATIVE INCREMENT OF THE WINDOW MUST"
      PRINT*,"   BE GREATER THAN 1.00***"
      PRINT*," "
      RETURN
```

```
 30   PRINT*," "
      PRINT*,"***THERE ARE ONLY EIGHT ALLOWED COMMANDS***"
      PRINT*," "
      RETURN
      END


      SUBROUTINE SIZEERR(LOCPAR1,LOCPAR2,I,ERR)


      REAL LOCPAR1(10),LOCPAR2(10)
      INTEGER I,ERR,SIZE1,SIZE2

C
C   THIS ROUTINE CHECKS IF TWO ARRAYS HAVE THE SAME SIZE.  ERR=1
C   IF THE ARRAYS HAVE THE SAME SIZE.  OTHERWISE ERR=0.
C

      SIZE1=IFIX(LOCPAR1(2) + .1)
      SIZE2=IFIX(LOCPAR2(2) + .1)

      IF (SIZE1 .EQ. SIZE2) ERR=1
      IF (ERR .EQ. 1) RETURN
      GOTO(10,20)I
 10   PRINT*," "
      PRINT*,"***ARRAYS ARE OF DIFFERENT SIZES IN DIFFRNC***"
      PRINT*," "
      RETURN
 20   PRINT*," "
      PRINT*,"***ARRAYS ARE OF DIFFERENT SIZES IN AVRGSET***"
      PRINT*," "
      RETURN
      END
```

II.5 DATPLOT

```
      PROGRAM DATPLOT(INPUT,OUTPUT,DATA29,TAPE1=INPUT,
     +TAPE2=OUTPUT,TAPE3=DATA29)
C
C   THIS PROGRAM READS 2000 POINTS FROM A ROCKET FILE AND PLOTS
C   THE POINTS AS A FUNCTION OF TIME.  THIS PARTICULAR VERSION ASSUMES
C   A RECORD LENGTH OF 250 (SEE OTHER ROCKET PROGRAMS FOR ROCKET FORMAT)
C   AND A DIGITIZING RATE OF 5000.  THE PLOTTING STARTS AT STRTIM
C   SECONDS INTO THE FILE, RELATIVE TO THE FILE'S BEGINNING.
C   THIS ALLOWS USE WITHOUT KNOWLEDGE OF THE ABSOLUTE TIME OF EACH
C   RECORD.  THE USER MUST ONLY KNOW THE DESIRED POSITION RELATIVE
C   TO THE PARTICULAR FILE'S STARTING TIME.
C   TO RUN THIS PROGRAM THE GCS PLOTTING LIBRARY MUST BE ACCESSED
C   WITH: GRAB,GCS(TEKT,3D).  THIS IS ENTERED PRIOR TO RUN.  THE
C   LIBRARY IS NOT NEEDED TO COMPILE DATPLOT.
C
      REAL ARRAY(1251),TIME(2000),CHAN(2000),TSTPRNT,STRTIM
      INTEGER IARRAY(1250),I,J,K,L,STRTREC,DIGRATE,SKIP,MAXMAG,
     *     QUES
      EQUIVALENCE (ARRAY(2),IARRAY(1))
C   DIGRATE IS THE DIGITIZING RATE OF THE DATA.
      DIGRATE=5000
C   MAXMAG IS THE LARGEST EXPECTED VALUE OF DATA.
      MAXMAG=256
      PRINT*,"THIS PROGRAM PLOTS 2000 POINTS.  IT ASSUMES"
      PRINT*,"A ROCKET FILE AS THE INPUT."
      PRINT*,"      "
      PRINT*,"AT HOW MANY SECONDS INTO THE FILE SHOULD THE PLOT BEGIN?"
      READ*,STRTIM
      CALL USTART
  30  REWIND 3
C
C   STRTREC IS THE FIRST RECORD WHICH WILL BE PLOTTED.
C   THE FOLLOWING LOOP PUTS THE FILE READ POINTER AT THE PROPER PLACE.
C   THE RECORD IS NOT READ.
C   THE "+ .1" HELPS PREVENT ROUNDOFF ERRORS FROM THE IFIX
C
      STRTREC=IFIX((FLOAT(DIGRATE/250))*STRTIM + .1)+1
      SKIP=STRTREC-1
      IF (SKIP .EQ. 0 ) GOTO 50
      DO 40 L=1,SKIP
        READ(3) ARRAY
  40  CONTINUE
  50  DO 300 K=1,8
      READ(3) ARRAY
      TIME((K-1)*250+1)=ARRAY(1)
      DO 100 I=2,250
        TIME(I+(K-1)*250)=TIME(I+(K-1)*250-1)+(1.0/(FLOAT(DIGRATE)))
  100 CONTINUE
C
C   NOW LOAD UP THE ARRAY CALLED CHAN.  NOTE THAT CHAN IS REAL AS
C   ALL GCS GRAPHICS ROUTINES REQUIRE REAL NUMBERS AS INPUTS.
      DO 200 J=1,250
        CHAN(J+(K-1)*250)=FLOAT(IARRAY(J*5-3))
  200 CONTINUE
  300 CONTINUE
C
C   SET UP A USER DEFINED AREA THE SIZE OF A TEKTRONIX SCREEN.
C   ALSO SET THE VIRTUAL UNITS IN THE RANGE OF THE DATA BY MEANS OF A
C   UWINDO COMMAND.
C
      CALL UPSET("PRECISION",5.)
      CALL USET("OWNSCALE")
      CALL UDAREA(0.0,7.0,0.0,5.7)
      CALL UWINDO(TIME(1),TIME(2000),0.00,FLOAT(MAXMAG))
      CALL UPLOT1(TIME,CHAN,2000.0)
      CALL UPAUSE
      PRINT*,"DO THE NEXT ONE?          1-YES"
      PRINT*,"                          2-NO"
```

```
READ*,QUES
CALL UERASE
STRTIM=STRTIM+.4
IF (QUES .EQ. 1)GOTO 30
CALL UEND
STOP
END
```

II.6 SPINFIX

```
      PROGRAM SPINFIX(INPUT,OUTPUT,DATAIN,DATOUT,TAPE1=INPUT,
     +          TAPE2=OUTPUT,TAPE3=DATAIN,TAPE4=DATOUT)
C
C
C          PROGRAM SPINFIX BY RODNEY STOLTZFUS   11/1/83
C
C
C     THIS PROGRAM FILTERS OUT THE SPIN FREQUENCY
C       FROM ROCKET DATA.  THIS FREQUENCY IS OF THE
C       ORDER OF 4-8 HZ.  THIS FILTERING INVOLVES CONVOLVING THE
C       THE DATA WITH A RECTANGULAR WINDOW 1 HIGH AND OF LENGTH
C       SPINPRD.  THIS CONVOLUTION TRANSFORMS TO MULTIPLYING THE
C       SPECTRUM BY A SIN SQUARED FUNCTION, PUTTING HOLE IN THE
C       SPECTRUM EVERY 1/SPINPRD HZ.  THE CONVOLUTION PERFORMED IS
C       NOT EXACTLY CONVENTIONAL.  INSTEAD OF ADDING UP THE WHOLE
C       INTERSECTING GROUP OF POINTS, THE LEAD POINT IS ADDED AND THE
C       TRAILING POINT IS SUBTRACTED FROM THE PREVIOUS SUM.  THE
C       INITIAL VALUE IS SET AT ZERO.  THE ONLY EFFECT THIS HAS IS TO
C       DISTORT THE OFFSET.  ALSO, EACH POINT IS NOT NORMALIZED BY
C       THE TIME INCREMENT BETWEEN POINTS.
C
C     ARRCNT SUBBLOCKS OF DATA ARE READ INTO A LARGE ARRAY.
C       THIS DATA IS ANALYZED UNTIL ANOTHER SUBBLOCK IS NEEDED,
C       WHEREUPON DATA IS READ IN AND PLACED IN THE APPROPRIATE
C       POSITION WITH RESPECT TO THE OTHERS.  THUS THE
C       DATA CYCLES THROUGH THE MAIN BLOCK.
C       THE MAIN BLOCK MAY BE VIEWED AS CIRCULAR. TWO WIPERS
C       ROTATE, SAMLING THE DATA.  WHEN THE TRAILING WIPER
C       FINISHES A SUBBLOCK A NEW ONE IS INSERTED.
C       THE COUNTER REDCNT RUNS FROM 1 TO HOWEVER MANY DATA
C       POINTS ARE DESIRED.  THIS WILL RUN INTO THE THOUSANDS.
C       EVERYTIME IT PASSES AN INCREMENT OF ARRCNT*250 THE FLAG OVERFLW
C       IS INCREMENTED.  THE COUNTER PNTCNT INDEXES THE SUBBLOCK
C       IDATA.  WHEN IDATA IS FULL IT IS WRITTEN INTO TAPE3.
C       PNTCNT IS RESET AFTER A DATA RECORD IS WRITTEN OUT.
C
C     WHEN RUNNING THE OUTPUT DATA THROUGH THE "SPECTRA"PROGRAM
C        YOU  MUST MULTIPLY THE SPECTRUM BY (CONSTANT)*(FRE-
C       QUENCY)**2 TO ADJUST FOR THE RECTANGULAR WINDOW.
C
C
C             I M P O R T A N T    N O T E
C          THIS PROGRAM ASSUMES DATA RECORDS IDENTICAL TO THOSE OF
C          ROCKET SHOTS 31.029 AND 31.028.  THAT MEANS A DIGITIZING
C          RATE OF 5000, RECORD SIZE OF 1250, AND FIVE DATA CHANNELS
C          PER FRAME, THE SECOND CHANNEL BEING THE ONE OF INTEREST.
C
C              VARIABLE DICTIONARY
C
C          TIMEL1 THE TIME MARKER OF THE RECORD PRIOR TO THE
C                 STARTING RECORD.
C
C          BLKCNT THE NEXT SUBBLOCK TO BE FILLED.
C
C          ARRAY CONTAINS 1251 DATA POINTS.  AS USUAL THE
C                  FIRST CONTAINS THE CORRESPONDING TIME.
C
C          IARRAY  IS THE EQUIVALENT OF ARRAY BUT IN INTEGER
C                  FORM.
C
C          IRAWDAT CONTAINS FOUR SUBBLOCKS WITH THE TIME AND THE
C                  FOUR OTHER DATA CHANNELS STRIPPED OFF.
C
C          SPINFRQ IS THE SPIN FREQUENCY OF THE ROCKET.
C
C          SPNPRD IS THE PERIOD OF THE SPIN IN TERMS OF
C                  DATA POINTS.
C
C          ARRCNT  IS THE NUMBER OF SUBBLOCKS IN THE MAIN BLOCK.
```

```
C           THERE SHOULD BE ENOUGH SUBBLOCKS TO COVER THE SPIN PERIOD
C           PLUS AN EXTRA SUBBLOCK.
C
C          LEFTOVR IS THE DIFFERENCE BETWEEN THE BLOCK LENGTH AND
C                   THE SPIN PERIOD.
C
C          IDATA CONTAINS THE INTEGER FORM OF THE PROCESSED DATA.
C
C          I,J      ARE ASSORTED COUNTERS.
C
C          NORM     IS THE NORMALIZED INDEX (POSITION IN IRAWDAT)
C                   OF THE DATA POINT SPNPRD AHEAD OF THE CURRENT POINT.
C          OVERFLW TELLS THE INCREMENT OF ARRCNT*250 THAT REDCNT
C                   IS ON.  SEE PROGRAM NOTES ABOVE THIS DICTIONARY.
C
C          REDCNT   INDEXES THE ARRAY IRAWDAT.  REDCNT IS UNBOUNDED.
C                   SEE OVERFLW.  REDCNT COUNTS THE POINTS THAT HAVE
C                   BEEN READ ALREADY.
C
C          PNTCNT   INDEXES THE ARRAY IDATA.  PNTCNT IS CYCLED FROM
C                   2 TO 251.
C
C
      REAL ARRAY(1251),SPINFRQ,STRTIME,TIME,TIMEL1,SPAN
      INTEGER SPNPRD,ARRCNT,LEFTOVR,IDATA(251),IRAWDAT(5000),
     +   I,J,BLKCNT,REDPNT,PNTCNT,OVERFLW,IARRAY(1250),SPANPTS
      EQUIVALENCE(ARRAY(2),IARRAY(1))
C
C         INPUT THE SPIN FREQUENCY.
C
      PRINT*,"WHAT IS THE SPIN FREQUENCY OF THE ROCKET"
      READ*,SPINFRQ
      PRINT*,"WHAT IS THE STARTING TIME IN U.T. SECONDS"
      READ*,STRTIME
C
C          PUT THE DATA CORRESPONDING TO STRTIME INTO ARRAY.
C
   10 READ(3) ARRAY
      TIMEL1=STRTIME-0.05100.
      IF (ARRAY(1) .GT. TIMEL1) GOTO 20
      GOTO 10

   20 CONTINUE
      TIME=ARRAY(1)
C
C          FIND SPIN PERIOD, BLOCK SIZE, AND LEFTOVER.
C
      SPNPRD=IFIX(5000.0/SPINFRQ)
      ARRCNT=2+((IFIX((5000.0/SPINFRQ)+.5))/250)
      LEFTOVR=(ARRCNT*250)-SPNPRD
C
C          LOAD UP IRAWDAT WITH ROCKET DATA
C
      DO 100 I=1,250
        IRAWDAT(I)=IARRAY((I-1)*5+2)
  100 CONTINUE
      DO 120 J=2,ARRCNT
        READ(3) ARRAY
        DO 110 I=1,250
          IRAWDAT(I+(J-1)*250)=IARRAY((I-1)*5+2)
  110   CONTINUE
  120 CONTINUE
C
C          BEGIN FILTERING
C
      BLKCNT=1
      IDATA(1)=0
      REDPNT=1
      PNTCNT=2
      OVERFLW=0
C
C       ASK FOR THE DESIRED NUMBER OF SECONDS.
C       MUST BE A MULTIPLE OF 0.05000   .
```

```
C
      PRINT*,"HOW MANY SECONDS OF DATA DO YOU WANT?"
      READ*,SPAN
      SPANPTS=IFIX(SPAN*5000.00+.1)
      DO 300 I=1,SPANPTS
      CALL PROCESS(PNTCNT,REDPNT,IRAWDAT,IDATA,SPNPRD,TIME,
     +      OVERFLW,BLKCNT,ARRCNT)
  300 CONTINUE
      STOP
      END
C
C
C          SUBROUTINES GETNEXT AND PROCESS
C
C
      SUBROUTINE GETNEXT(BLKCNT,LOCIRAW)
C
      REAL LOCARRY(1251)
      INTEGER LOCIARR(1250),I,J,LOCIRAW(2000),BLKCNT
      EQUIVALENCE(LOCARRY(2),LOCIARR(1))
      READ(3) LOCARRY
C
C       PUT DATA INTO LOCIRAW AT THE POSITION BLKCNT.
C
      DO 400 I=1,250
        LOCIRAW((BLKCNT-1)*250+I)=LOCIARR((I-1)*5+2)
  400 CONTINUE
      RETURN
      END


      SUBROUTINE PROCESS(LPNTCNT,LREDPNT,IRAWDAT,IDATA,
     +           SPNPRD,TIME,OVERFLW,BLKCNT,ARRCNT)
      REAL OUTPUT(1251),TIME
      INTEGER IOUTPUT(1250),LPNTCNT,LREDPNT,IRAWDAT(2000),IDATA(251),
     +      SPNPRD,OVERFLW,BLKCNT,NORM,OFFSET,ARRCNT
      EQUIVALENCE(OUTPUT(2),IOUTPUT(1))
      IF ((LREDPNT) .GT. (ARRCNT*250*(OVERFLW+1))) OVERFLW=
     +  OVERFLW+1
C
C .       SUBTRACT ARRCNT*250 FROM THE IRAWDAT INDEX IF THE INDEX
C         BECOMES GREATER THAN ARRCNT*250.
C
      NORM=LREDPNT-ARRCNT*250*OVERFLW+SPNPRD
      IF (NORM .GT. ARRCNT*250) NORM=NORM-ARRCNT*250
      IDATA(LPNTCNT)=IDATA(LPNTCNT-1)-IRAWDAT(LREDPNT-ARRCNT*
     +   250*OVERFLW)+IRAWDAT(NORM)
C
C
C     IF THERE ARE 250 ELEMENTS IN DATA, THEN WRITE OUT.
      IF (LPNTCNT .LT. 251) GOTO 700
      OUTPUT(1)=TIME
C
C     LOAD UP THE FIRST, THIRD, FOURTH, AND FIFTH CHANNELS OF THE
C     DATA FRAME WITH JUNK.
C     ALSO PUT IN AN OFFSET AS THE DATA OTHERWISE WILL BE CENTERED
C     AROUND ZERO.
C
      OFFSET=0000
      DO 500 I=1,250
        IOUTPUT((I-1)*5+1)=IRAWDAT(I)
        IOUTPUT((I-1)*5+2)=IDATA(I+1)+OFFSET
        IOUTPUT((I-1)*5+3)=IRAWDAT(I+250)
        IOUTPUT((I-1)*5+4)=IRAWDAT(I+500)
        IOUTPUT((I-1)*5+5)=IRAWDAT(I+750)
  500 CONTINUE
      IDATA(1)=IDATA(251)
      WRITE(4) OUTPUT
      LPNTCNT=1
      TIME=TIME+.050000
```

```
C
C     WHEN REDPNT IS PAST A SUBBLOCK, THAT SUBBLOCK MAY
C     BE DISCARDED ANDREPLACED BY A NEW ONE.  THIS IS DONE
C     VIA THE GETNEXT SUBROUTINE.
C
  700 CONTINUE
      DO 800 I=1,ARRCNT
        IF ((LREDPNT-ARRCNT*250*OVERFLW) .EQ. 250*I) CALL
     +     GETNEXT(I,IRAWDAT)
  800 CONTINUE
      LREDPNT=LREDPNT+1
      LPNTCNT=LPNTCNT+1
      RETURN
      END
```

REFERENCES

Banks, P. M., and G. Kockarts (1973), Aeronomy Part B, Academic Press, New York.

Batchelor, G. K. (1953), The Theory of Homogeneous Turbulence, Cambridge University Press, Cambridge, UK.

Batchelor, G. K. (1959), Small-scale variation of convected quantities like temperature in turbulent fluid, Part 1. General discussion and the case of small conductivity, J. Fluid Mech., 5, 113-133.

Batchelor, G. K., I. D. Howells, and A. A. Townsend (1959), Small-scale variation of convected quantities like temperature in tubulent fluid, Part 2. The case of large conductivity, J. Fluid Mech., 5, 134-139.

Booker, J. R., and F. P. Bretherton (1967), The critical layer for internal gravity waves in a shear flow, J. Fluid Mech., 27, 1-27.

Boston, N. E., and R. W. Burling (1972), An investigation of high wave number temperature and velocity spectra in air, J. Fluid Mech., 55, 473-492.

Chandrasekhar, S. (1961), Hydrodynamic and Hydromagnetic Instability, Oxford University Press, New York.

Chen, F. F. (1965), Electric probes, in Plasma Diagnostic Techniques, edited by R. H. Huddlestone and S. L. Leonard, Academic Press, New York, 113-200.

Cicerone, R. J., and S. A. Bowhill (1967), Positive ion collection by a spherical probe in a collision-dominated plasma, Aeron. Rep. No. 21, Aeron. Lab., Dep. Elec. Eng., Univ. IL, Urbana-Champaign.

Corrsin, S. (1964), Further generalization of Onsager's cascade model for turbulent spectra, Phys. Fluids, 7, 1156-1159.

Edwards, B. (1976), Editor, Research in Aeronomy, Prog. Rep. No. 76-1, Aeron. Lab., Dep. Elec. Eng., Univ. IL, Urbana-Champaign.

Edwards, B. (1977), Editor, Research in Aeronomy, Prog. Rep. No. 77-1, Aeron. Lab., Dep. Elec. Eng., Univ. IL, Urbana-Champaign.

Fritts, D. C. (1978), The nonlinear gravity wave-critical level interaction, J. Atmos. Sci., 35, 397-413.

Fukao, S., T. Sato, R. M. Harper, and S. Kato (1980), Radio wave scattering from the tropical mesosphere observed with the Jicamarca radar, Radio Sci., 15, 447-457.

Geller, M. A., H. Tanaka, and D. C. Fritts (1975), Production of turbulence in the vicinity of critical levels for internal gravity waves, J. Atmos. Sci., 32, 2125-2135.

Gossard, E. E., J. H. Richter, and D. Atlas (1970), Internal waves in the atmosphere from high-resolution radar measurements, J. Geophys. Res., 75, 3523-3536.

Gossard, E. E., and K. C. Yeh (1980), Foreword, Radio Sci.,15, 147-150.

Heicklen, J. (1976), Atmospheric Chemistry, Academic Press, New York.

Hill, R. J. (1978), Models of the scalar spectrum for turbulent advection, J. Fluid Mech., 88, 541-562.

Hill, R. J., and S. A. Bowhill (1976), Small-scale fluctuations in D-region ionization due to hydrodynamic turbulence, Aeron. Rep. No. 75, Aeron. Lab., Dep. Elec. Eng., Univ. IL, Urbana-Champaign.

Hinze, J. O. (1975), Turbulence, McGraw Hill Co., New York, Second Edition.

Hocking, W. K., and R. A. Vincent (1982), A comparison between HF partial reflection profiles from the D-region and simultaneous Langmuir probe electron density measurements, J. Atmos. Terr. Phys., 44, 843-854.

Hodges, R. R., Jr. (1967), Generation of turbulence in the upper atmosphere by internal gravity waves, J. Geophys. Res., 72, 3455-3458.

Howard, L. N. (1961), Note on a paper of John W. Miles, J. Fluid Mech., 10, 509-512.

Howells, I. D. (1960), An approximate equation for the spectrum of a conserved scalar quantity in a turbulent field, J. Fluid Mech., 9, 104.

Klaus, D. E., and L. G. Smith (1978), Rocket observations of electron-density irregularities in the equatorial ionosphere below 200 km, Aeron. Rep. No. 80, Aeron. Lab., Dep. Elec. Eng., Univ. IL, Urbana-Champaign.

Kolmogorov, A. (1941), The local structure of turbulence in incompressible viscous fluid for very large Reynolds' numbers, in Turbulence, Classic Papers on Statistical Theory, edited by S. K. Friedlander and L. Topper, Interscience Publishers, New York, 1961, 151-155.

Kraichnan, R. H. (1968), Small-scale structure of a scalar field convected by turbulence, Phys. Fluids, 11, 945-953.

Lemaire, J., and M. Scherer (1970), Model of the polar ion-exosphere, Planet. Space Sci., 18, 103-120.

Lumley, J. L. and H. A. Panofsky (1964), The Structure of Atmospheric Turbulence, Monographs and Texts in Physics and Astronomy, Vol. XII, Interscience Publishers, New York.

McInerney, M. K., and L. G. Smith (1984), Rocket observations of the ionosphere during the eclipse of 26 February 1979, Aeron. Rep. No. 113, Aeron. Lab., Dep. Elec. Computer Eng., Univ. IL, Urbana-Champaign.

Mechtly, E. A., S. A. Bowhill, L. G. Smith, and H. W. Knoebel (1967), Lower ionosphere electron concentration and collision frequency from rocket

measurements of Faraday rotation, differential absorption, and probe current, J. Geophys. Res., 72, 5239-5245.

Miles, J. W. (1961), On the stability of heterogeneous shear flows, J. Fluid Mech., 10, 496-508.

Mjolsness, R. C. (1975), Diffusion of a passive scalar at large Prandtl numbers according to the abridged Lagrangian interaction theory, Phys. Fluids, 18, 1393-1394.

Oppenheim, A. V., and R. W. Schafer (1975), Digital Signal Processing, Prenctice Hall, Inc., Englewood Cliffs, NJ.

Pao, Y-H. (1964), Statistical behavior of a turbulent multicomponent mixture with first-order reactions, AIAA J., 2, 1550-1555.

Patnaik, P. C., F. S. Sherman, and G. M. Corcos (1976), A numerical simulation of Kelvin-Helmhotlz waves of finite amplitude, J. Fluid Mech., 73, 215-240.

Prakash, S., B. H. Subbaraya, and S. P. Gupta (1969), A study of the lower ionosphere over the geomagnetic equator at Thumba using a Langmuir and plasma noise probe, Space Res. IX, edited by K. S. W. Champion, P. A. Smith, and R. L. Smith-Rose, North-Holland Publ. Co., Amsterdam, 237-245.

Prakash, S., S. P. Gupta, B. H. Subbaraya, and R. Pandey (1980), A review of the electron density irregularities in the equatorial D and E region, in Low Latitude Aeronomical Processes, edited by A. P. Mitra, Pergamon, Oxford, 3-16.

Rastogi, P. K. and S. A. Bowhill (1976), Scattering of radio waves from the mesosphere -- 2. Evidence for intermittent mesospheric turbulence, J. Atmos. Terr. Phys., 38, 449-462.

Roth, P. (1982a), Editor, Research in Aeronomy, Prog. Rep. No. 82-1,

Aeron. Lab., Dep. Elec. Eng., Univ. IL, Urbana-Champaign.

Roth, P. (1982b), Editor, Research in Aeronomy. Prog. Rep. No. 82-2, Aeron. Lab., Dep. Elec. Eng., Univ. IL, Urbana-Champaign.

Rottger, J., P. K. Rastogi, and R. F. Woodman (1979), High-resolution VHF radar observations of turbulence structures in the mesosphere, Geophys. Res. Lett., 6, 617-620.

Royrvik, O., and L. G. Smith (1984), Comparison of mesospheric VHF radar echoes and rocket probe electron concentration measurements, J. Geophys. Res., 89, 9014-9022.

Smith, L. G. (1965), Langmuir probes for measurements in the ionosphere, GCA Tech. Rep. No. 65-25-N.

Smith, L. G. (1969), Langmuir probes in the ionosphere, in Small Rocket Instrumentation Techniques, North-Holland Publ. Co., Amsterdam.

Smith, L. G., and D. E. Klaus (1978), Rocket observations of electron density irregularities in the equatorial E region, Space Res. XVIII, edited by M. J. Rycroft and A. C. Stickland, Pergamon, Oxford, 261-264.

Smith, L. G., and O. Royrvik (1985), Electron-density irregularities in the daytime equatorial ionosphere, J. Atmos. Terr. Phys., in press.

Tatsumi, T., S. Kida, and J. Mizushima (1978), The multiple-scale cumulant expansion for isotropic turbulence, J. Fluid Mech., 85, 97-142.

Tennekes, H., and J. L. Lumley (1972), A First Course in Turbulence, The MIT Press, Cambridge, MA.

Thrane, E. V., and B. Grandal (1981), Observations of fine scale structure in the mesosphere and lower thermosphere, J. Atmos. Terr. Phys., 43, 179-189.

Welch, P. D. (1967), The use of fast Fourier transform for the estimation of power spectra: a method based on time averaging over short, modified

periodograms, IEEE Trans. Audio Electroacoustics, AU-15, 70-73.

Zimmerman, R. K., Jr., and L. G. Smith (1980), Rocket measurements of electron temperature in the E region, Aeron. Rep. No. 92, Aeron. Lab., Dep. Elec. Eng., Univ. IL, Urbana-Champaign.